NASA TECHNICAL NOTE

NASA TN D-2643

NASA TN D-2643

LOAN COPY: R
AFWL (W
KIRTLAND AFI
0154784
TECH LIBRARY KAFB, NM

PARAMETRIC PERFORMANCE ANALYSIS FOR LUNAR ORBIT BRAKING AND DESCENT

by Charles M. Akridge and Sam H. Harlin

George C. Marshall Space Flight Center
Huntsville, Ala.

NATIONAL AERONAUTICS AND SPACE ADMINISTRATION • WASHINGTON, D. C. • FEBRUARY 1965

1cy
NASA
D-2643

ERRATA

NASA TECHNICAL NOTE D-2643

PARAMETRIC PERFORMANCE ANALYSIS FOR LUNAR ORBIT BRAKING AND DESCENT

By Charles M. Akridge and Sam H. Harlin

February 1965

Page viii: The symbol for the definition of Range, km (X) the eighth symbol from the bottom; is correctly written as follows:

x Range, km

Page viii: The correct definition for the symbol ζ, the sixth symbol from the bottom (Propellant mass fraction, W_p/W_o) is correctly defined as:

ζ Propellant mass fraction, W_ϑ/Wo

Page 7: The introductory phrase to equation (9)(The range and pericenter altitude can then be calculated by the relations) is correctly stated:

The range and altitude can be calculated by the relations

Page 7: Delete the term $\frac{r_{☾}}{r}$ in the right side of equation (9). The equation is correctly stated:

$$x = \int v \sin \vartheta \, dt$$

Page 7: Delete the Moon subscript (☾) in the right hand side of equation (11). The equation is correctly written:

$$\psi = \int \frac{\dot{x}}{r} \, dt$$

Page 7: Change the term W_c in equation (13). The equation is correctly written as follows:

$$W_o = W_f + W_\vartheta$$

ERRATA (Cont'd)

Page 8: Delete the large parentheses around the expression $\left(1 - \frac{V_o^2 r_o}{\mu_{\mathbb{C}}}\right)$ of equation (19). The equation should appear:

$$\nu_o = \cos^{-1}\left[\frac{(V_a r_a)^2/\mu_{\mathbb{C}} - r_o}{r_o \sqrt{1 - \frac{V_o^2 r_o}{\mu_{\mathbb{C}}} \left(2 - \frac{V_o^2 r_o}{\mu_{\mathbb{C}}}\right) \sin^2 \vartheta_o}}\right]$$

Page 9: The figure reference of the first sentence in the third paragraph of Section IV part A. (Figure 14) is correctly stated:

The characteristic impulse velocity, shown in Figure 13, is ...

Page 9: The following figure references are changed:

Sixth line from bottom, Figures 15a and 15b to Figures 14a and 14b.

Fourth line from botton, Figures 16a and 16b to Figures 15a and 15b.

Third line from bottom, Figures 17a and 17b to Figures 16a and 16b.

Page 10: The following figure references are changed:

Fourth line from top, Figures 18a and 18b to Figures 17a and 17b.

Sixth line from top, Figures 19a and 19b to Figures 18a and 18b.

Eighth line from top, Figures 20a and 20b to Figures 19a and 19b.

Tenth line from top, Figures 21a and 21b to Figures 20a to 20b.

Third line from bottom, Figures 12a, 12b, 12c, and 12d to Figures 21a, 21b, 21c, and 21d.

Second line from bottom, Figures 13a and 13b to Figures 22a and 22b.

Issued 5-24-65

NASA-Langley, 1965

TECH LIBRARY KAFB, NM
0154784

PARAMETRIC PERFORMANCE ANALYSIS FOR LUNAR ORBIT BRAKING AND DESCENT

By Charles M. Akridge and Sam H. Harlin

George C. Marshall Space Flight Center
Huntsville, Ala.

NATIONAL AERONAUTICS AND SPACE ADMINISTRATION

For sale by the Office of Technical Services, Department of Commerce,
Washington, D.C. 20230 -- Price $3.00

TABLE OF CONTENTS

	Page
SUMMARY	1
SECTION I. INTRODUCTION	2
SECTION II. ASSUMPTIONS	3
SECTION III. ANALYSIS	4
SECTION IV. RESULTS AND CONCLUSIONS	
A. BRAKE TO LUNAR ORBIT	9
B. DESCENT TO LUNAR SURFACE	9
SECTION V. GRAPHIC PRESENTATIONS	
A. BRAKE TO LUNAR ORBIT	11
B. DESCENT TO LUNAR SURFACE	41
BIBLIOGRAPHY	66

LIST OF ILLUSTRATIONS

Figure	Title	Page
1	Pericenter Velocity for Earth Lunar Transfer . . .	12
2	Time to Pericenter for Brake to Lunar Orbit	
	a. h_p = 50 km	13
	b. h_p = 100 km	14
	c. h_p = 200 km	15
	d. h_p = 300 km	16
3	Characteristic Velocity for Brake to Lunar Orbit .	17
4	Stage Propellant Mass Fraction for Brake to Lunar Orbit	
	a. h_p = 50 km	18
	b. h_p = 100 km	19
	c. h_p = 200 km	20
	d. h_p = 300 km	21
5	Change in Altitude for Brake to Lunar Orbit	
	a. h_p = 50 km	22
	b. h_p = 100 km	23
	c. h_p = 200 km	24
	d. h_p = 300 km	25

LIST OF ILLUSTRATIONS (Continued)

Figure	Title	Page
6	Change in Flight Path Angle for Brake to Lunar Orbit	
	a. h_p = 50 km	26
	b. h_p = 100 km	27
	c. h_p = 200 km	28
	d. h_p = 300 km	29
7	Change in Central Angle for Brake to Lunar Orbit	
	a. h_p = 50 km	30
	b. h_p = 100 km	31
	c. h_p = 200 km	32
	d. h_p = 300 km	33
8	Burning Time for Brake to Lunar Orbit	
	a. h_p = 50 km	34
	b. h_p = 100 km	35
	c. h_p = 200 km	36
	d. h_p = 300 km	37
9	Velocity Losses for Brake to Lunar Orbit	
	a. h_p = 50 and 100 km	38
	b. h_p = 200 and 300 km	39

LIST OF ILLUSTRATIONS (continued)

Figure	Title	Page
10	Apocenter and Pericenter Velocities Versus Apocenter and Pericenter Altitudes	42
11	Chart for Determining Elevation and Slant Range of Lunar Spacecraft (0 to 1100 km)	43
12	Characteristic Velocity as a Function of Propellant Mass Fraction and Specific Impulse . . .	44
13	Characteristic Impulse Velocity to Attain Transfer Ellipse with r_p = 1748.3 km	45
14	Characteristic Velocity for Lunar Descent	
	a. I_{sp} = 300 sec	46
	b. I_{sp} = 420 sec	47
15	Propellant Mass Fraction for Lunar Descent	
	a. I_{sp} = 300 sec	48
	b. I_{sp} = 420 sec	49
16	Change in Altitude for Lunar Descent	
	a. I_{sp} = 300 sec	50
	b. I_{sp} = 420 sec	51
17	Change in Flight Path Angle for Lunar Descent	
	a. I_{sp} = 300 sec	52
	b. I_{sp} = 420 sec	53

LIST OF ILLUSTRATIONS (Concluded)

Figure	Title	Page
18	Change in Central Angle for Lunar Descent	
	a. I_{sp} = 300 sec	54
	b. I_{sp} = 420 sec	55
19	Surface Range for Lunar Descent	
	a. I_{sp} = 300 sec	56
	b. I_{sp} = 420 sec	57
20	True Anomaly at Initiation of Lunar Descent	
	a. I_{sp} = 300 sec	58
	b. I_{sp} = 420 sec	59
21	Burning Time for Lunar Descent	
	a. h_a = 50 km	60
	b. h_a = 100 km	61
	c. h_a = 200 km	62
	d. h_a = 300 km	63
22	Velocity Losses for Lunar Descent	
	a. I_{sp} = 300 sec	64
	b. I_{sp} = 420 sec	65

DEFINITION OF SYMBOLS

Symbol	Definition
F	Thrust, N
F/W_o	Initial thrust-to-weight ratio (based on weight at sea level)
g	Gravitational acceleration, m/sec^2
$g_\oplus$	Earth gravitational acceleration, 9.80665 m/sec^2
h	Altitude, km
I_{sp}	Specific impulse, sec
m	Mass, kg
r	Radius, km
t	Time, sec
S	Surface range, km
V	Velocity, m/sec
V^*	Comparative velocity, m/sec
ΔV	Stage characteristic velocity, m/sec
W_o	Gross mass, kg
W_8	Propellant mass, kg
X	Range, km
α	Thrust vector orientation angle measured from the velocity to the thrust vector (positive down), deg
ζ	Propellant mass fraction, W_P/W_o
ϑ	Flight path angle from vertical, deg
μ	Gravitational constant for the moon, 4906 km^3/sec^2
ν	True anomaly, deg
ψ	Central angle from arbitrary reference, deg
Δ	Denotes a change

DEFINITION OF SYMBOLS (Concluded)

Subscript	Definition
a	Apocenter
B	Burnout
co	Circular Orbit
ex	Exhaust
f	Final
id	Ideal
o	Initial
p	Pericenter
⊕	Earth
☾	Moon

PARAMETRIC PERFORMANCE ANALYSIS FOR LUNAR ORBIT BRAKING AND DESCENT

SUMMARY

The effects of thrust-to-weight ratio, specific impulse, and altitude on trajectory parameters have been investigated for braking to lunar orbit and descent to the lunar surface from this lunar parking orbit. A single stage with constant thrust directed against the velocity vector was used in all instances. Specific impulses of 300 and 420 seconds and earth-to-moon transfer times for braking of 50, 60, and 72 hours were used for comparison.

The results of the study show the variations of the braking trajectory parameters for earth thrust-to-weight ratios from 0.1 to 1.0. The descent variations are limited to earth thrust-to-weight ratios from 0.2 to 0.5. These parameters include true anomaly, change in altitude, flight path angle, range angle during thrusting, burning time, characteristic velocity, propellant fraction, and velocity losses.

SECTION I. INTRODUCTION

Orbital operations are of great interest in lunar exploration because of requirements imposed by the landing site, energy, and tracking. Preliminary analysis of lunar missions requires a rapid method of sufficient accuracy for determining trajectory parameters.

The purpose of this report is to present trajectory parameters for the powered lunar braking and lunar landing maneuvers. The parameters presented are the following: velocity, altitude change, change in flight path angle, change in central angle, true anomaly, burning time, propellant mass fraction, and velocity losses.

The approach used for the braking maneuver was to determine the arrival velocity for a given transfer time and initiate burning so that circular orbit conditions were attained at burnout.

For the descent maneuver, an impulse was applied in a parking orbit to attain a transfer ellipse with a 10-kilometer pericenter altitude. At the proper point on the transfer ellipse, powered braking was initiated to arrive at a 300-meter altitude with zero velocity. In both cases, the analysis was limited to planar trajectories with all aerodynamic and perturbative forces being neglected. The equations were integrated on a digital computer, using a Runge-Kutta numerical integration procedure.

SECTION II. ASSUMPTIONS

A summary of the basic assumptions used in this analysis follows:

1. For braking, deceleration using a single propulsive stage from earth-moon transfer to circular lunar orbit, using constant thrust directed against the velocity vector.

2. For descent, deceleration using a single propulsive stage from a transfer ellipse to a 300-meter (hover) altitude and zero velocity using constant thrust directed against the velocity vector.

3. Initial pericenter and parking orbit altitudes:

$h = 50$ km

$h = 100$ km

$h = 200$ km

$h = 300$ km

4. For comparison, specific impulses of 300 and 420 seconds were used.

5. The thrust-to-weight ratio for a chemical stage was varied parametrically from 0.1 to 1.0.

6. Mean spherical moon:

$\mu_{☾} = 4906 \text{ km}^3/\text{sec}^2$

$r_{☾} = 1738.3$ km

SECTION III. ANALYSIS

In lunar mission programs, it is assumed that one mode of lunar flight and landing will be by way of transfer from a circular orbit around the moon. In general, a spacecraft will approach the vicinity of the moon with a relative hyperbolic flight velocity.

The velocity requirements for injection from a lunar transfer were calculated using the equations of motion for a vehicle flying into orbit with the thrust directed against the velocity vector. Relations of velocity and pericenter altitude from sphere-of-influence calculations were used for the earth-lunar transfer (Figure 1). These velocities, though not exact, are sufficient for preliminary calculations. Referring to the sketch below, computations were made for a point mass moving in a plane.

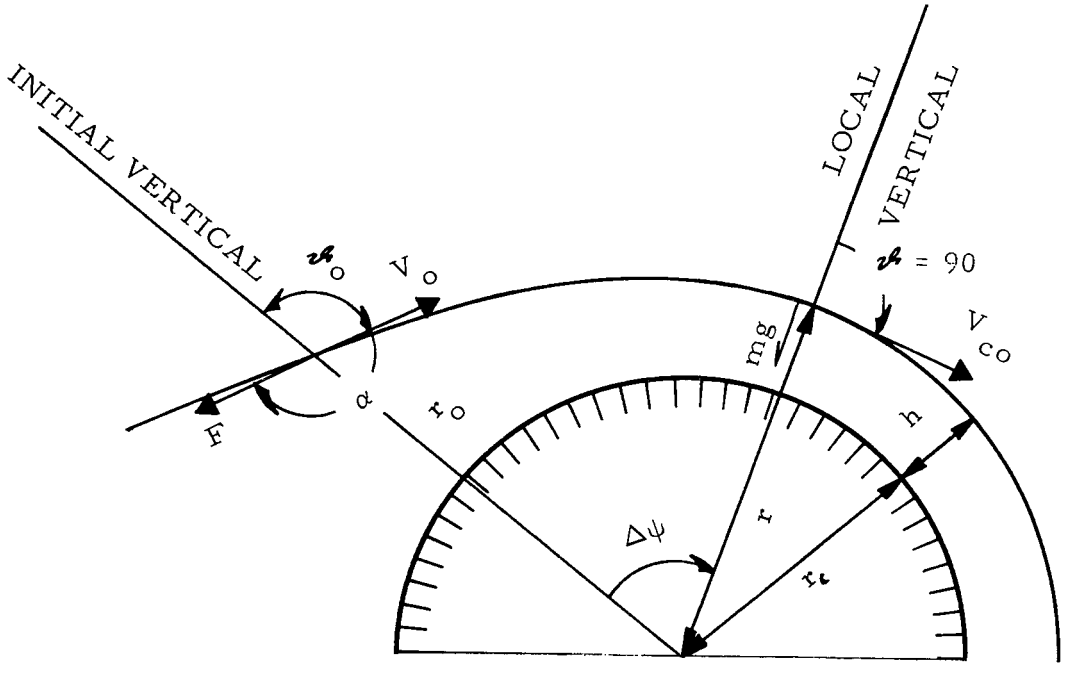

The method of landing on the lunar surface was to direct the thrust against the velocity vector (α = 180°) and follow a gravity turn path. The sketch below illustrates the conditions at initiation of burning.

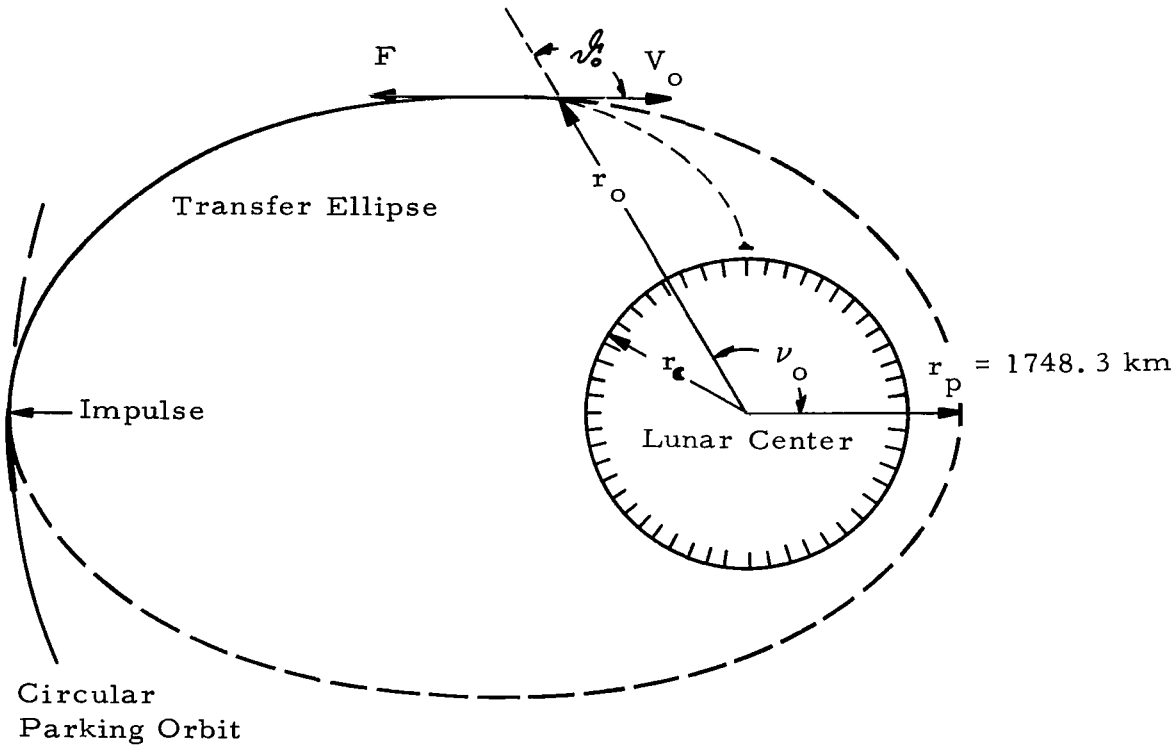

First, an impulse was applied against the velocity vector to attain the transfer ellipse. The pericenter altitude of the transfer ellipse was taken as 10 kilometers to insure against collision with the surface if powered descent were not initiated. The pericenter altitude was selected because of surface irregularities, guidance errors, retro-thrust errors, etc. From a performance viewpoint, it is preferable to expend the energy at as low an altitude as possible.

The true anomaly at initiation of powered descent (measured from the undisturbed Keplerian pericenter radius) varies with thrust-to-weight ratio and parking orbit altitude. It is seen that, as parking orbit altitude decreases, the initial true anomaly will increase (maximum of 180°).

The sketch below shows the initial and final trajectory parameters, as well as change in flight path angle, altitude, and central range angle.

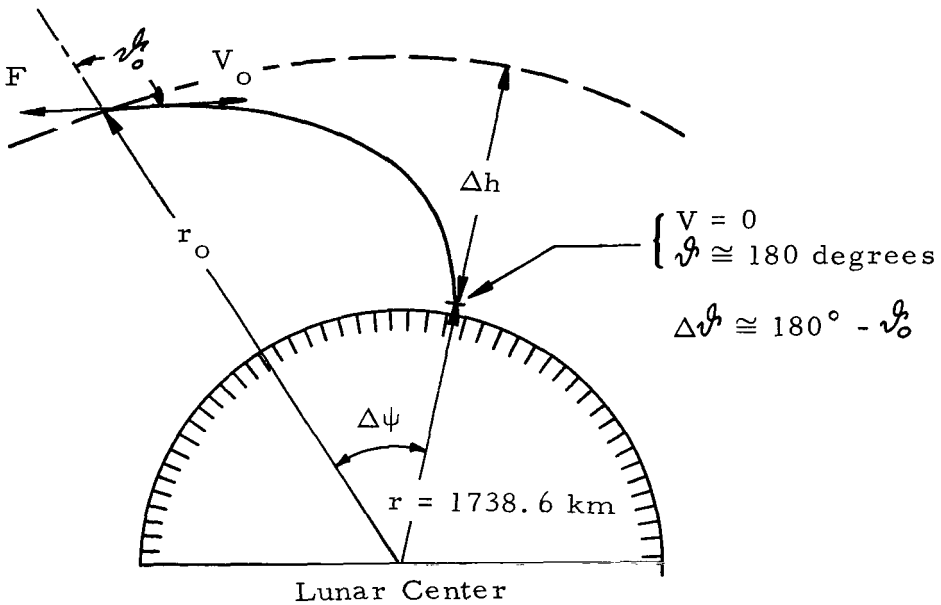

The line of sight and angular range can be determined from Figure 12, using initial conditions. The equations of motion were numerically integrated from initial conditions to 300 meters above the surface. The initial conditions were found by iteration to give the desired end conditions.

The following point mass, planar equations of motion were used with $\alpha = 180°$ in all instances:

$$\dot{V} = \frac{F \cos \alpha}{m} - \frac{g_{\mathbb{C}} r_{\mathbb{C}}^2}{r^2} \cos \vartheta \tag{1}$$

$$V \dot{\vartheta} = \frac{F \sin \alpha}{m} + \left[\frac{g_{\mathbb{C}} r_{\mathbb{C}}^2}{r^2} - \frac{V^2}{r} \right] \sin \vartheta \tag{2}$$

$$\dot{r} = V \cos \vartheta \tag{3}$$

$$\dot{\psi} = \frac{V \sin \vartheta}{r} \tag{4}$$

where

$$m = m_o + \int \dot{m}\, dt \tag{5}$$

and

$$\dot{m} = - \frac{F}{V_{ex}} \tag{6}$$

The velocity and flight path angle may be obtained by integrating the equation of motion

$$V = \int \dot{V}\, dt \tag{7}$$

$$\vartheta = \int \dot{\vartheta}\, dt \tag{8}$$

accurate The range and pericenter altitude can then be calculated by the relations

accurate $$x = \int \frac{r_{\mathbb{C}}}{r}\, v \sin \vartheta\, dt \tag{9}$$

$$h = h_o + \int \dot{r}\, dt \tag{10}$$

and the central angle

accurate $$\psi = \int \frac{\dot{x}}{r_{\mathbb{C}}}\, dt \tag{11}$$

and surface range

$$S = r_{\mathbb{C}}\, \Delta\psi \tag{12}$$

The initial weight of the vehicle is

accurate $$W_o = W_c + W_8 \tag{13}$$

The arrival velocities for altitude versus transfer time were calculated using the sphere-of-influence method and are shown in Figure 1. This method is based on the sphere-of-influence concept, reducing the n-body problem to two 2-body problems. These velocities, though not exact, are sufficient for preliminary calculations.

The velocity expended by a vehicle is the characteristic velocity, or

$$\Delta V = V_{ex} \ln \frac{1}{1 - \zeta} \tag{14}$$

Then the velocity losses are the difference between the characteristic velocity and the change in comparative velocity, or

$$\Delta V_{loss} = \Delta V - \Delta V^* \tag{15}$$

where the comparative velocity is

$$V^* = \sqrt{V_o^2 + 2\mu_{\mathbb{C}}\left(\frac{1}{r} - \frac{1}{r_o}\right)} \tag{16}$$

and the change in comparative velocity during descent from $r = r_o$ to $r = r_f$ is

$$\Delta V^* = \sqrt{V_o^2 + 2\mu_{\mathbb{C}}\left(\frac{1}{r_f} - \frac{1}{r_o}\right)} - V_f \tag{17}$$

By substituting an original equation for velocity losses

$$\Delta V_{loss} = V_{ex} \ln\left(\frac{1}{1 - \zeta}\right) - \sqrt{V_o^2 + 2\mu_{\mathbb{C}}\left(\frac{1}{r_f} - \frac{1}{r_o}\right)} - V_f \tag{18}$$

The undisturbed Keplerian true anomaly at initiation of powered descent is

$$\nu_o = \cos^{-1}\left[\frac{(V_a r_a)^2/\mu_{\mathbb{C}} - r_o}{r_o\sqrt{\left(1 - \frac{V_o^2 r_o}{\mu_{\mathbb{C}}}\right)\left(2 - \frac{V_o^2 r_o}{\mu_{\mathbb{C}}}\right)\sin^2 \vartheta_o}}\right] \tag{19}$$

SECTION IV. RESULTS AND CONCLUSIONS

The results of this analysis are shown in Figures 2 through 23, separated according to pericenter and parking orbit altitudes. For convenience, most variables are shown as a function of initial vehicle thrust-to-weight ratio. All variables for the braking maneuvers are plotted for 50-, 60-, and 72-hour earth-lunar transfer times and specific impulses of 300 and 420 seconds. These specific impulses are representative of present day storable and cryogenic stages.

A. BRAKE TO LUNAR ORBIT

The time of initiation of burning prior to Keplerian pericenter is shown in Figure 2. The characteristic velocity required to brake to lunar orbit is shown in Figure 3 and the corresponding stage propellant mass fraction is shown in Figures 4a through 4d. The change in other parameters for braking to orbit are shown in Figures 5 through 8.

Figures 9a and 9b show the velocity losses due to gravity for the braking maneuver. Beyond an earth thrust-to-weight ratio of 0.4, these gravity losses are small and considered to zero. It should be noted that these losses are the difference between characteristic and change in comparative velocities during burning, i.e., true gravity losses.

The characteristic impulse velocity, shown in Figure 14, is the velocity necessary to attain a transfer ellipse from a circular parking orbit altitude. The apocenter altitude of the transfer ellipse is assumed to be circular parking orbit altitude and the pericenter altitude is 10 kilometers in all instances. Since losses were negligible, an impulsive velocity was assumed.

B. DESCENT TO LUNAR SURFACE

The characteristic velocity for descent to 300 meters above the lunar surface is shown in Figures 15a and 15b for specific impulses of 300 and 420 seconds, respectively. The corresponding propellant mass fraction is shown in Figures 16a and 16b.

Figures 17a and 17b show the altitude change, Δh, during powered descent for specific impulses of 300 sec and 420 sec, respectively. A limit is reached, for a gravity turn ($\alpha = 180°$), when the altitude change

becomes equal to the apocenter altitude. This limit determines the minimum initial thrust-to-weight ratio for continuous burn from parking orbit to 300 meters above the surface. This limit is reflected in the change in flight path angle, $\Delta\vartheta$ (Figures 18a and 18b), when $\Delta\vartheta = 90°$.

The change in central angle, $\Delta\psi$ (angular range), during powered descent is given in Figures 19a and 19b. The product of $\Delta\psi$ (in radians) and the mean lunar radius is the surface range and is shown in Figures 20a and 20b. The limit shown for $\Delta\psi$ and S is reached when powered descent is initiated at apocenter.

The true anomaly, ν_o, shown in Figures 21a and 21b, is measured from the undisturbed Keplerian pericenter radius to the radius at initiation of powered descent. True anomaly equals 180° for the limit of minimum thrust-to-weight ratio. Burning times for the powered descent are given in Figures 12a, 12b, 12c, and 12d. The true gravity losses are shown in Figures 13a and 13b. Burning times and gravity losses are a maximum in the limiting case.

SECTION V. GRAPHIC PRESENTATIONS

BRAKE TO LUNAR ORBIT

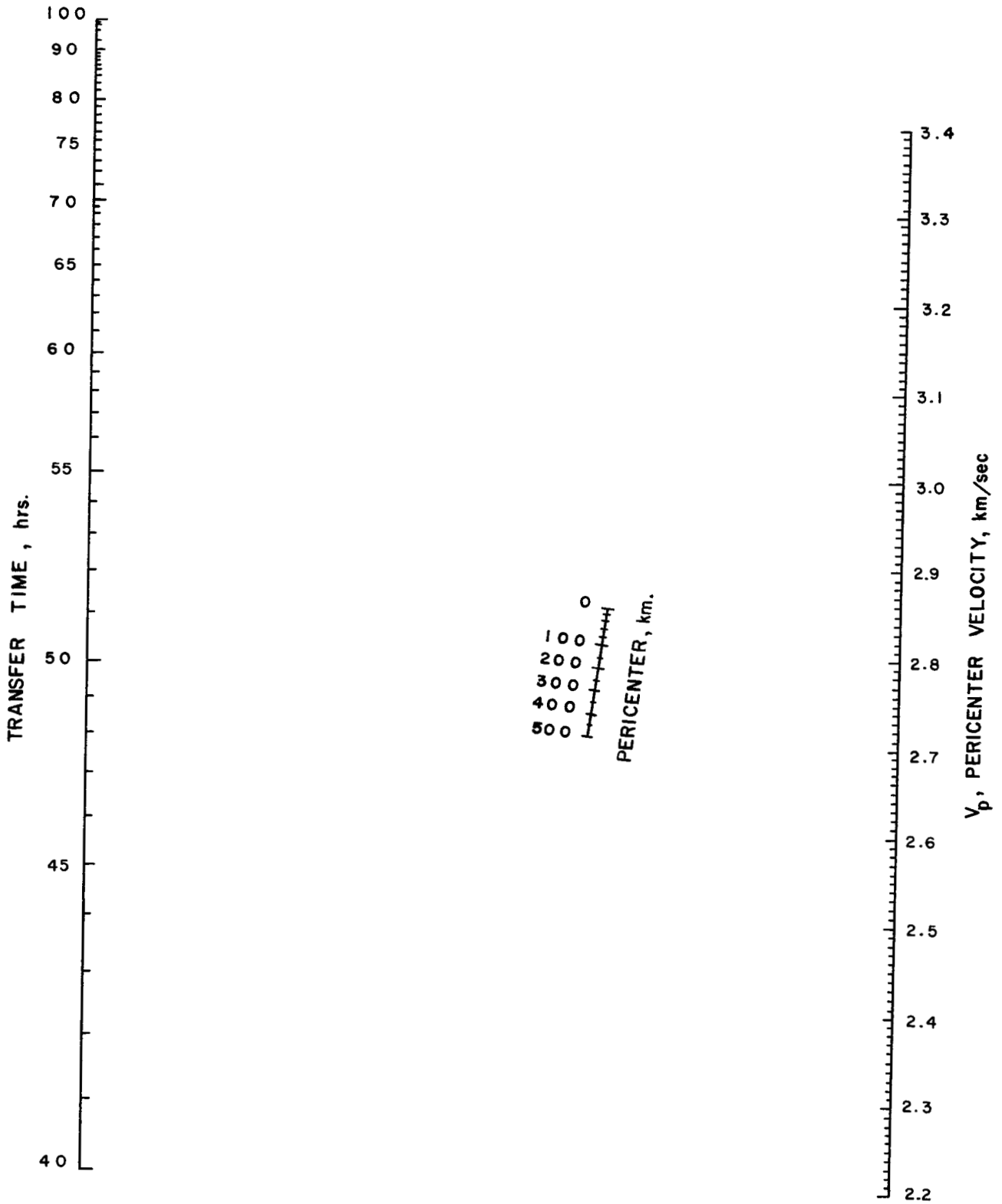

FIGURE 1. PERICENTER VELOCITY FOR EARTH-LUNAR TRANSFER.

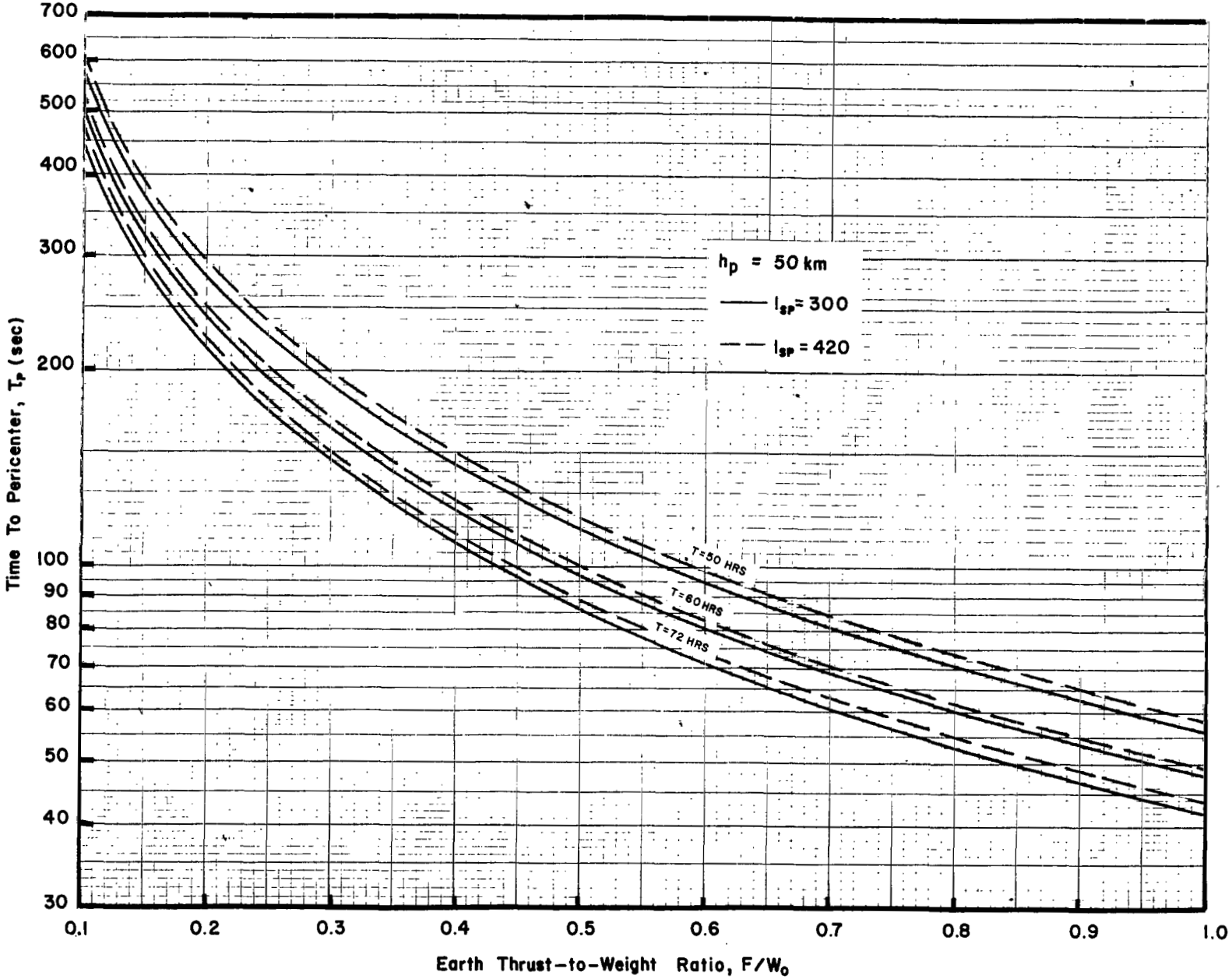

FIGURE 2a. TIME TO PERICENTER FOR BRAKE TO LUNAR ORBIT - h_p = 50 km.

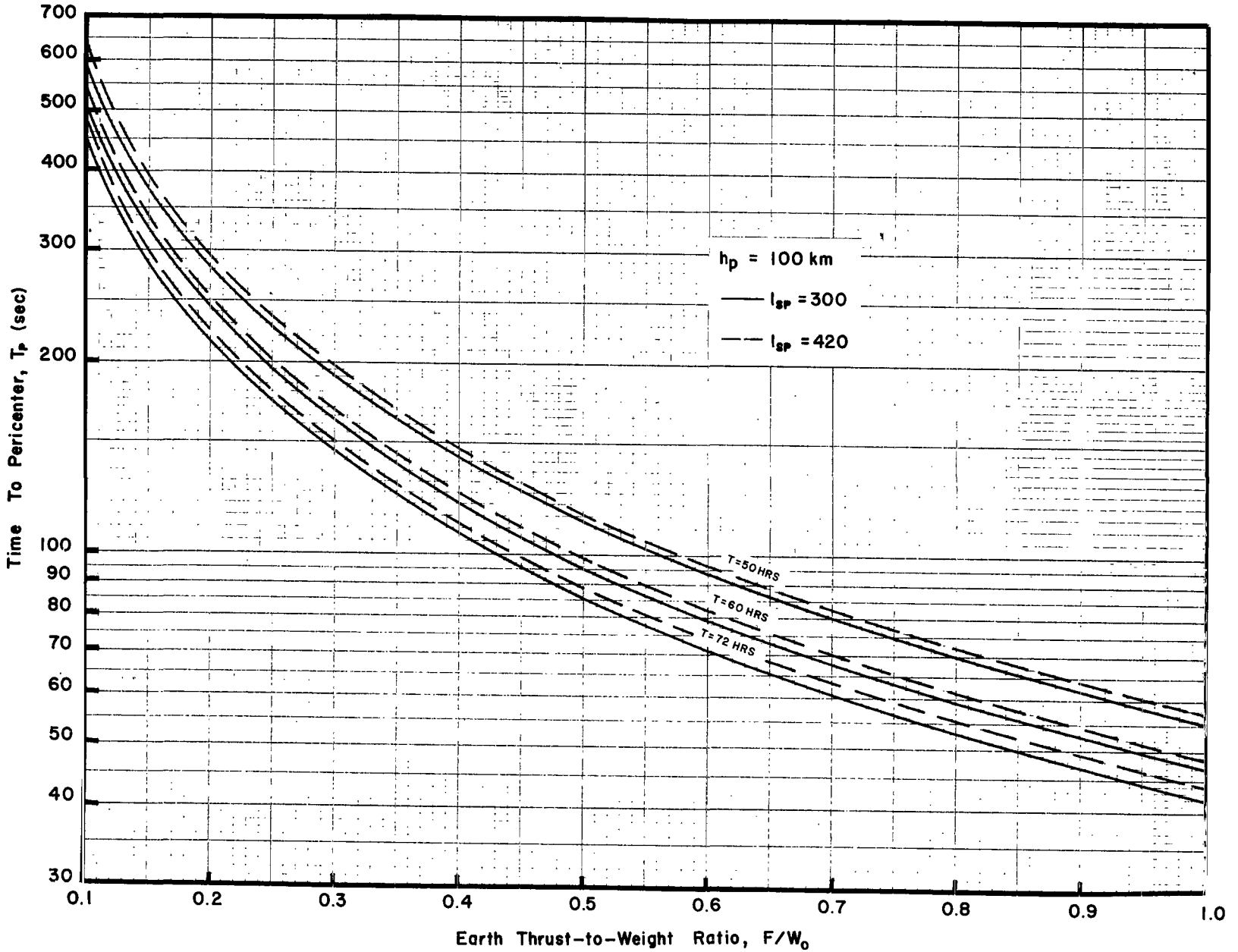

FIGURE 2b. TIME TO PERICENTER FOR BRAKE TO LUNAR ORBIT - h_p = 100 km.

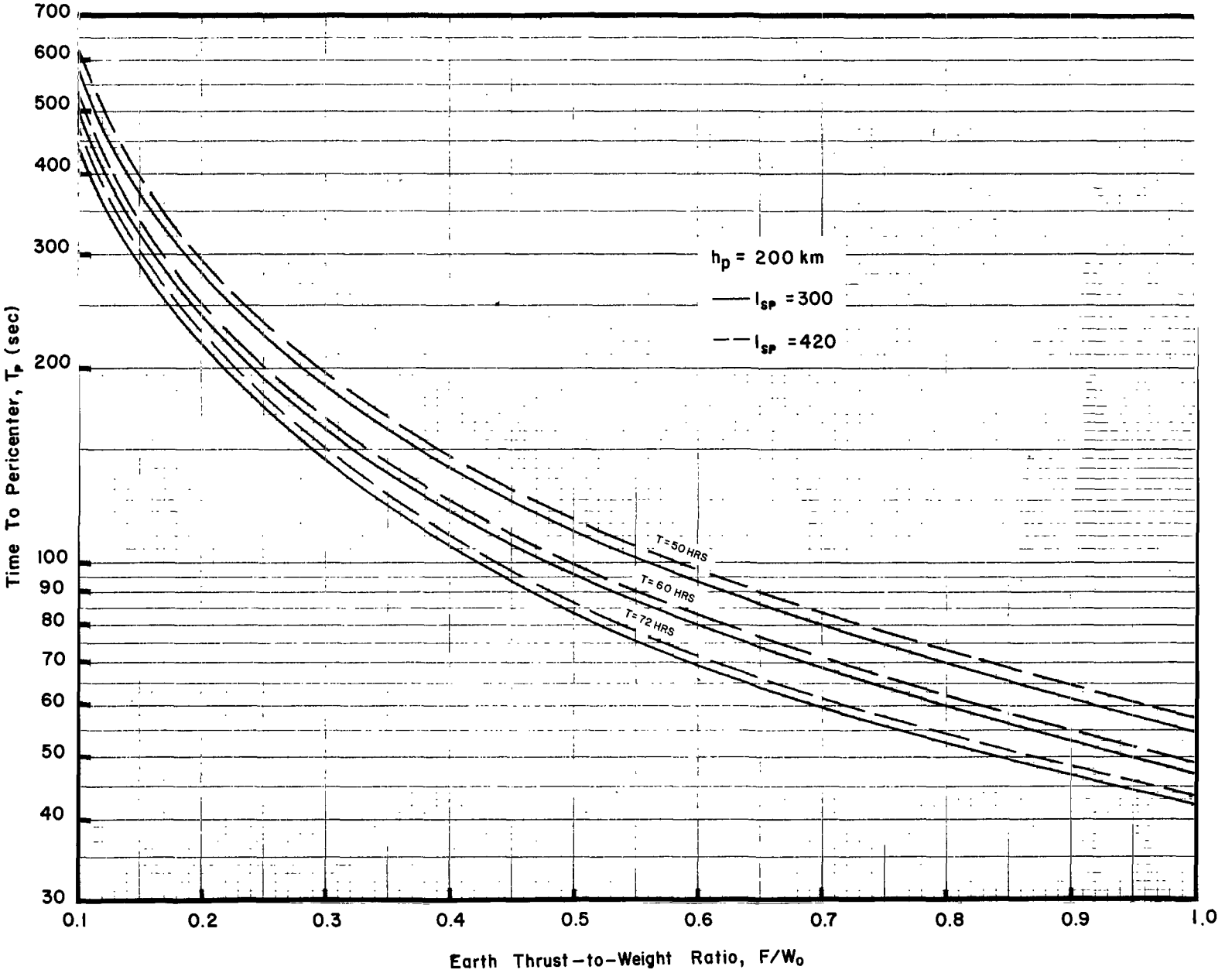

FIGURE 2c. TIME TO PERICENTER FOR BRAKE TO LUNAR ORBIT - h_p = 200 km.

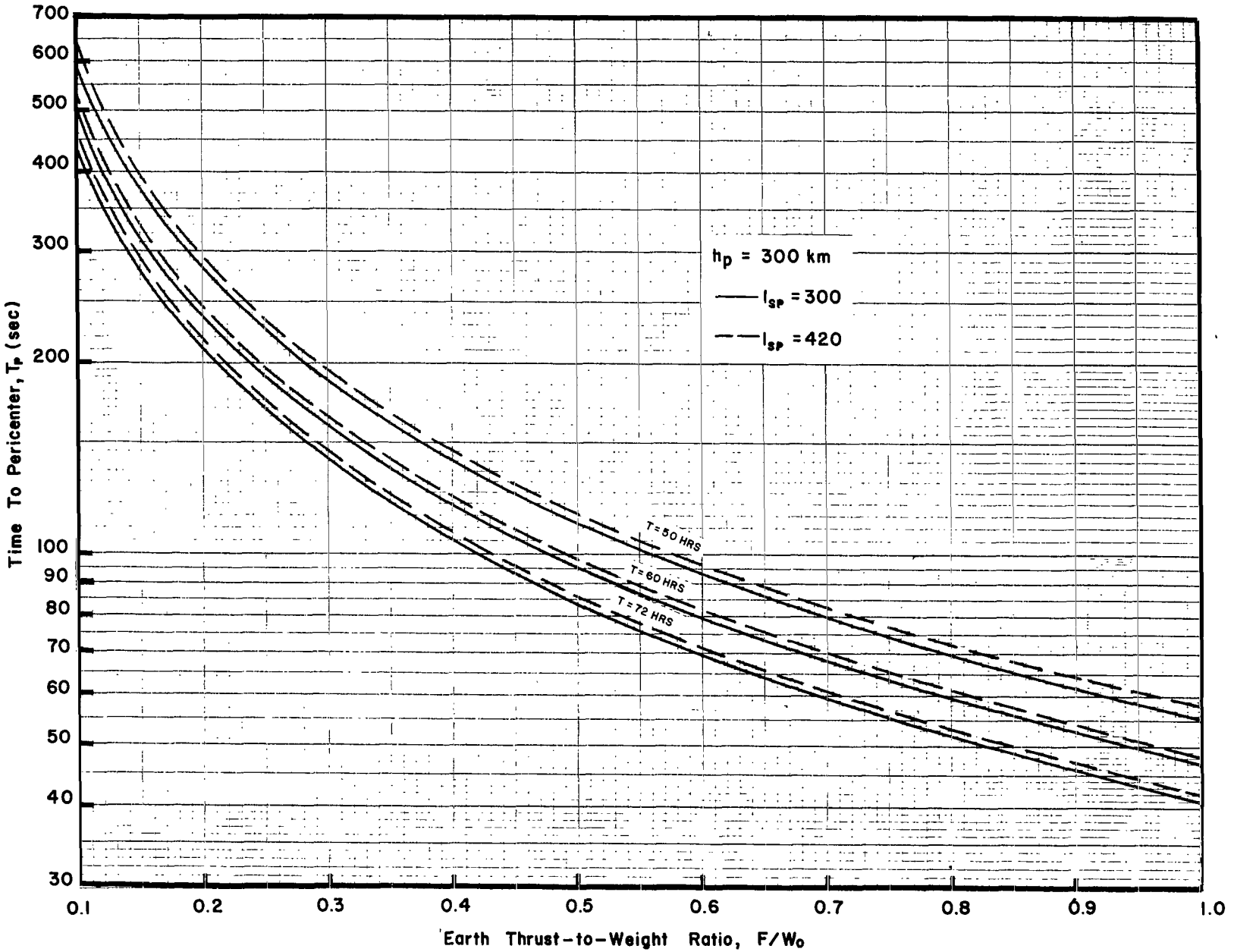

FIGURE 2d. TIME TO PERICENTER FOR BRAKE TO LUNAR ORBIT - h_p = 300 km.

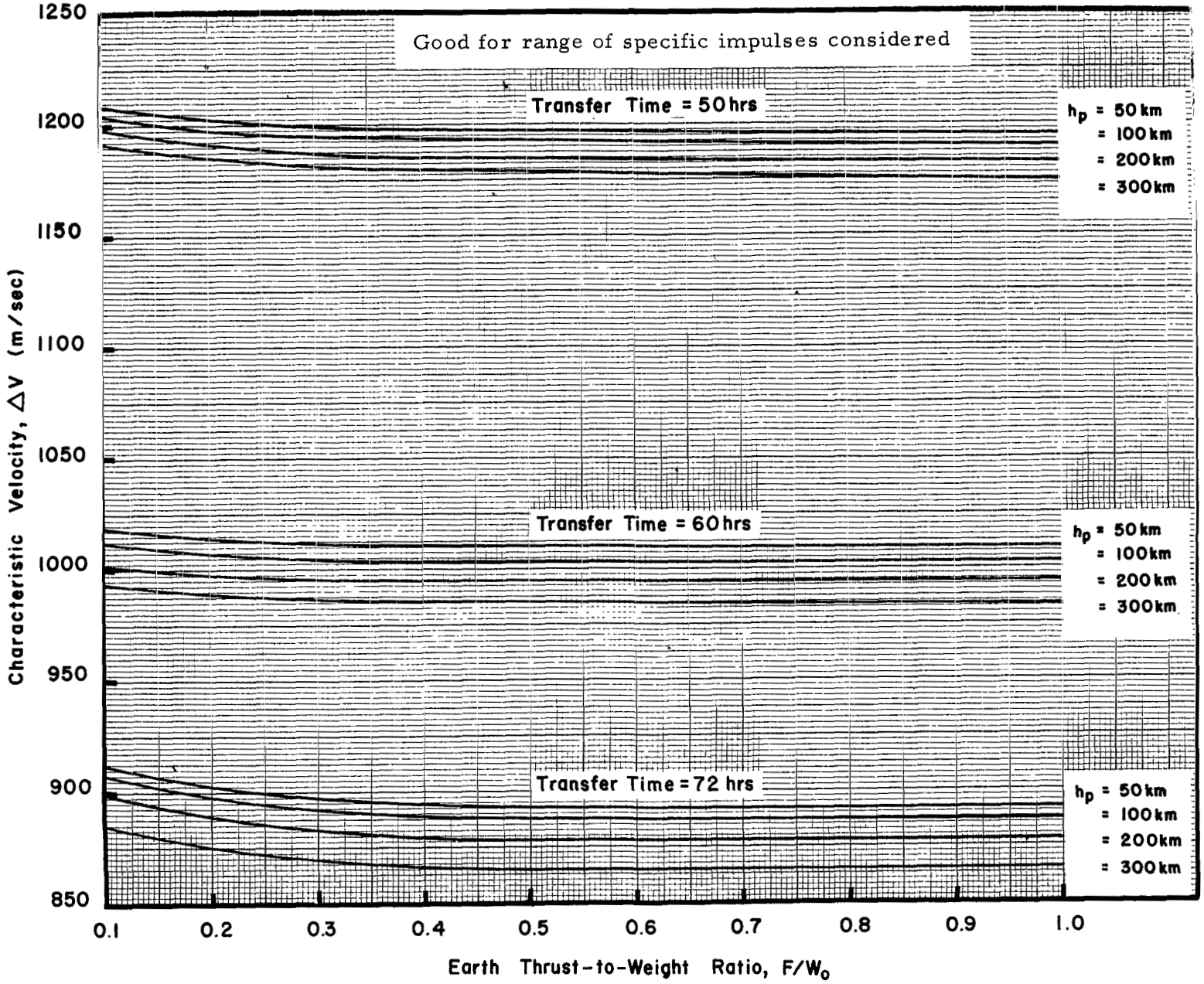

FIGURE 3. CHARACTERISTIC VELOCITY FOR BRAKE TO LUNAR ORBIT.

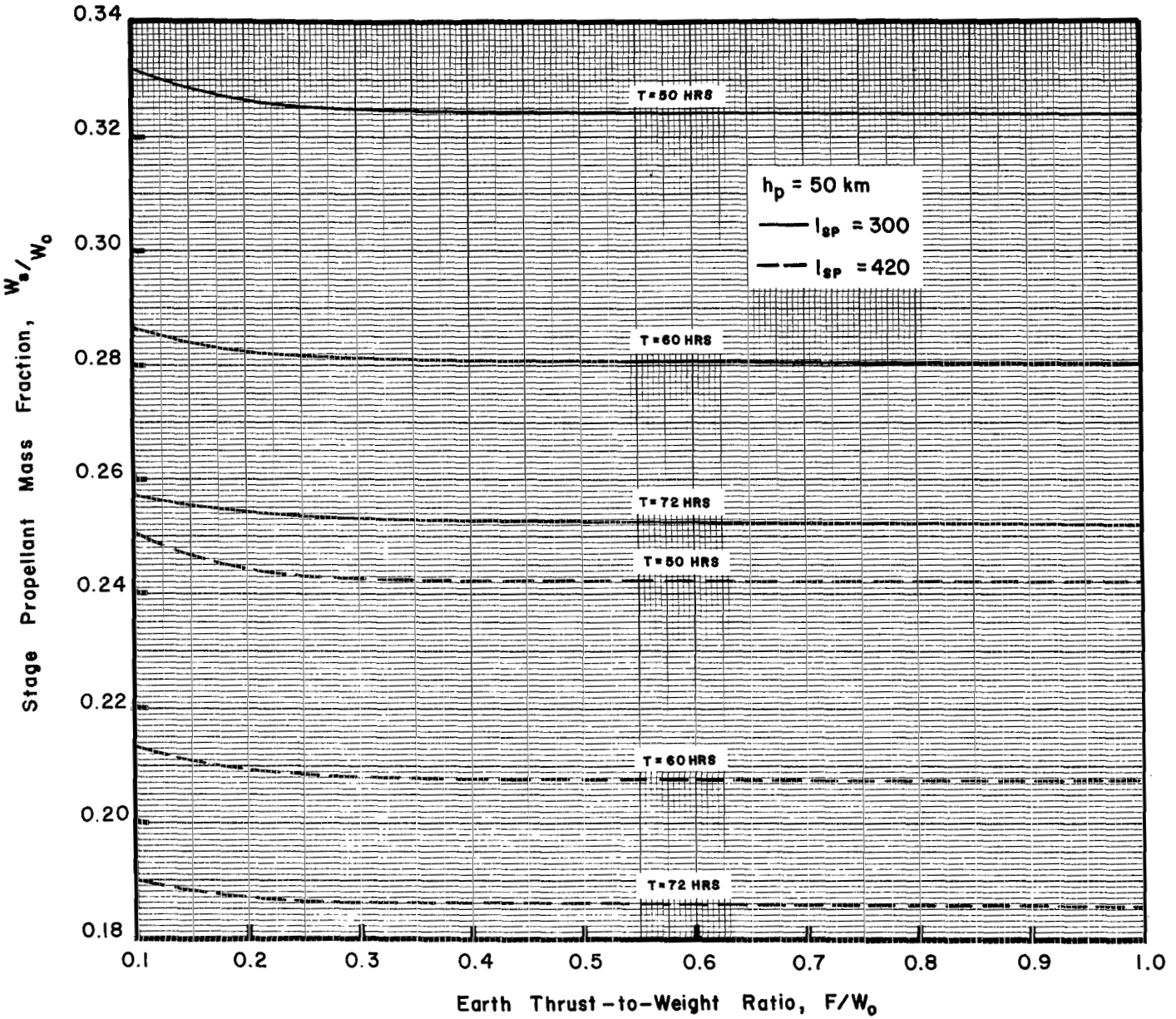

FIGURE 4a. STAGE PROPELLANT MASS FRACTION FOR BRAKE TO LUNAR ORBIT - h_p = 50 km.

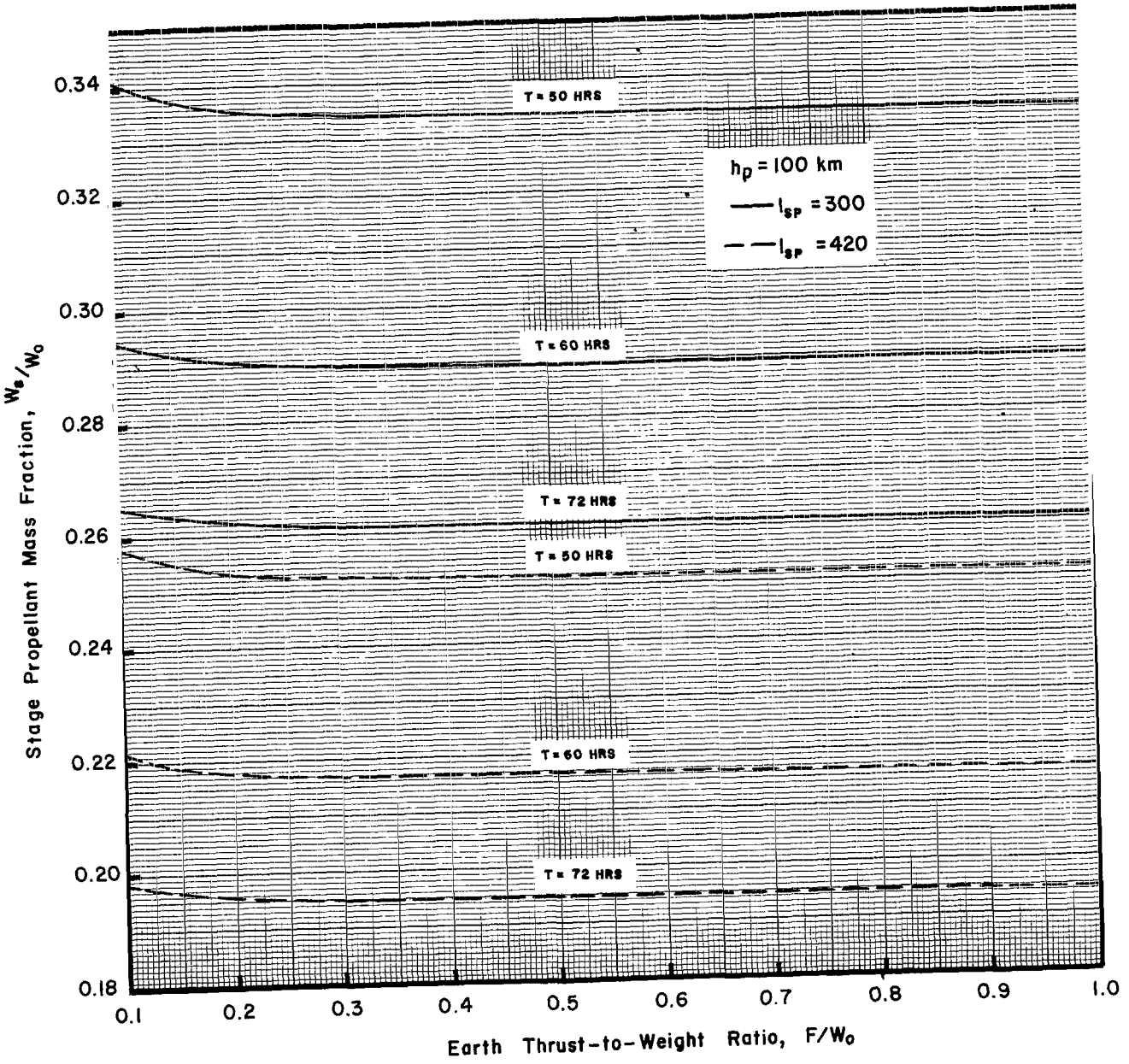

FIGURE 4b. STAGE PROPELLANT MASS FRACTION FOR BRAKE TO LUNAR ORBIT - h_p = 100 km

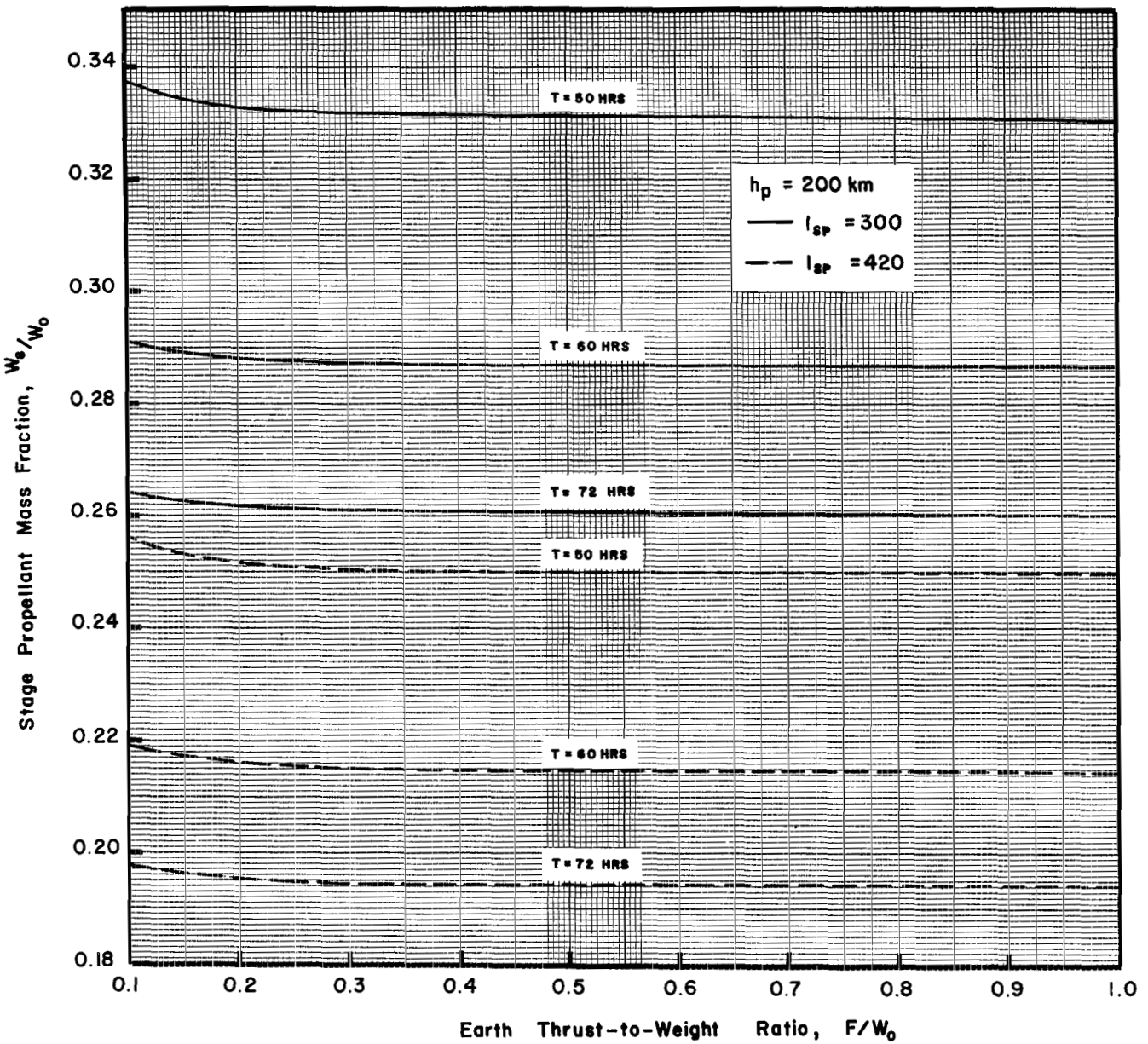

FIGURE 4c. STAGE PROPELLANT MASS FRACTION FOR BRAKE TO LUNAR ORBIT - h_p = 200 km.

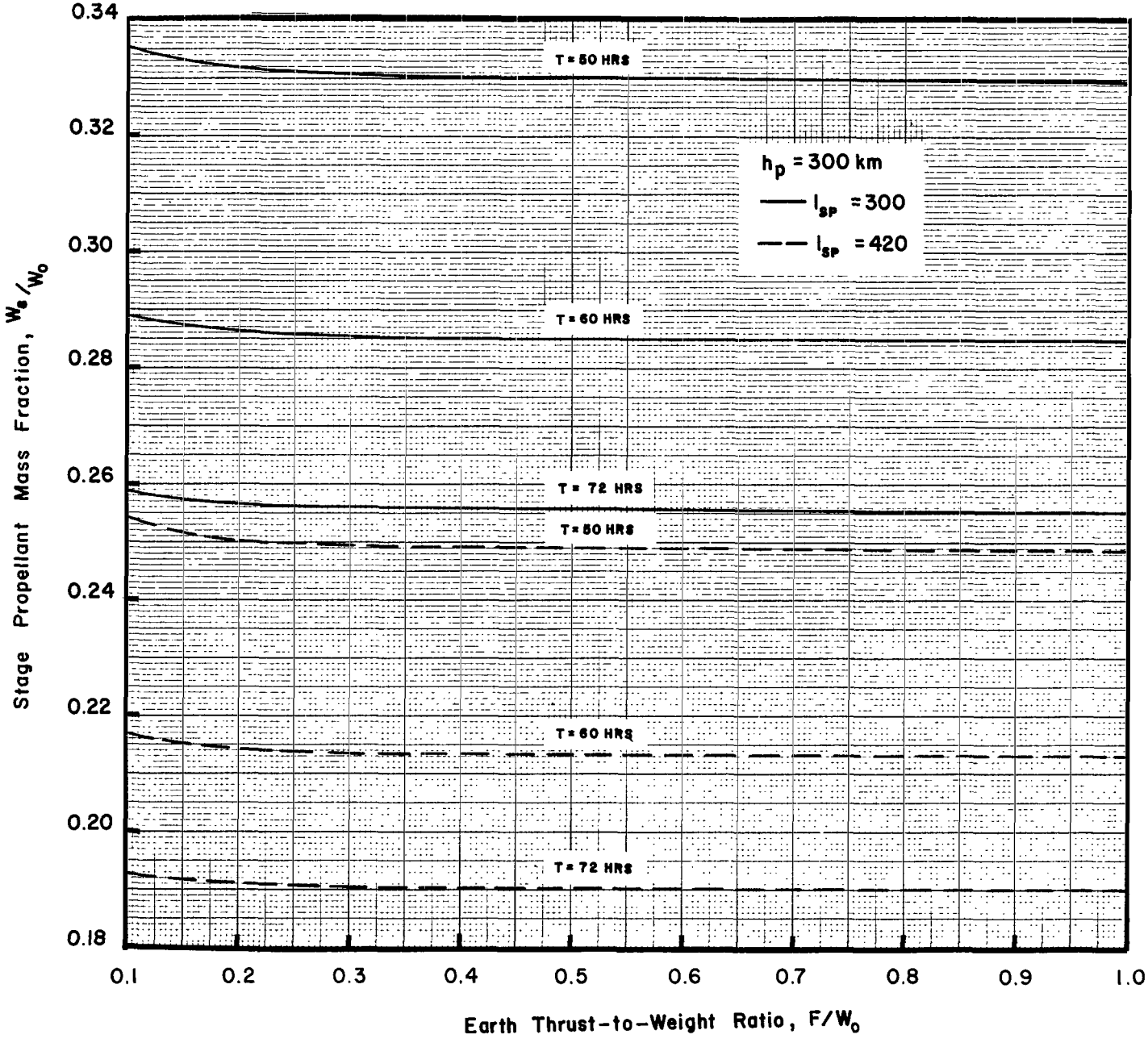

FIGURE 4d. STAGE PROPELLANT MASS FRACTION FOR BRAKE TO LUNAR ORBIT - h_p = 300 km.

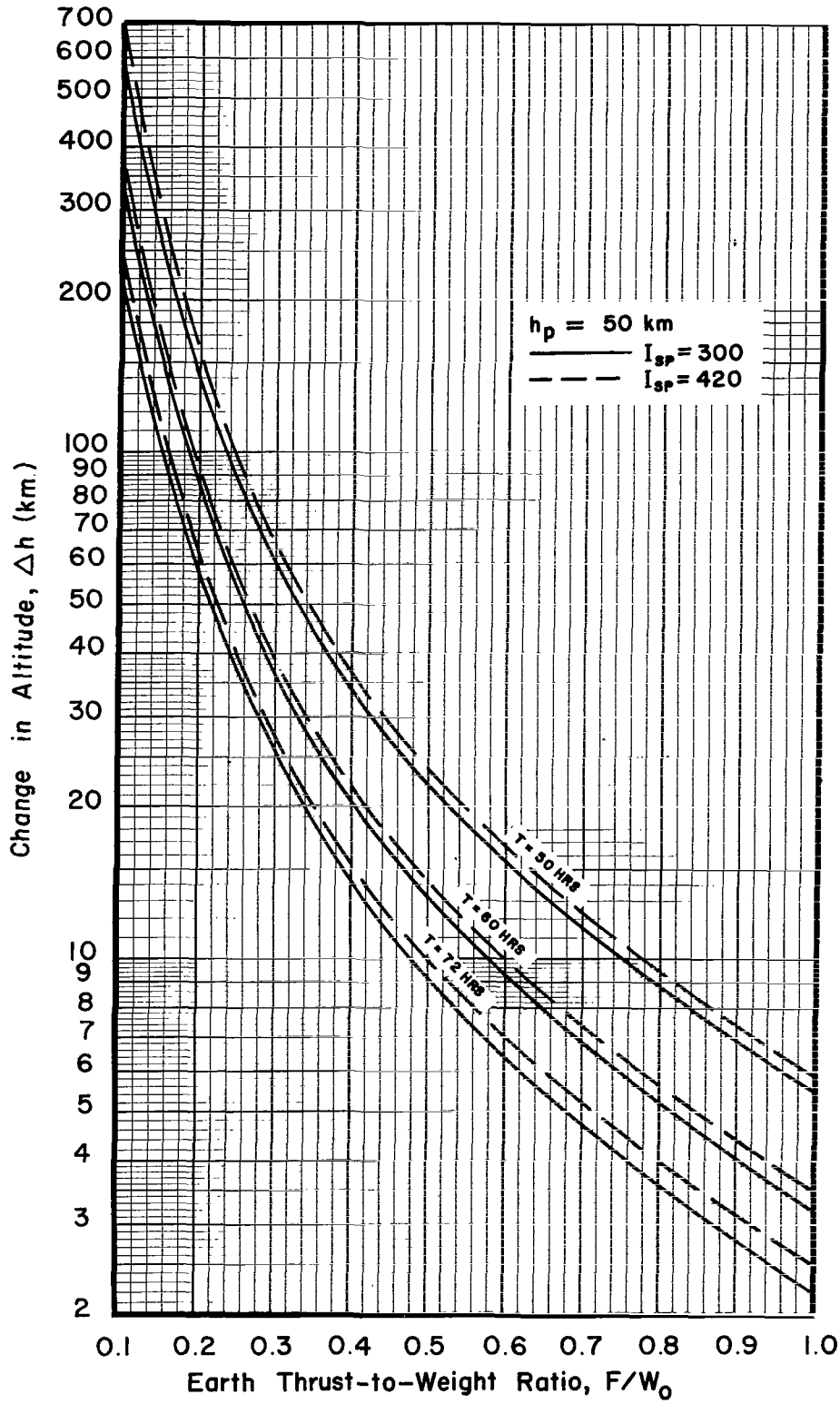

FIGURE 5a. CHANGE IN ALTITUDE FOR BRAKE TO LUNAR ORBIT - h_p = 50 km.

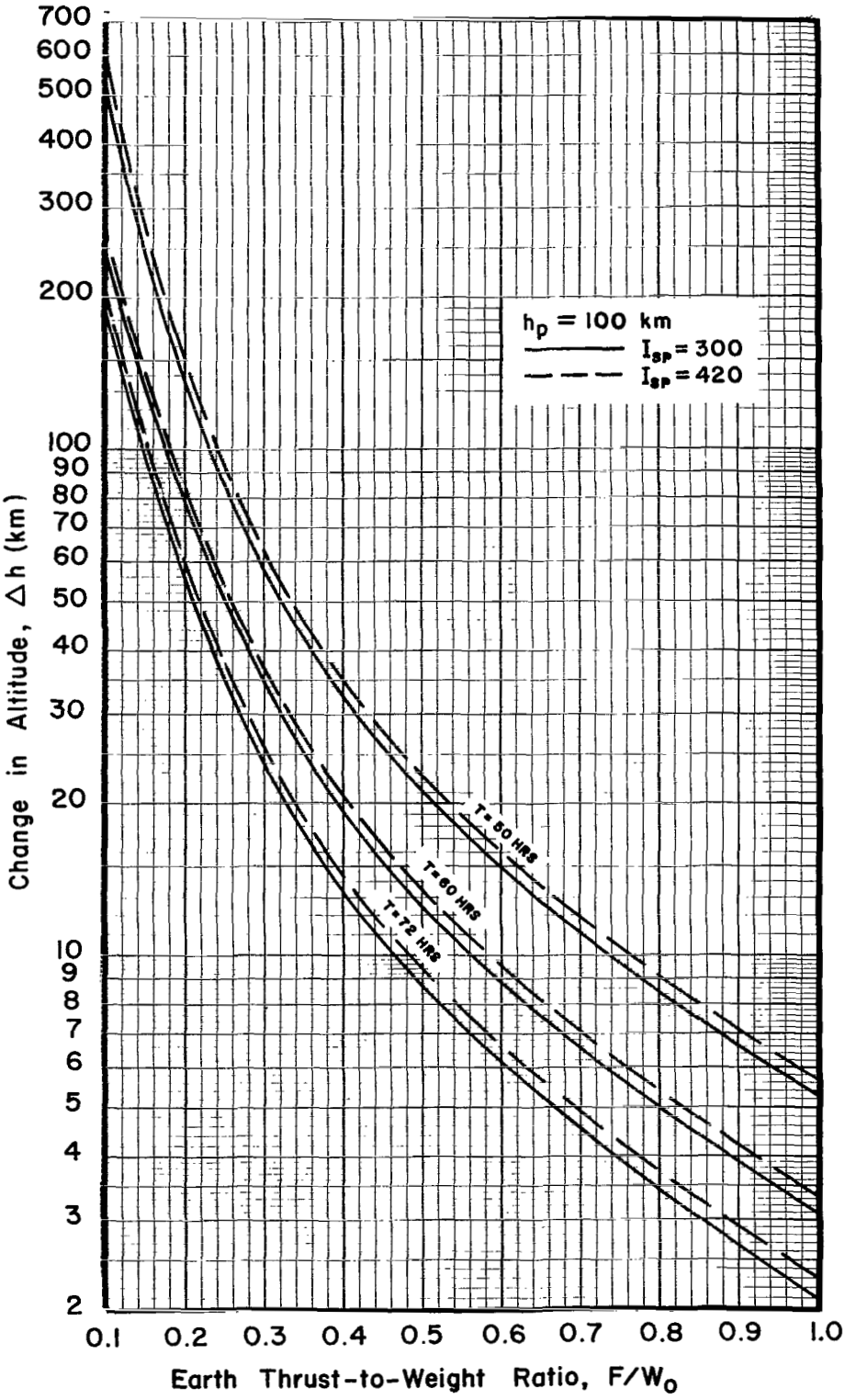

FIGURE 5b. CHANGE IN ALTITUDE FOR BRAKE TO LUNAR ORBIT - h_p = 100 km.

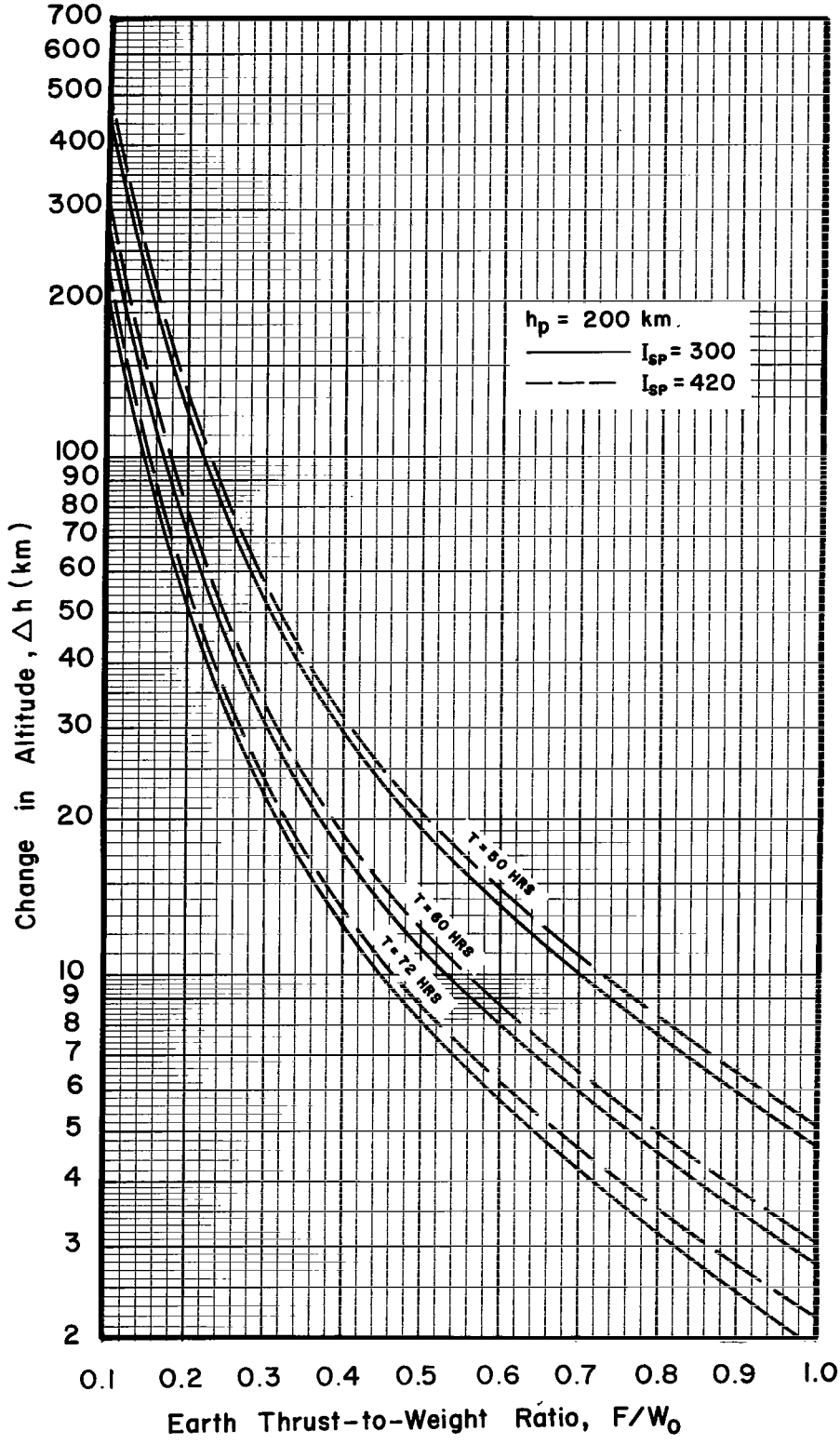

FIGURE 5c. CHANGE IN ALTITUDE FOR BRAKE TO LUNAR ORBIT - h_p = 200 km.

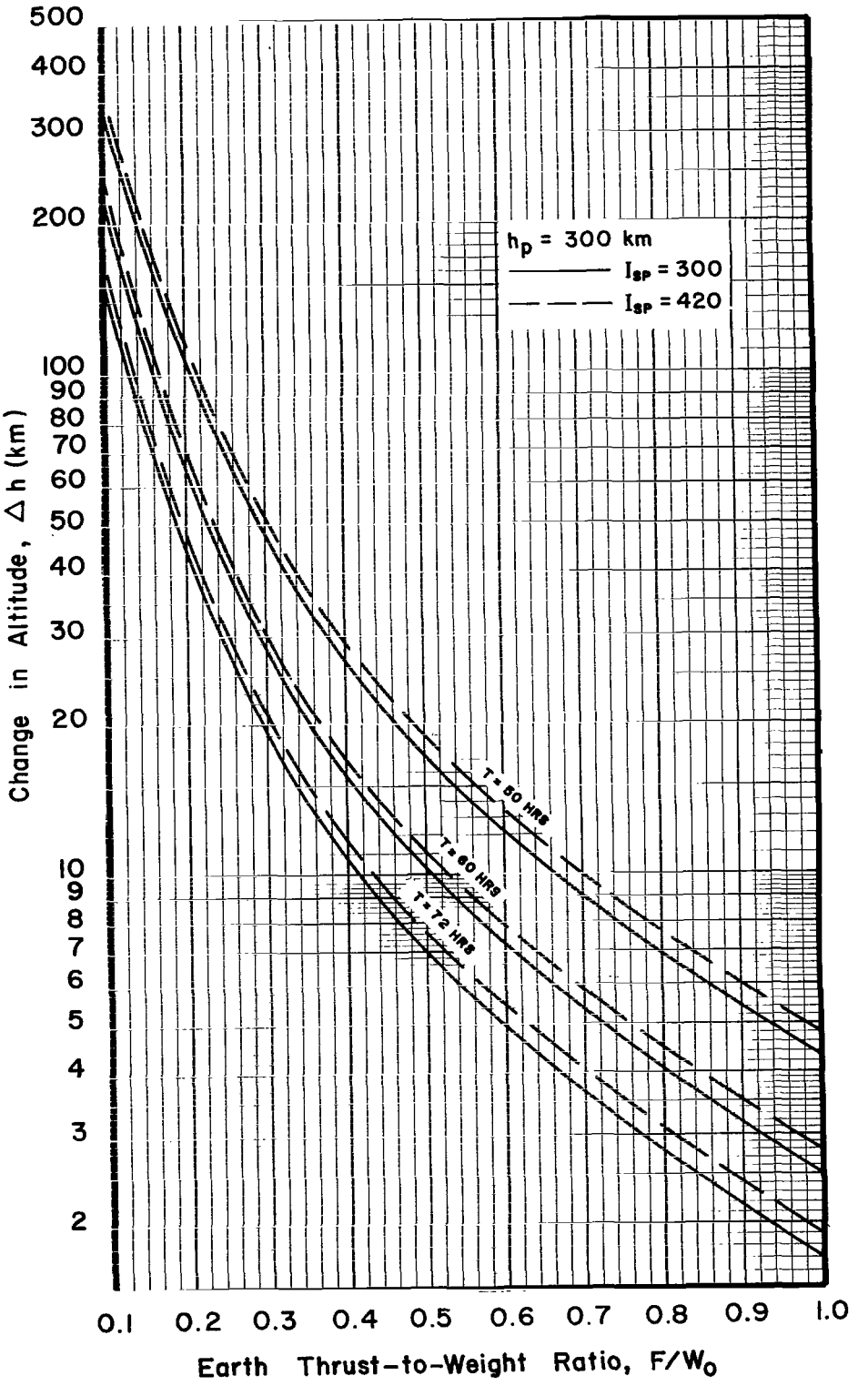

FIGURE 5d. CHANGE IN ALTITUDE FOR BRAKE TO LUNAR ORBIT - h_p = 300 km.

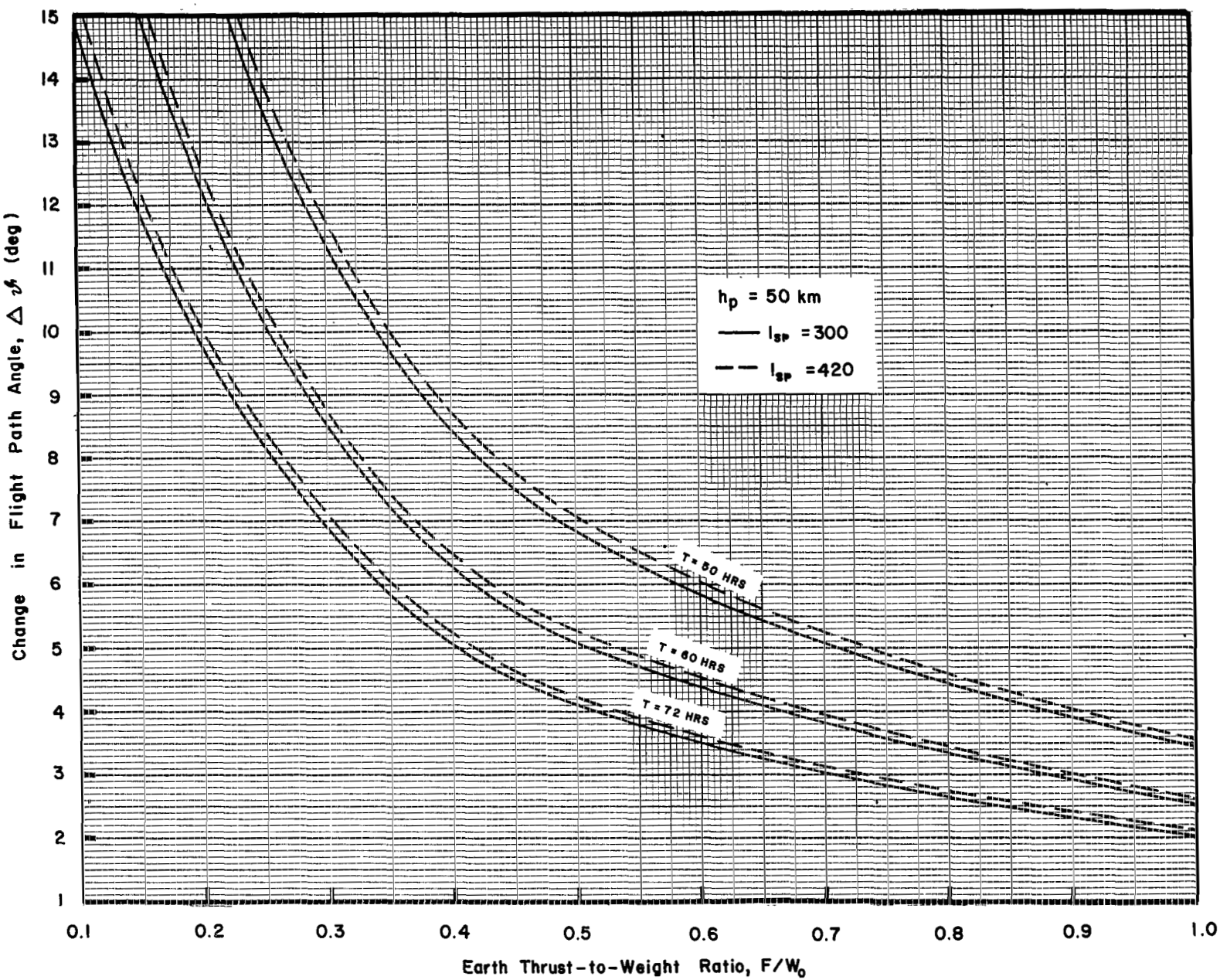

FIGURE 6a. CHANGE IN FLIGHT PATH ANGLE FOR BRAKE TO LUNAR ORBIT - h_p = 50 km

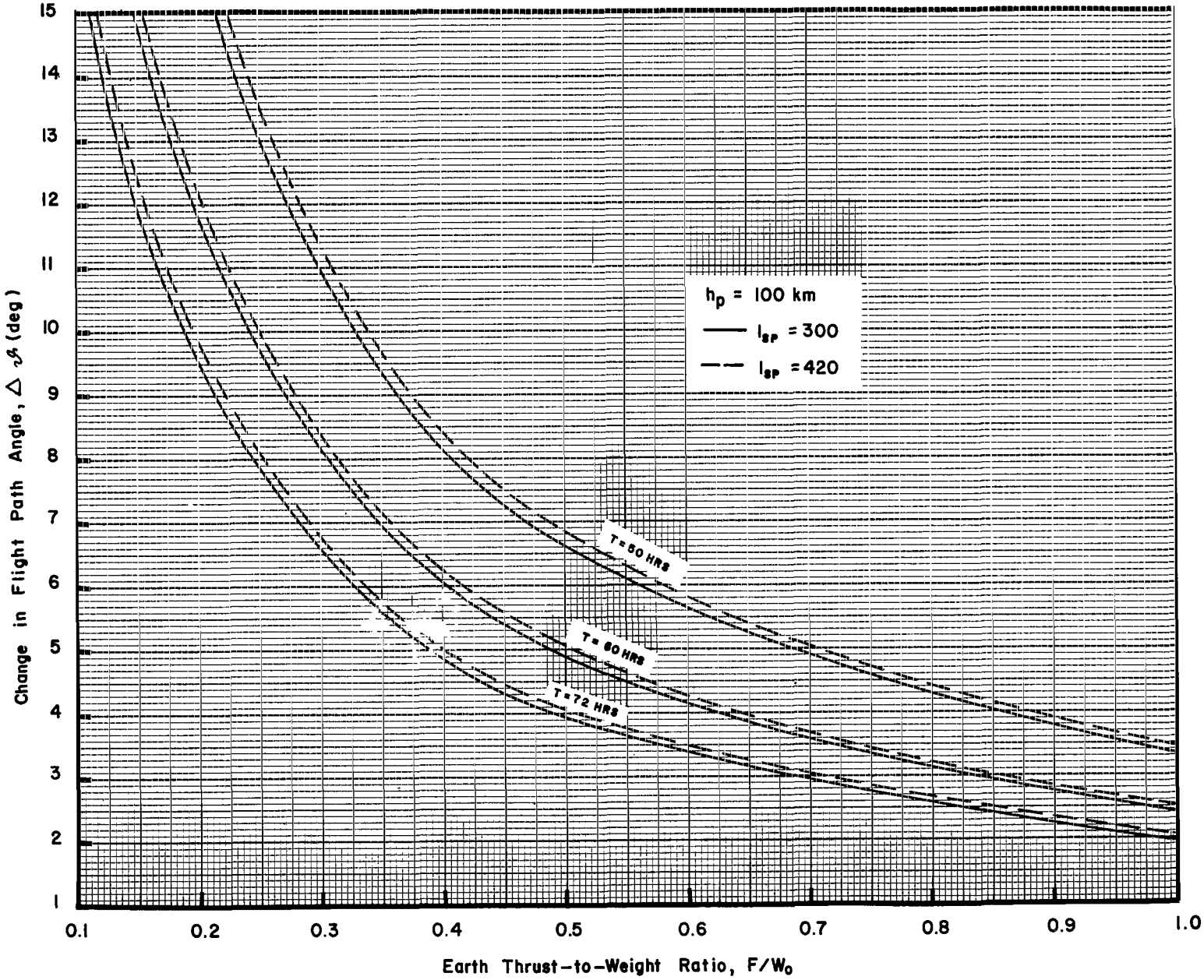

FIGURE 6b. CHANGE IN FLIGHT PATH ANGLE FOR BRAKE TO LUNAR ORBIT - h_p = 100 km

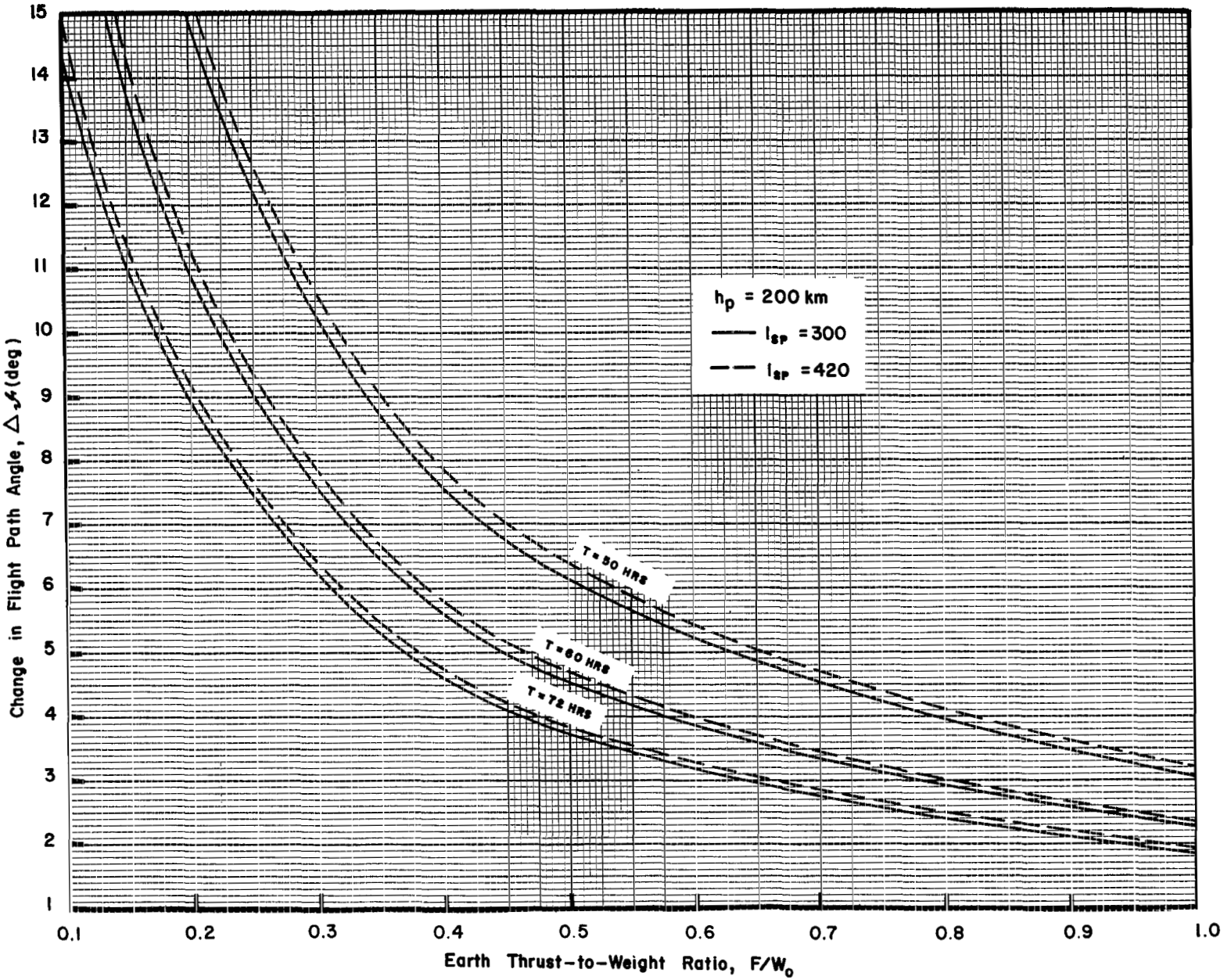

FIGURE 6c. CHANGE IN FLIGHT PATH ANGLE FOR BRAKE TO LUNAR ORBIT - h_p = 200 km

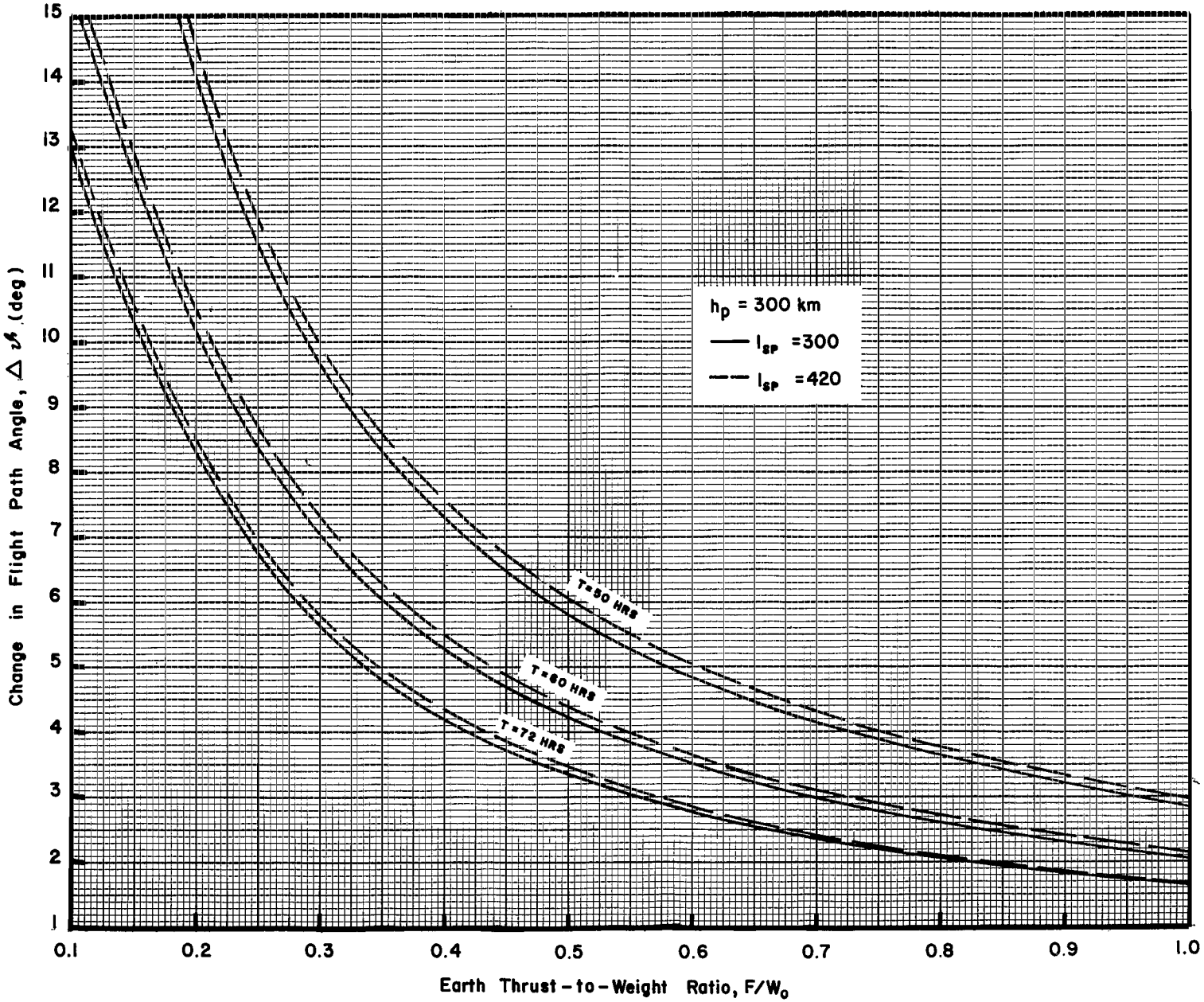

FIGURE 6d. CHANGE IN FLIGHT PATH ANGLE FOR BRAKE TO LUNAR ORBIT - h_p = 300 km.

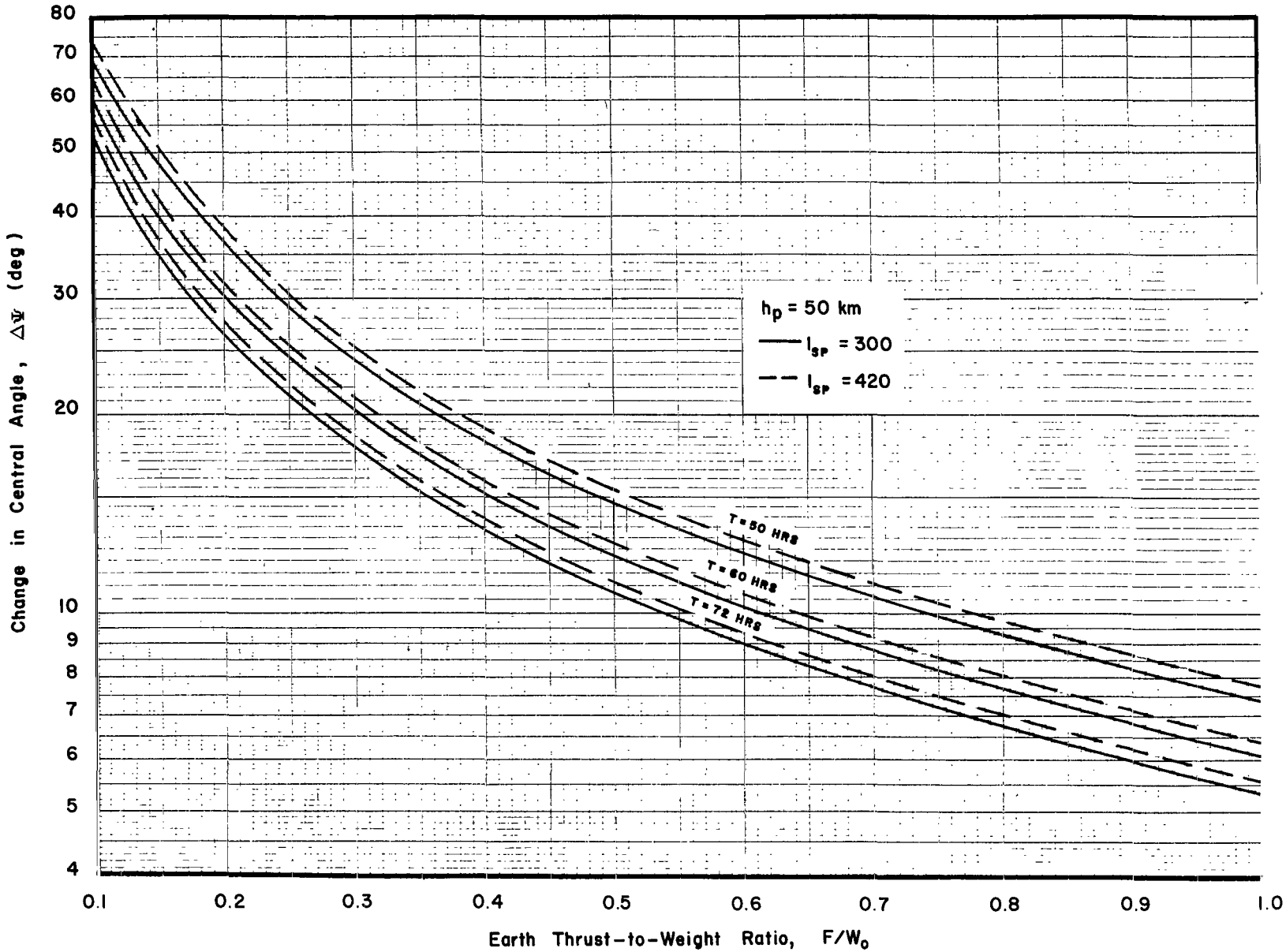

FIGURE 7a. CHANGE IN CENTRAL ANGLE FOR BRAKE TO LUNAR ORBIT - h_p = 50 km

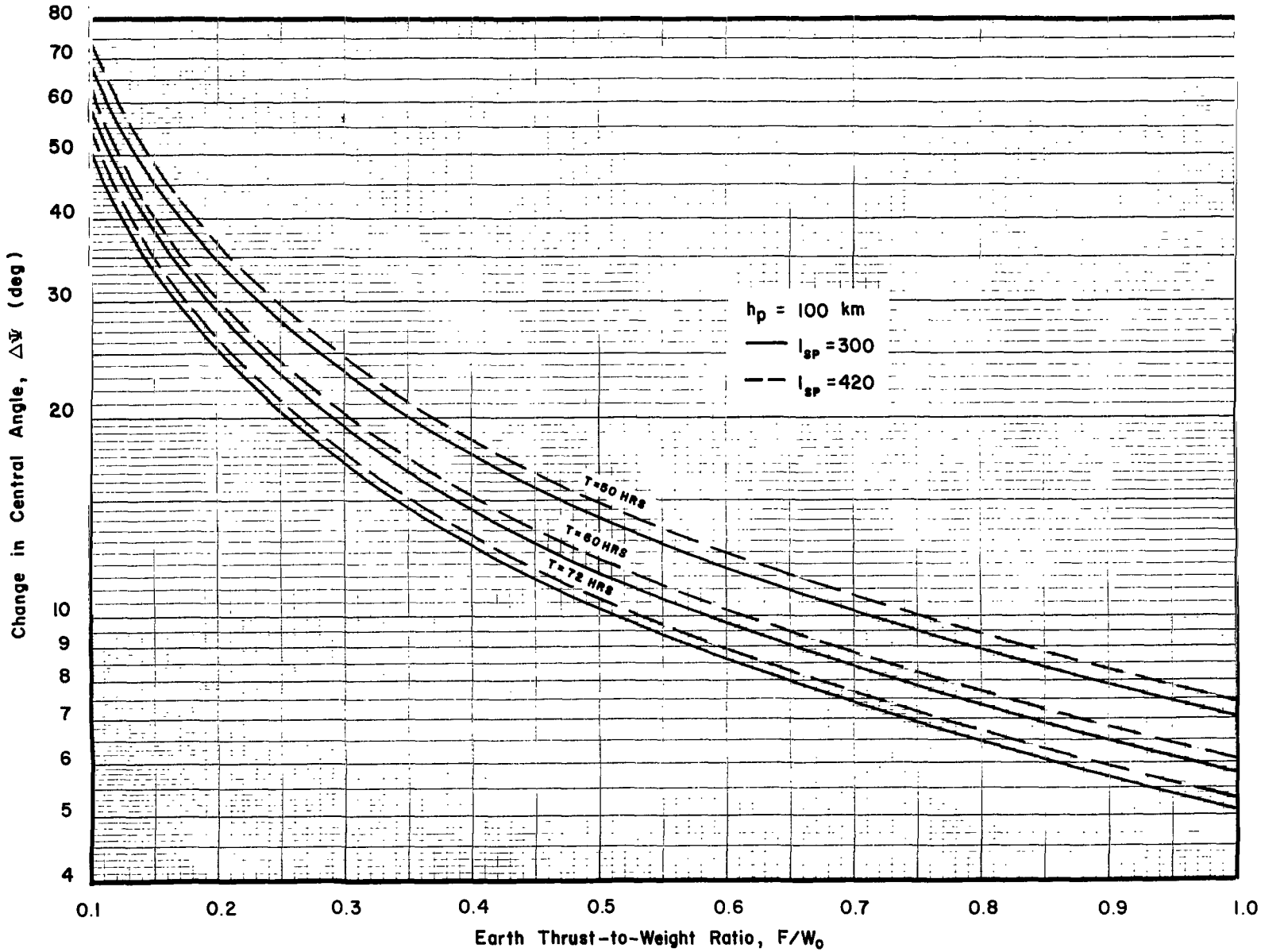

FIGURE 7b. CHANGE IN CENTRAL ANGLE FOR BRAKE TO LUNAR ORBIT - h_p = 100 km.

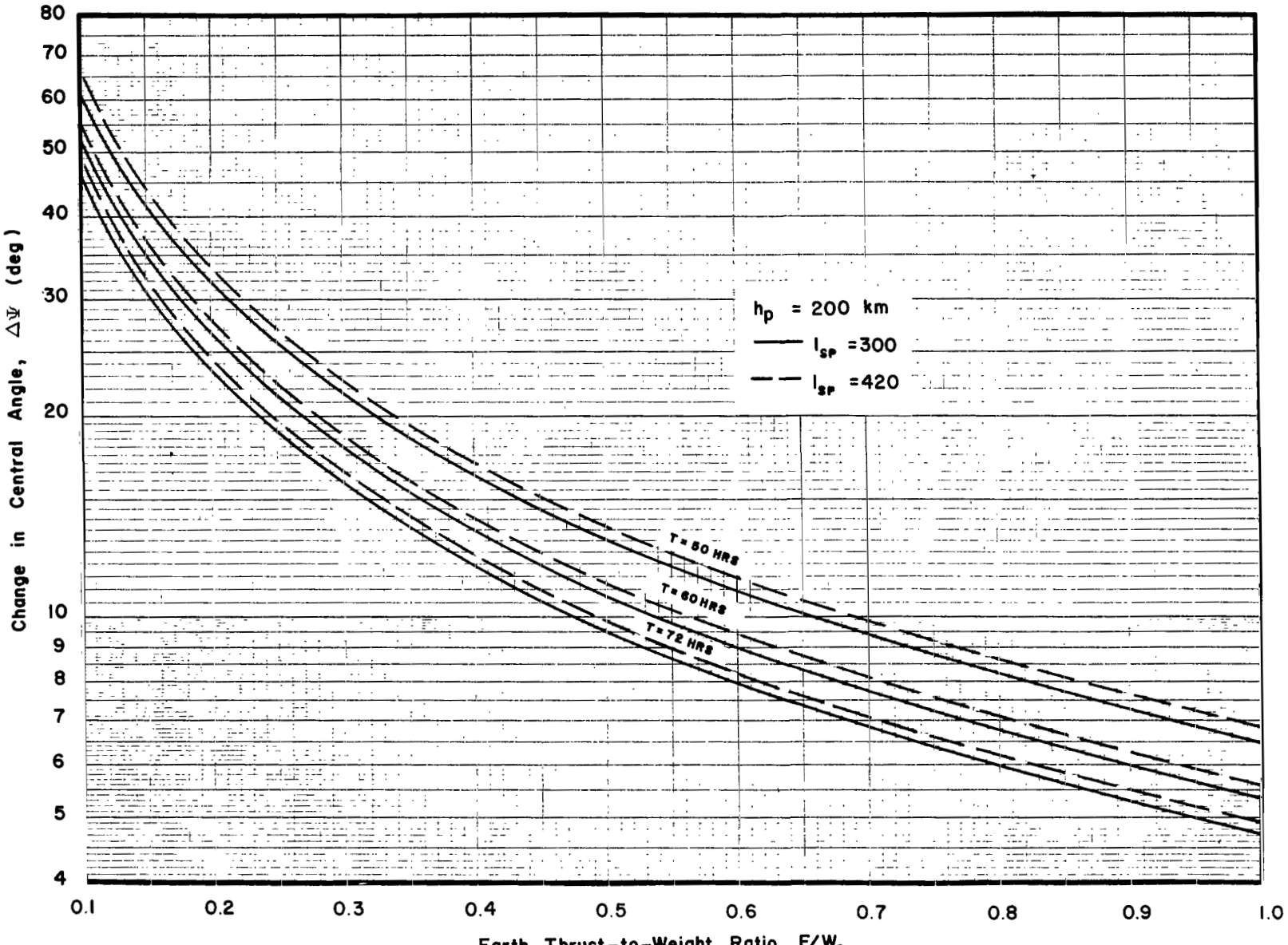

FIGURE 7c. CHANGE IN CENTRAL ANGLE FOR BRAKE TO LUNAR ORBIT - h_p = 200 km

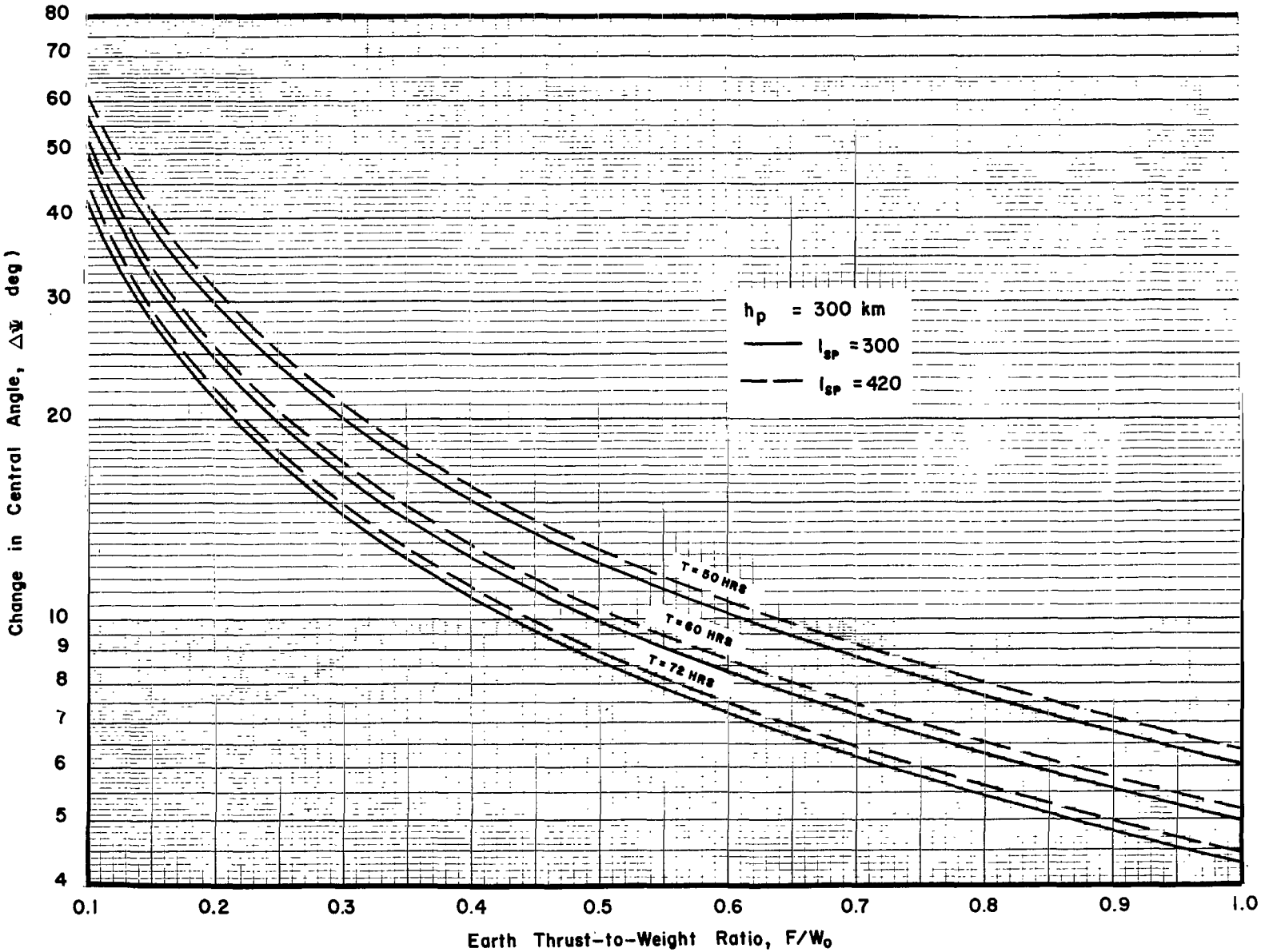

FIGURE 7d. CHANGE IN CENTRAL ANGLE FOR BRAKE TO LUNAR ORBIT - h_p = 300 km

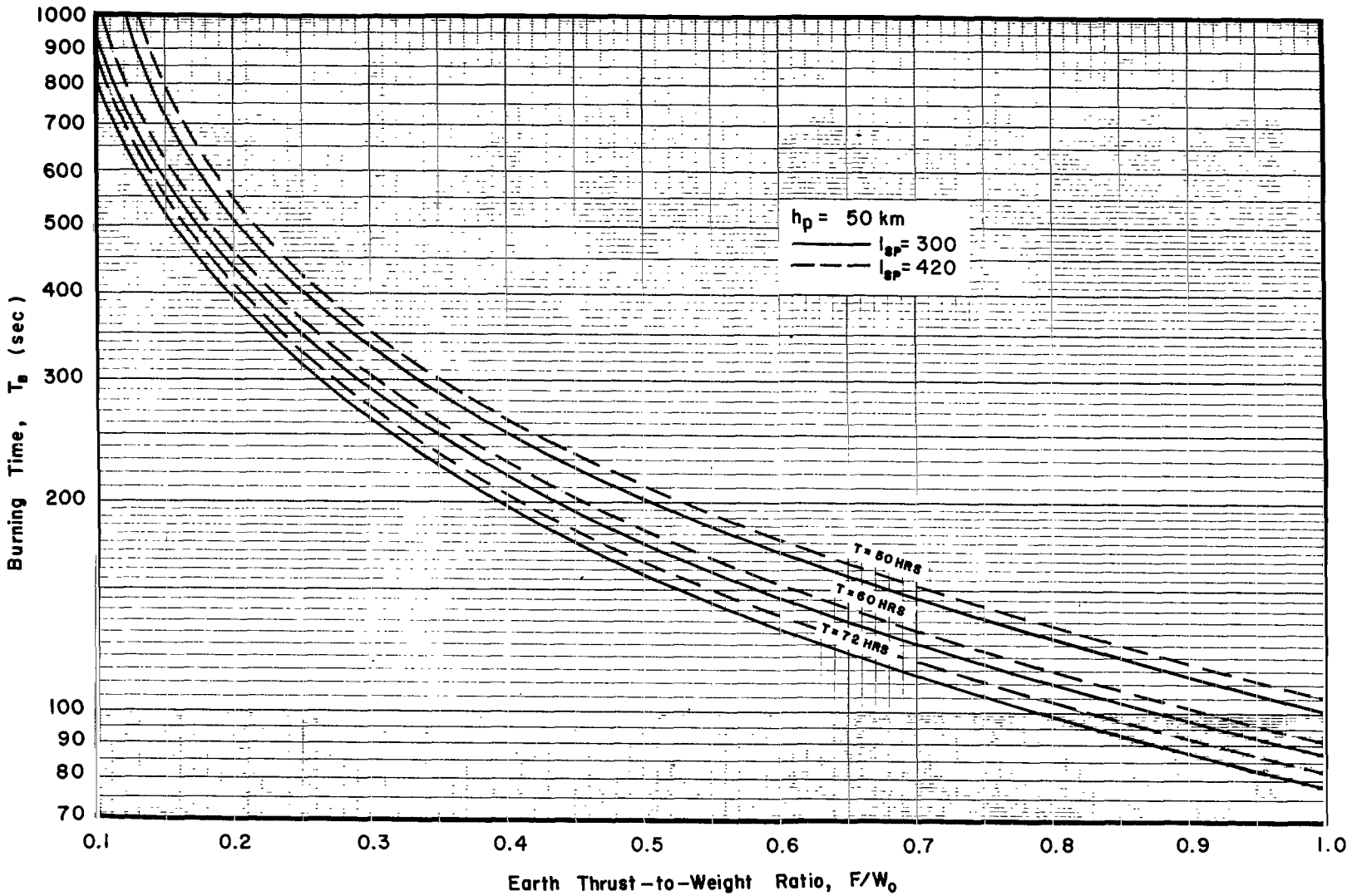

FIGURE 8a. BURNING TIME FOR BRAKE TO LUNAR ORBIT - h_p = 50 km.

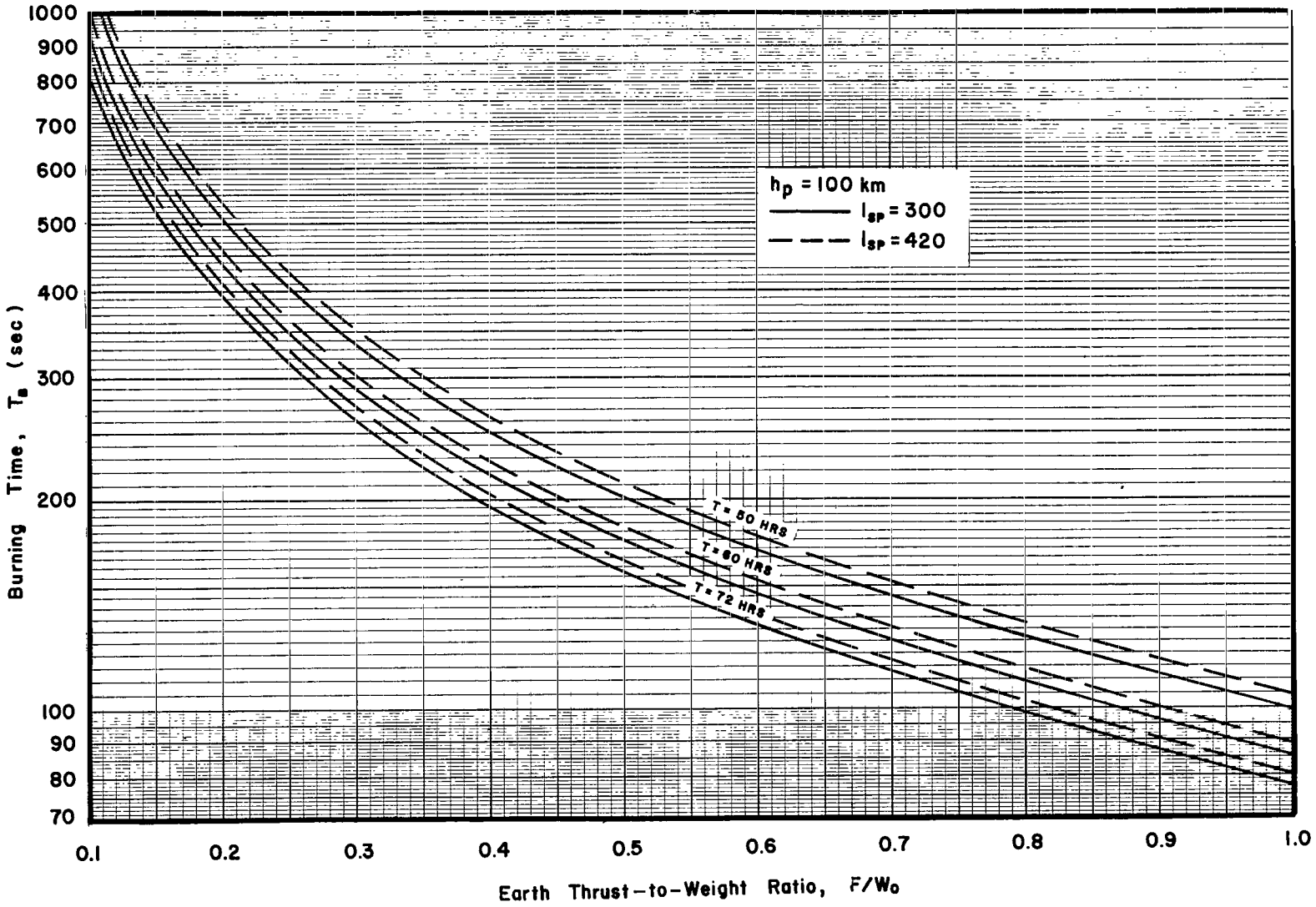

FIGURE 8b. BURNING TIME FOR BRAKE TO LUNAR ORBIT - h_p = 100 km.

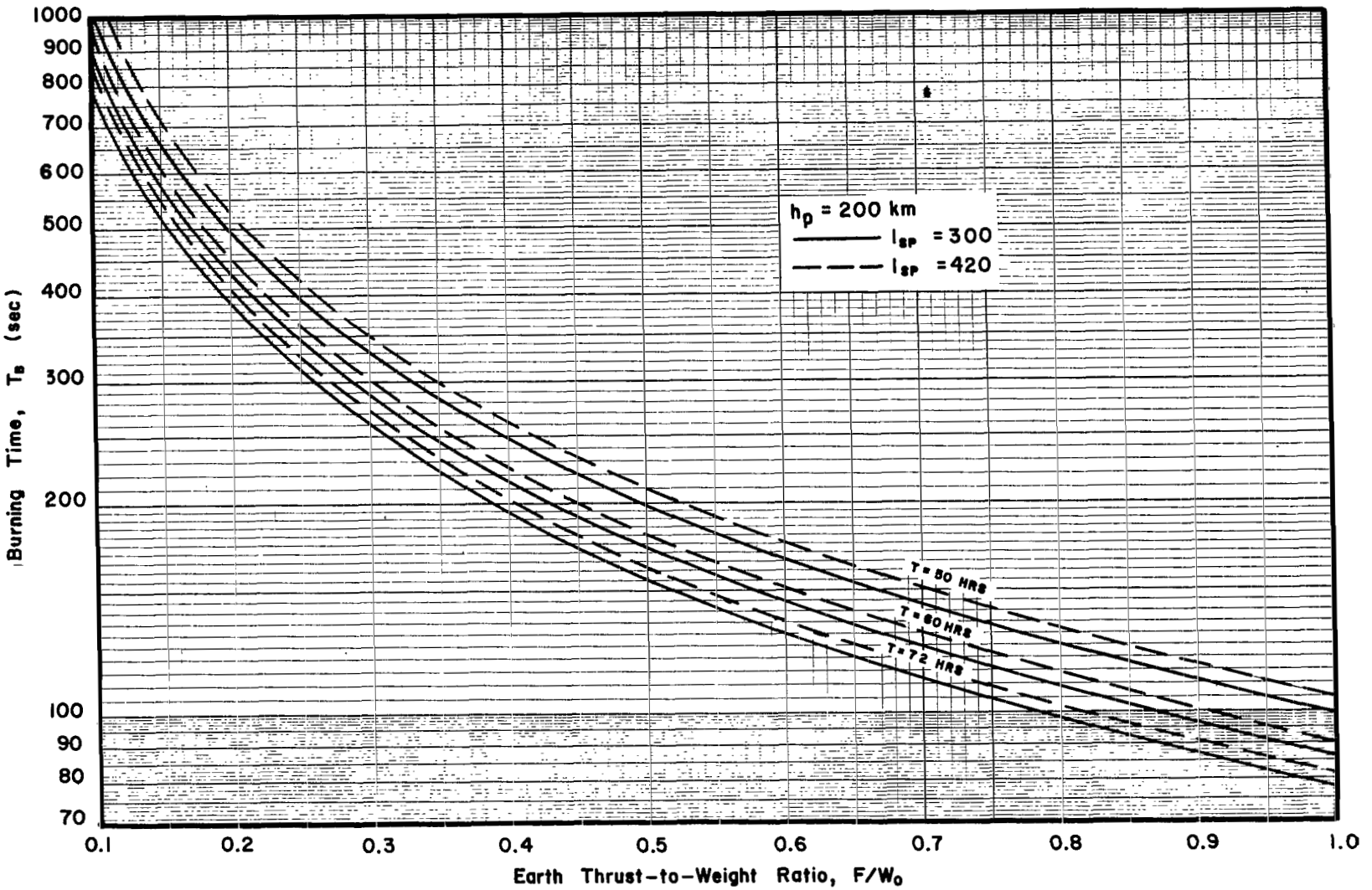

FIGURE 8c. BURNING TIME FOR BRAKE TO LUNAR ORBIT - h_p = 200 km.

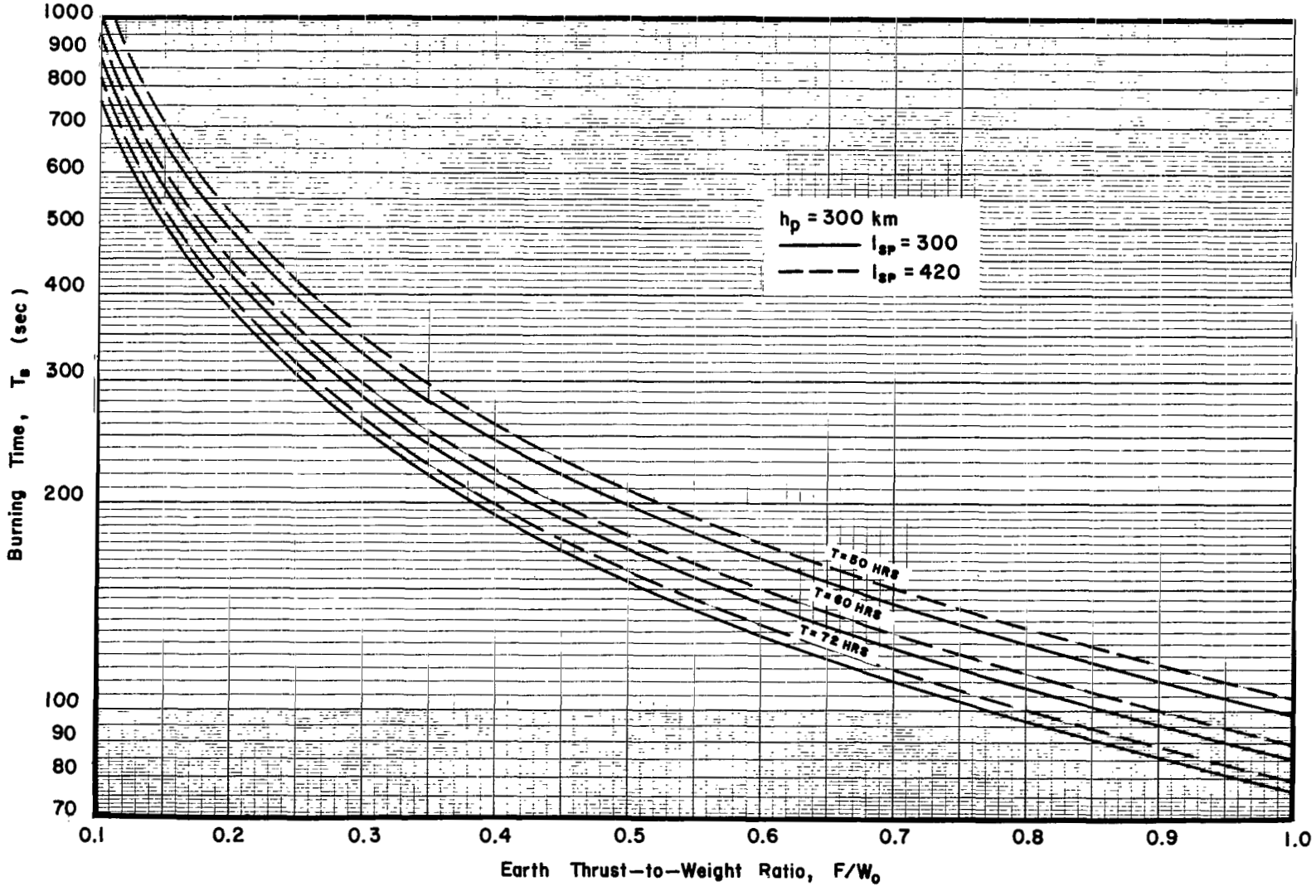

FIGURE 8d. BURNING TIME FOR BRAKE TO LUNAR ORBIT - h_p = 300 km.

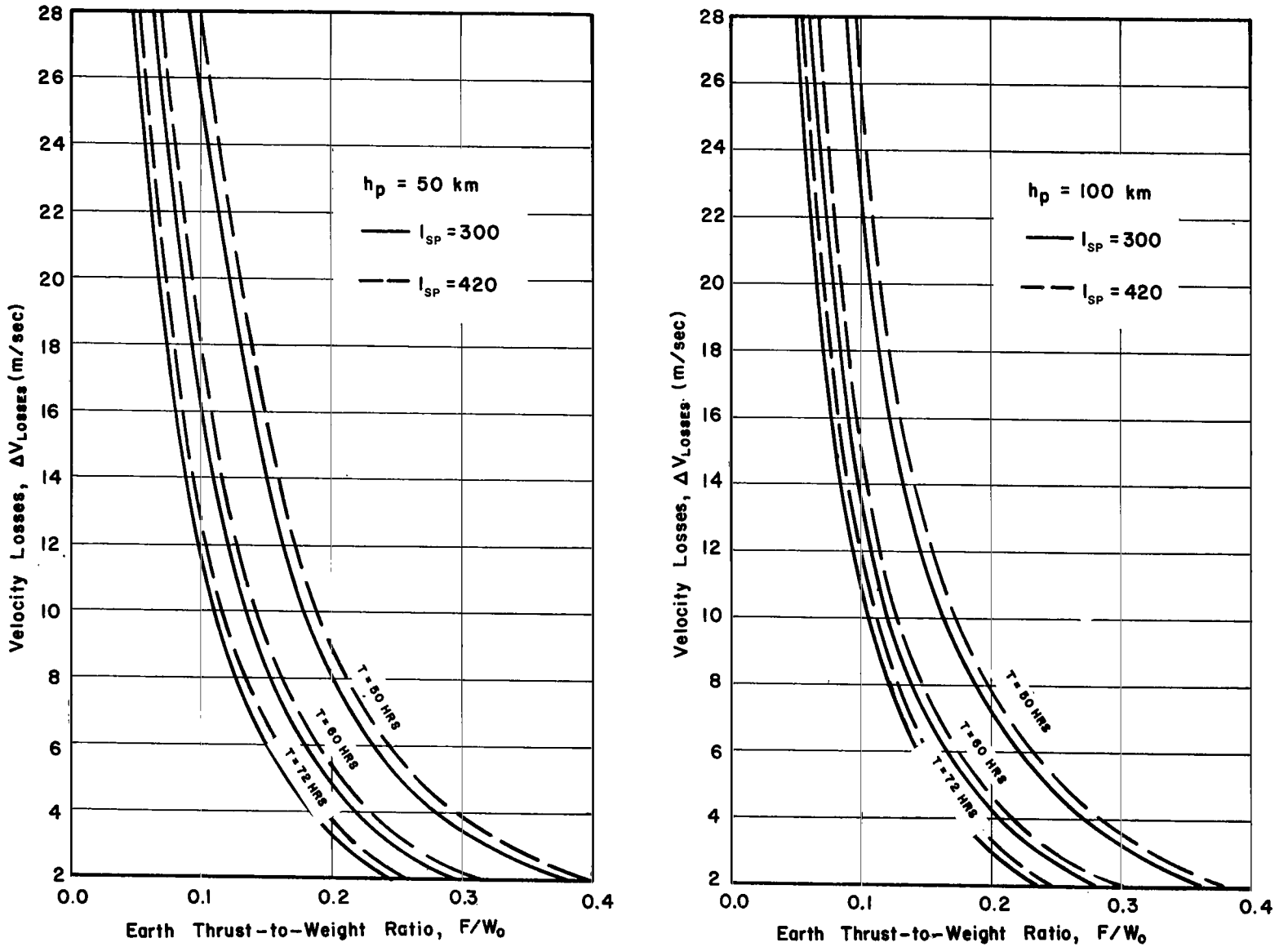

FIGURE 9a. VELOCITY LOSSES FOR BRAKE TO LUNAR ORBIT.

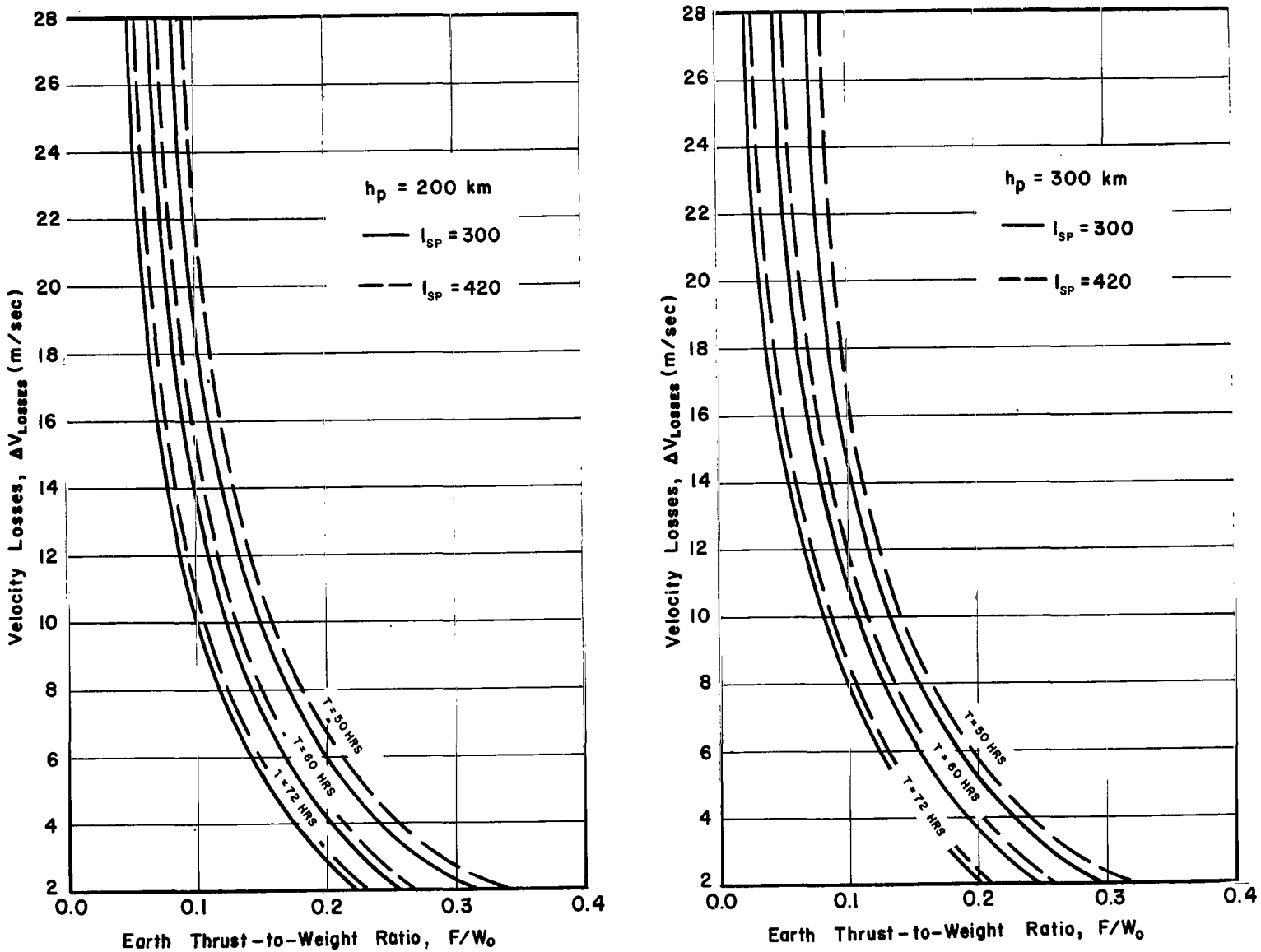

FIGURE 9b. VELOCITY LOSSES FOR BRAKE TO LUNAR ORBIT.

SECTION V. GRAPHIC PRESENTATIONS

DESCENT TO LUNAR SURFACE

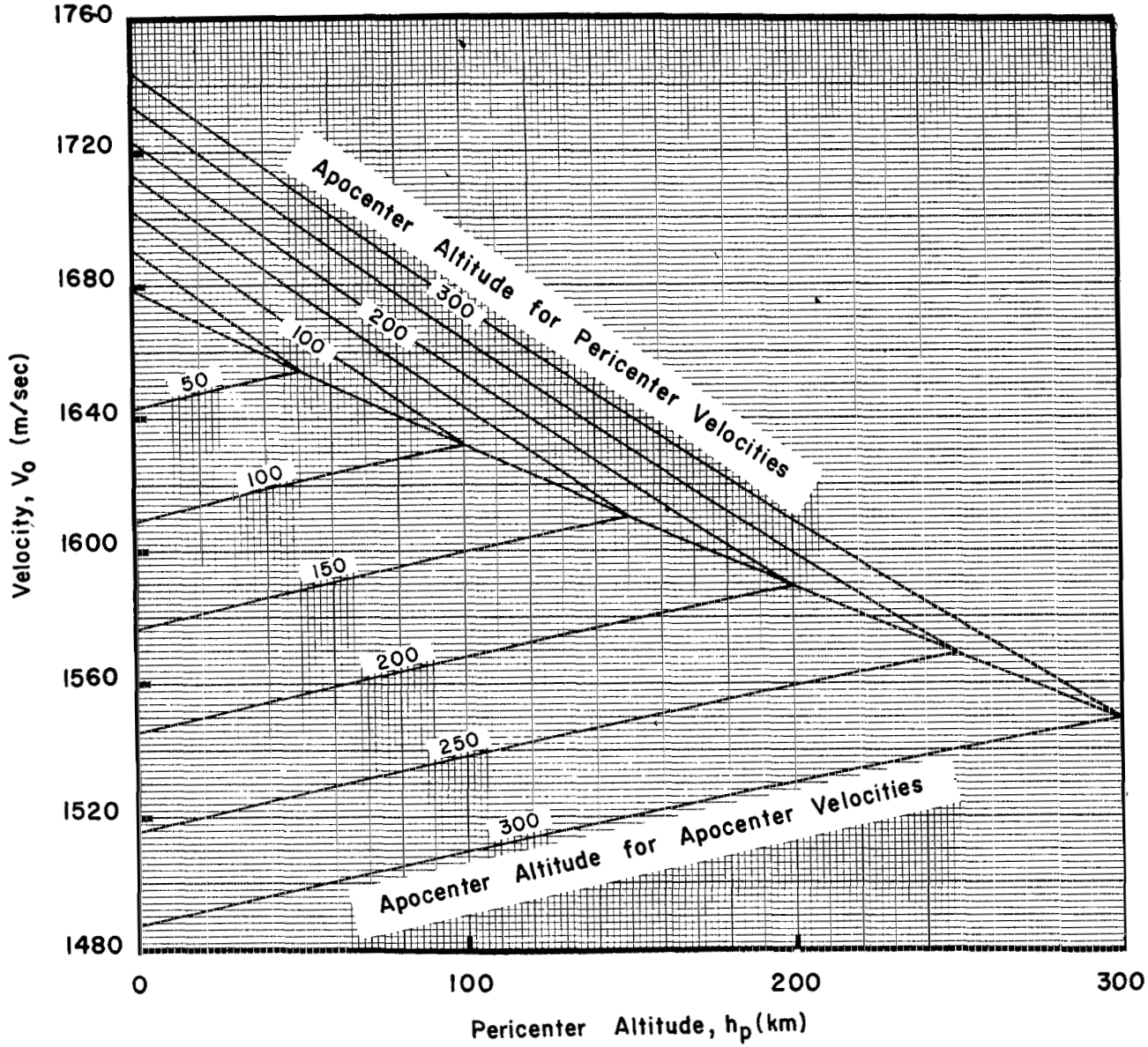

FIGURE 10. APOCENTER AND PERICENTER VELOCITIES VERSUS APOCENTER AND PERICENTER ALTITUDES

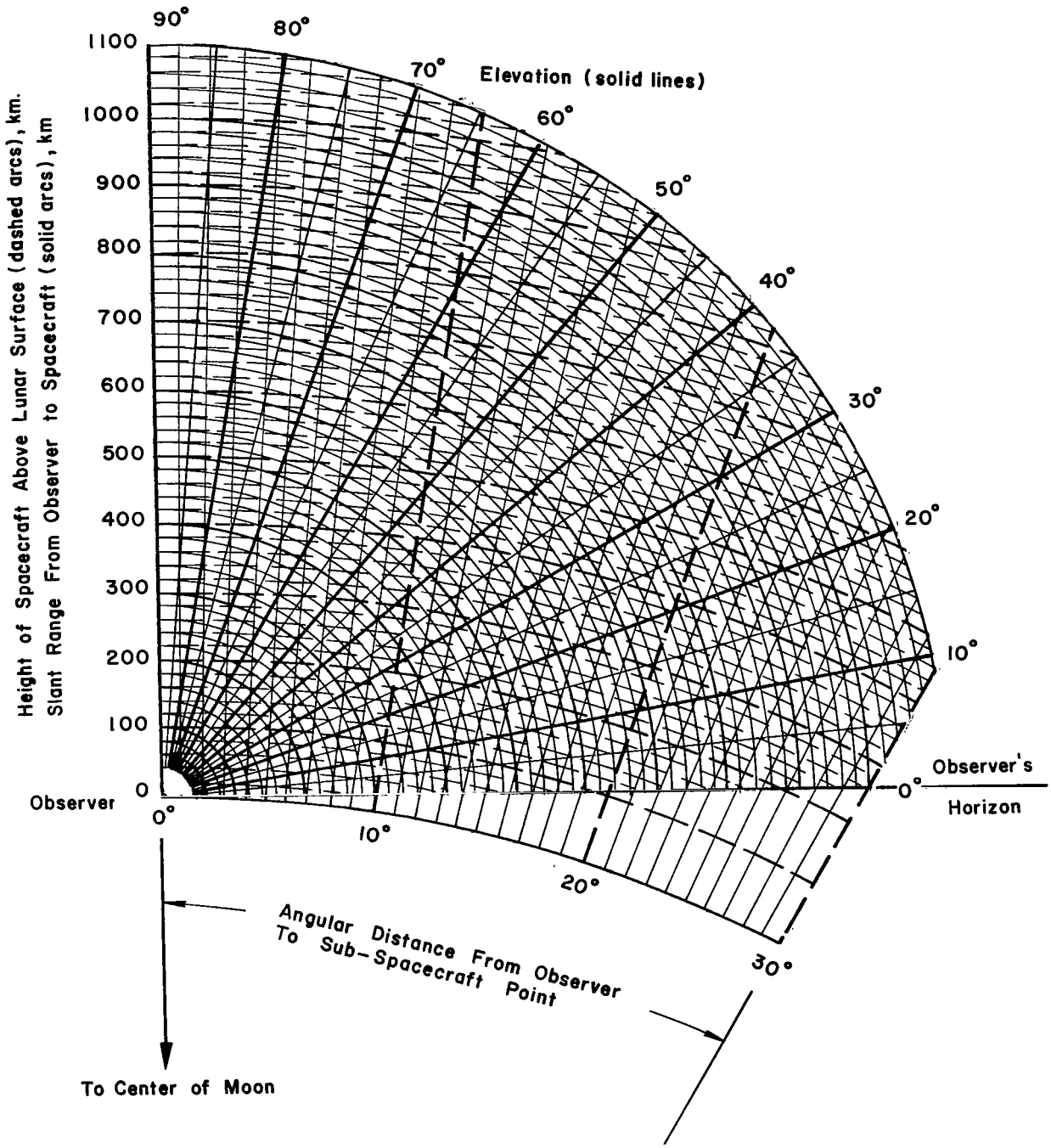

FIGURE 11. CHART FOR DETERMINING ELEVATION AND SLANT RANGE OF LUNAR SPACECRAFT (0 TO 1100 km)

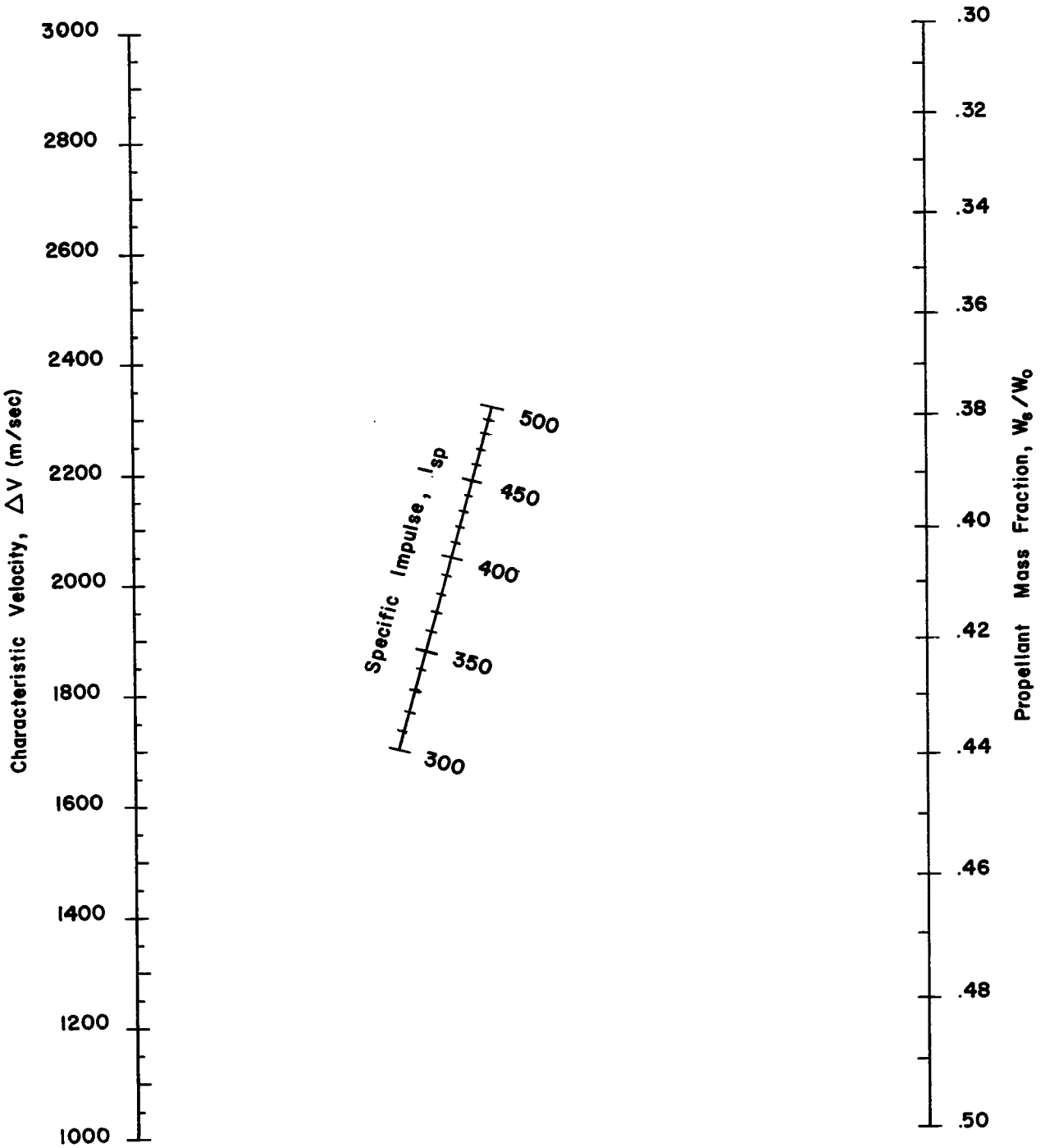

FIGURE 12. CHARACTERISTIC VELOCITY AS A FUNCTION OF PROPELLANT MASS FRACTION AND SPECIFIC IMPULSE

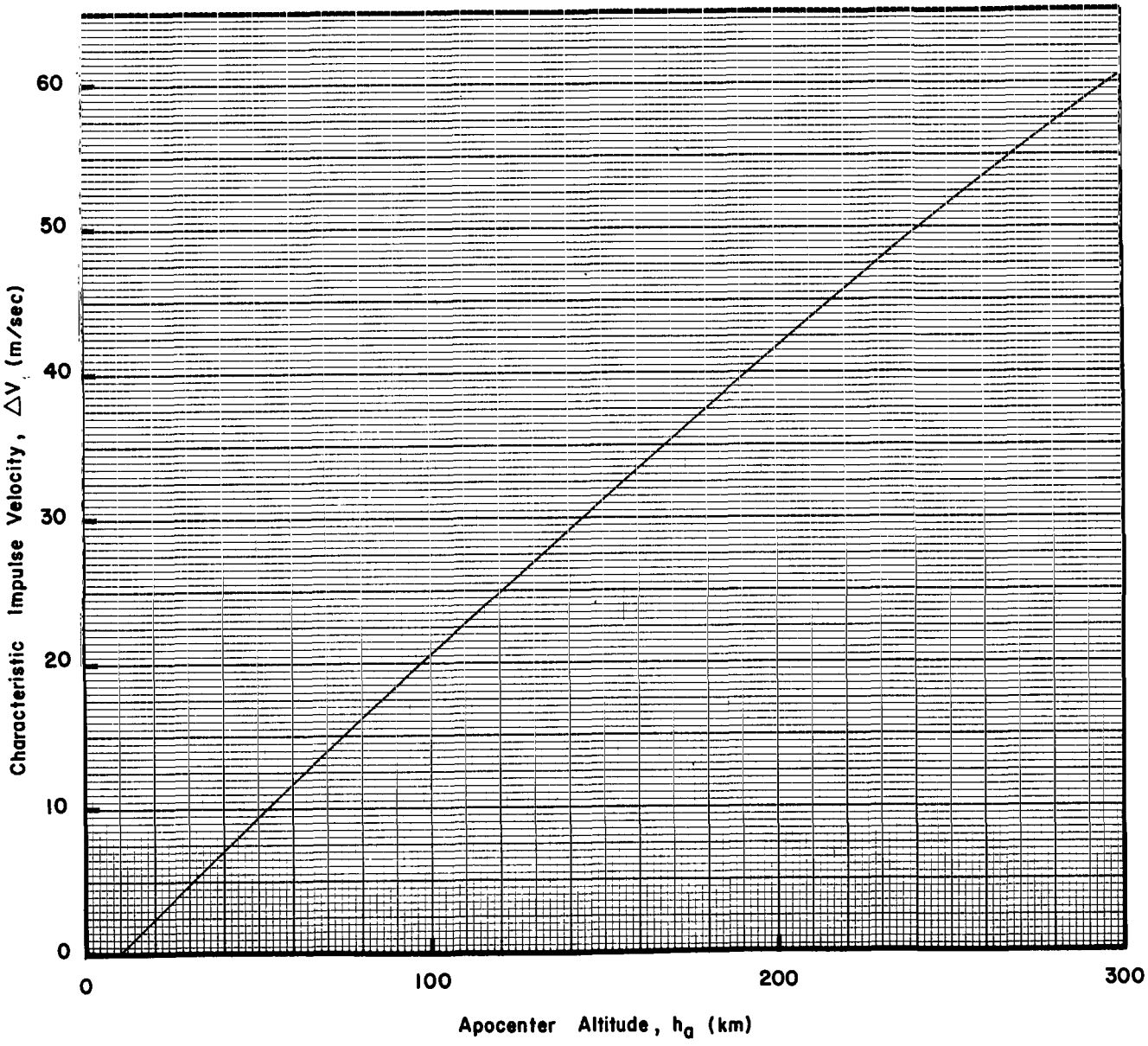

FIGURE 13. CHARACTERISTIC IMPULSE VELOCITY TO ATTAIN TRANSFER ELLIPSE WITH r_p = 1748.3 km

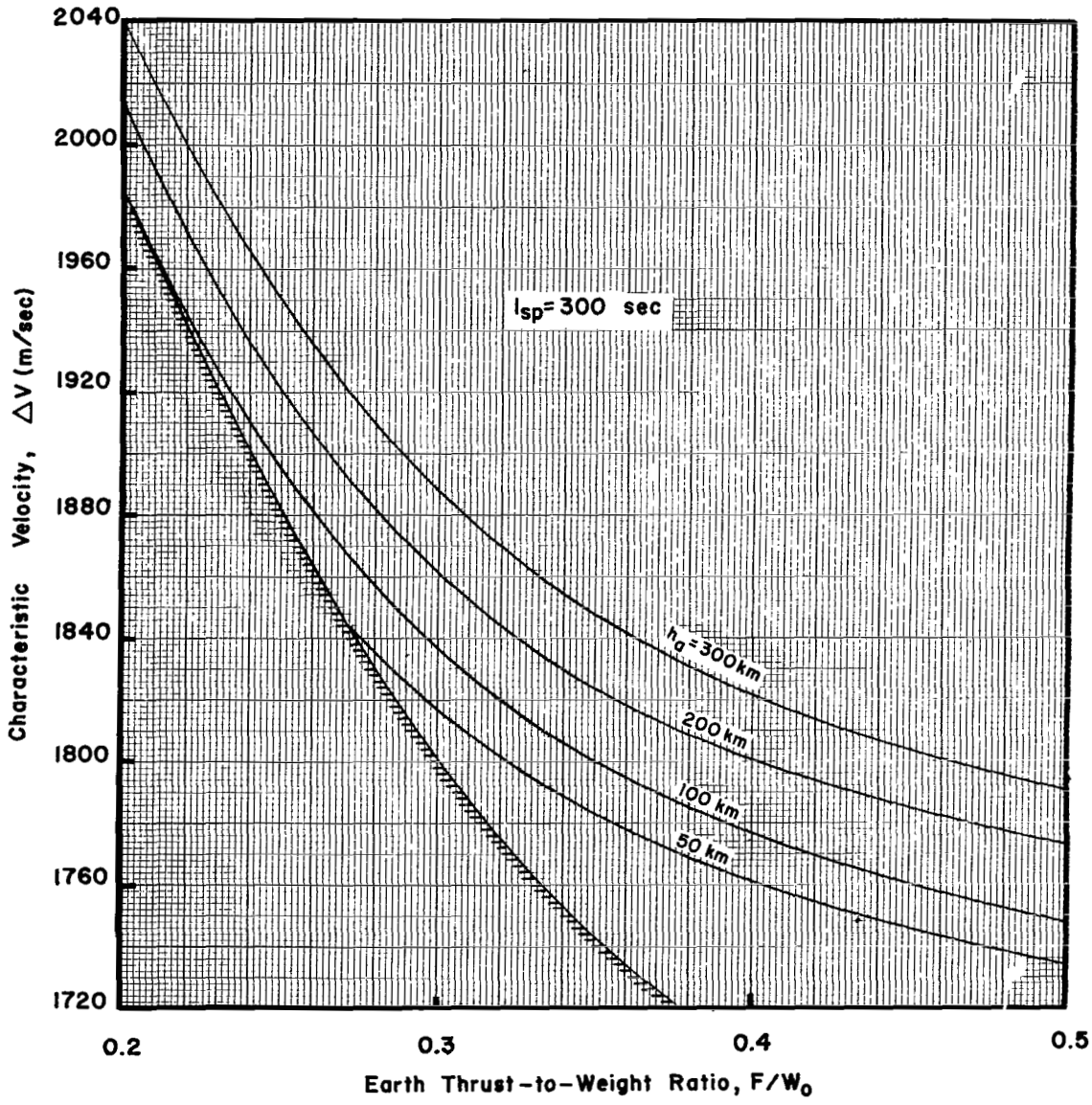

FIGURE 14a. CHARACTERISTIC VELOCITY FOR LUNAR DESCENT - I_{sp} = 300 sec

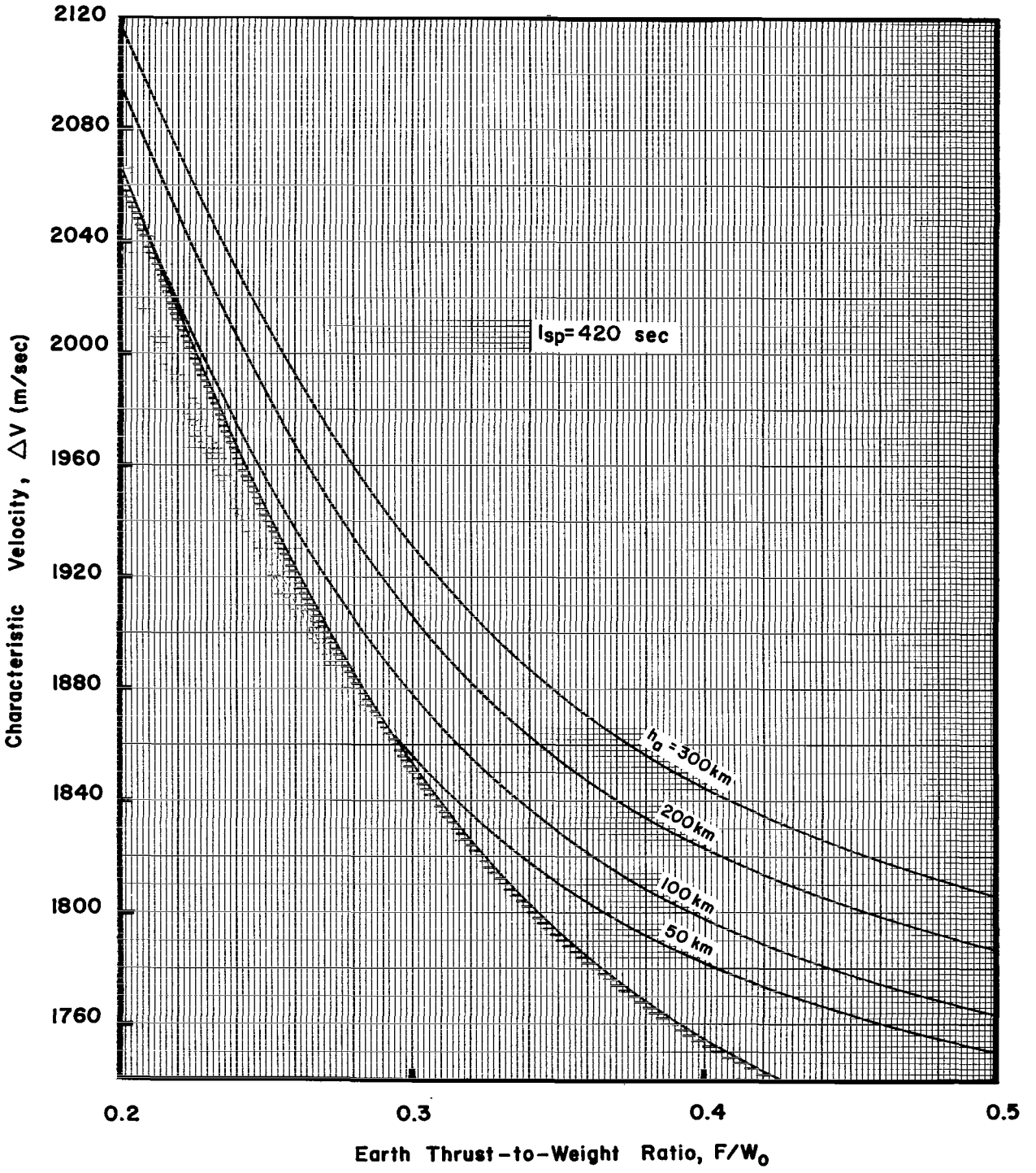

FIGURE 14b. CHARACTERISTIC VELOCITY FOR LUNAR DESCENT - I_{sp} = 420 sec

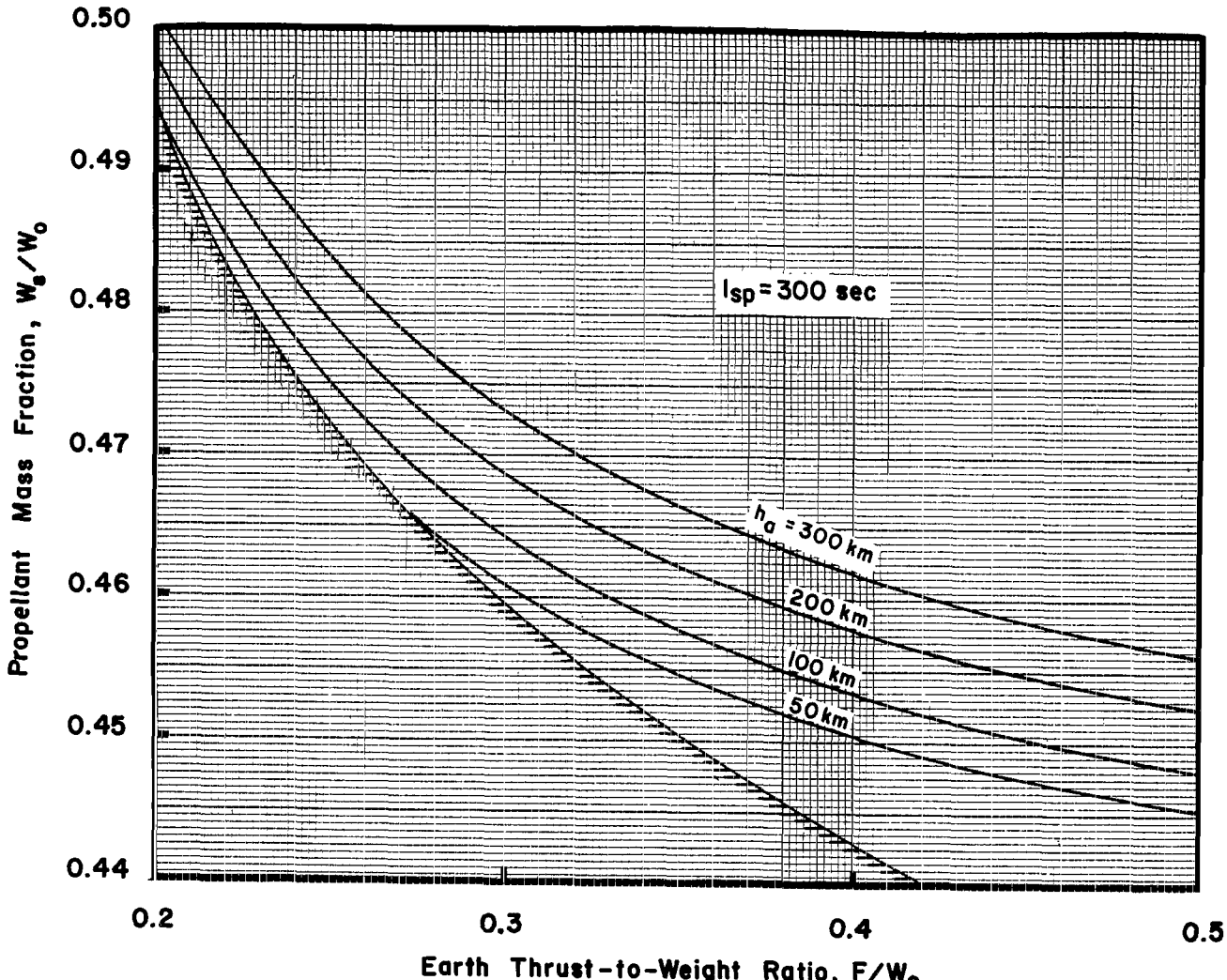

FIGURE 15a. PROPELLANT MASS FRACTION FOR LUNAR DESCENT - I_{sp} = 300 sec

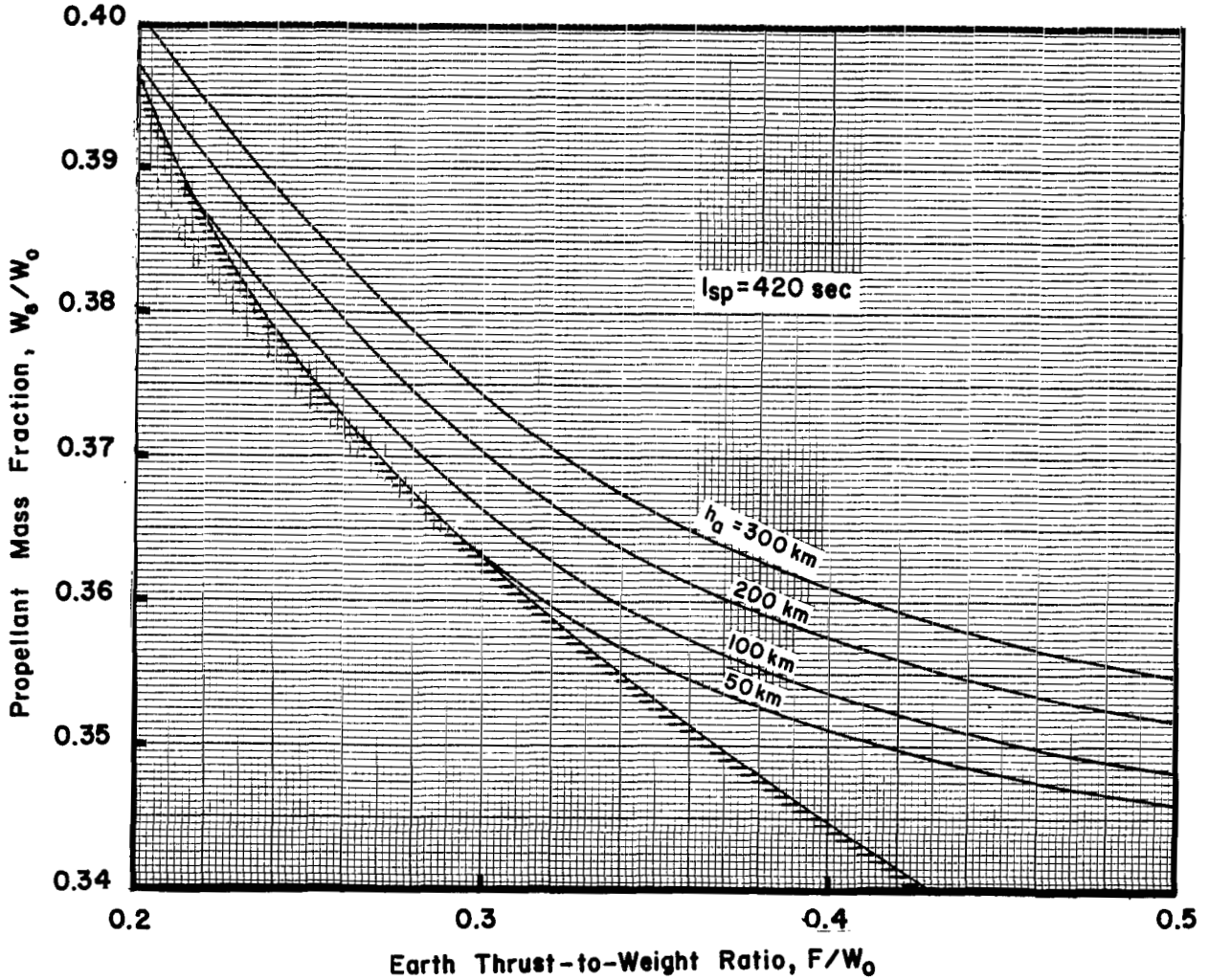

FIGURE 15b. PROPELLANT MASS FRACTION FOR LUNAR DESCENT - I_{sp} = 420 sec

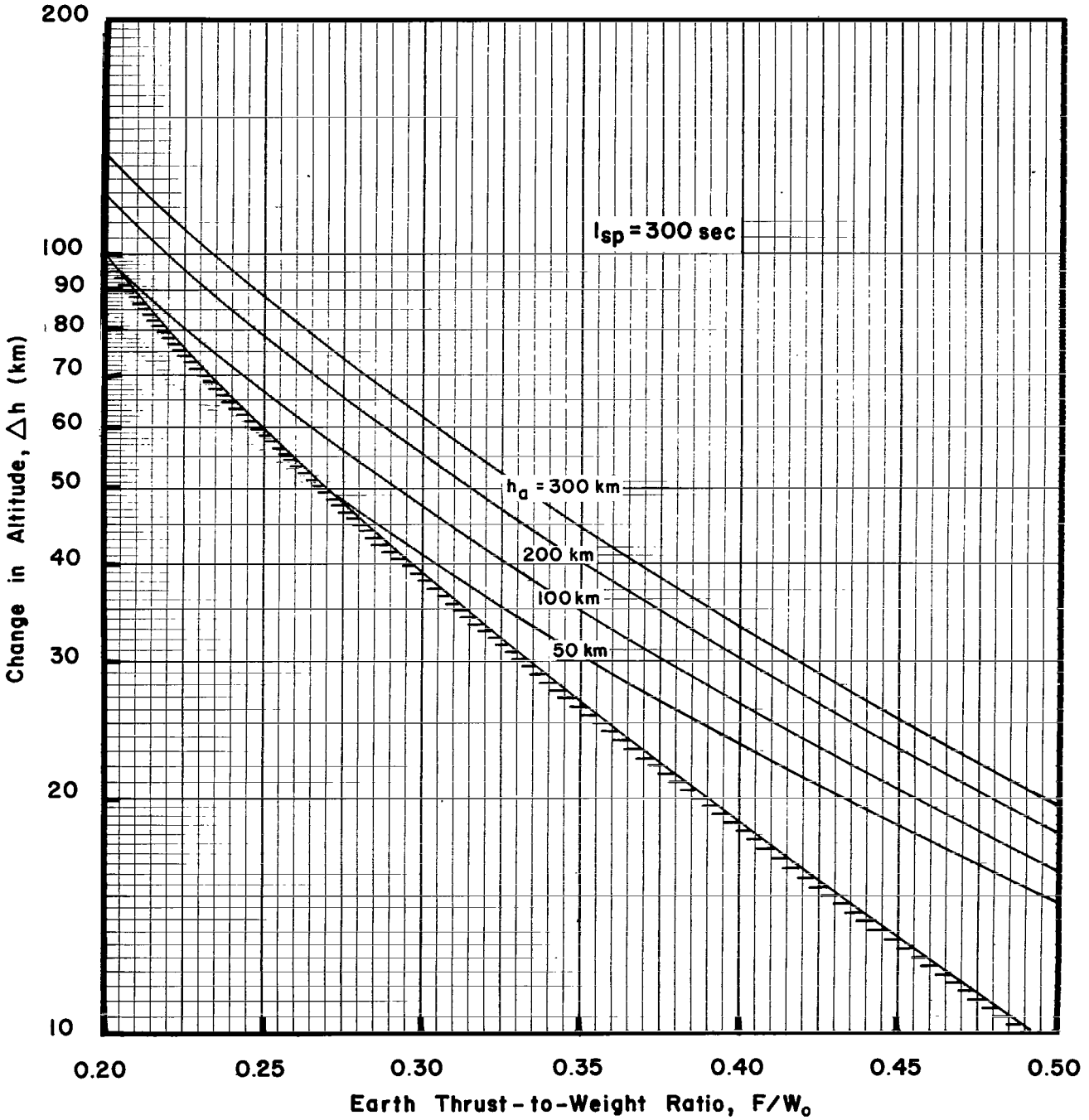

FIGURE 16a. CHANGE IN ALTITUDE FOR LUNAR DESCENT - I_{sp} = 300 sec

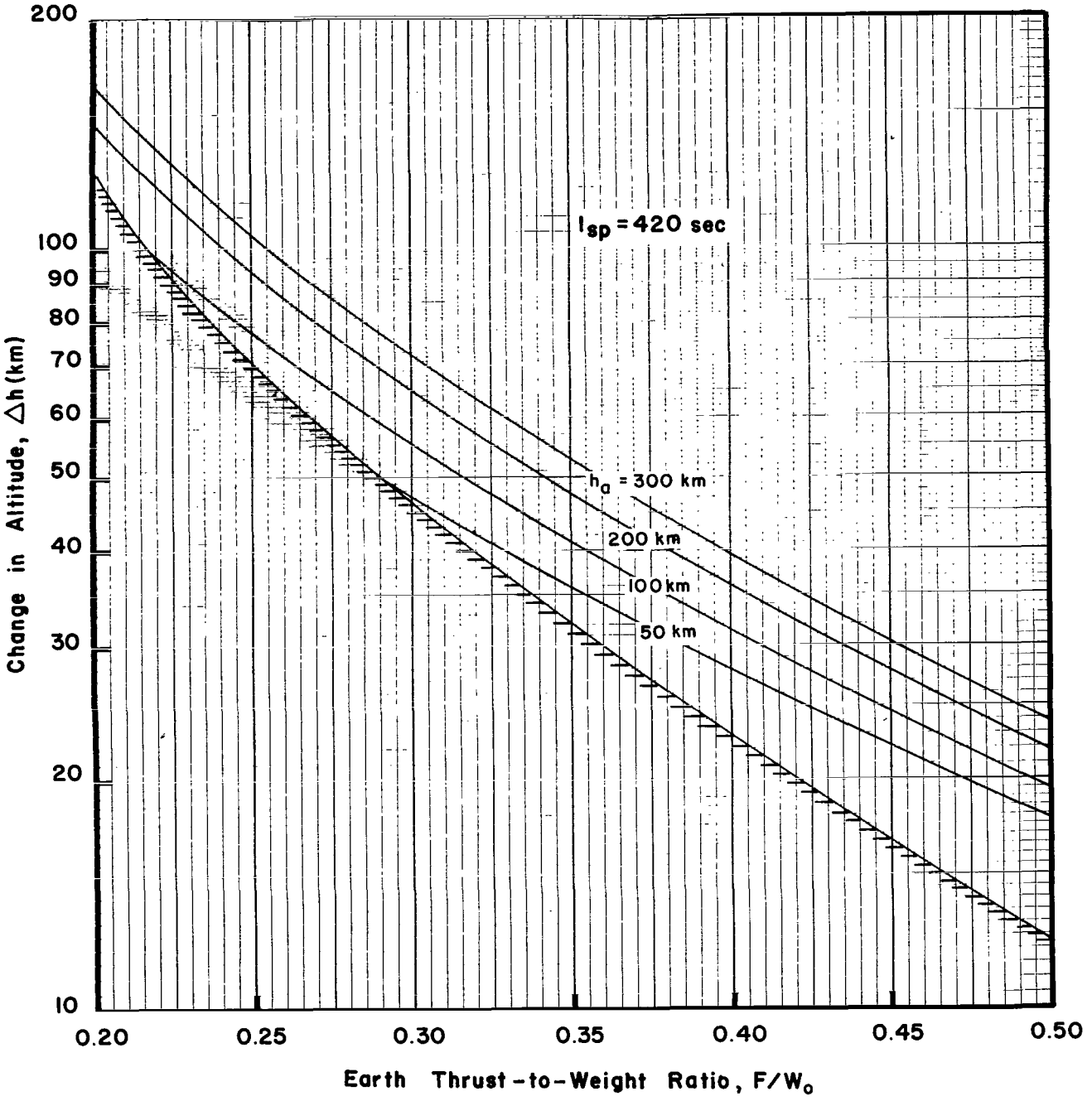

FIGURE 16b. CHANGE IN ALTITUDE FOR LUNAR DESCENT - I_{sp} = 420 sec

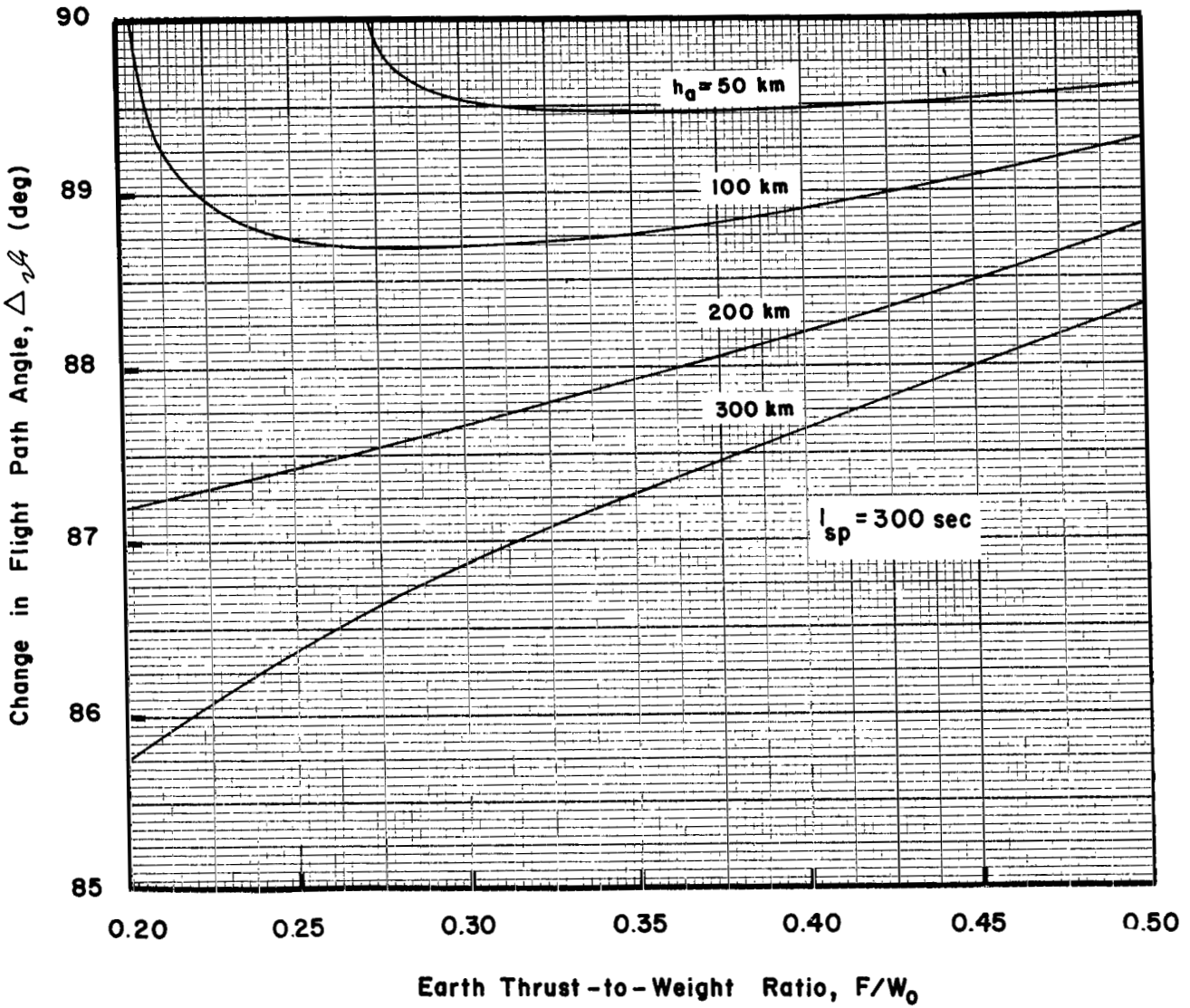

FIGURE 17a. CHANGE IN FLIGHT PATH ANGLE FOR LUNAR DESCENT - I_{sp} = 300 sec

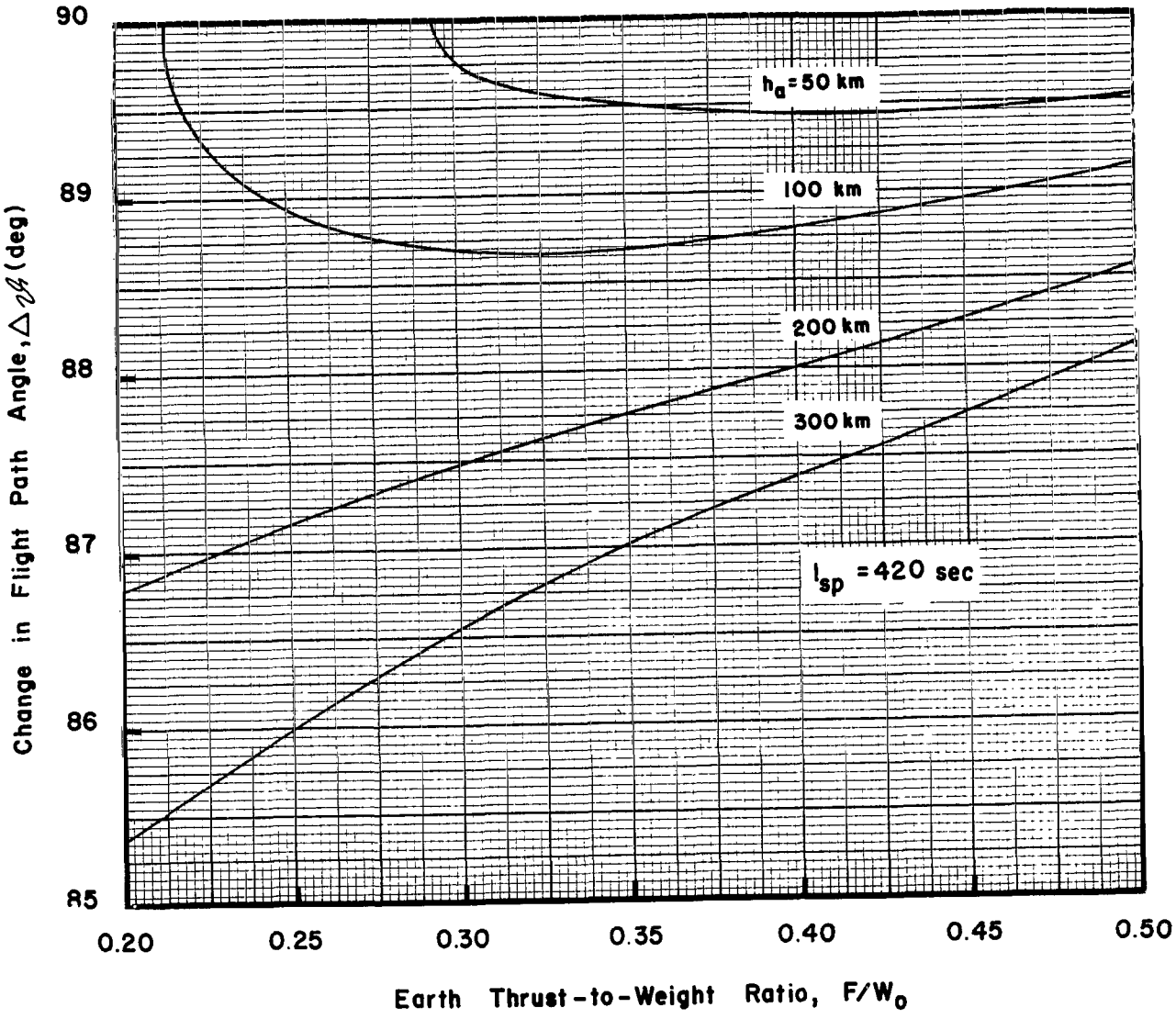

FIGURE 17b. CHANGE IN FLIGHT PATH ANGLE FOR LUNAR DESCENT - I_{sp} = 420 sec

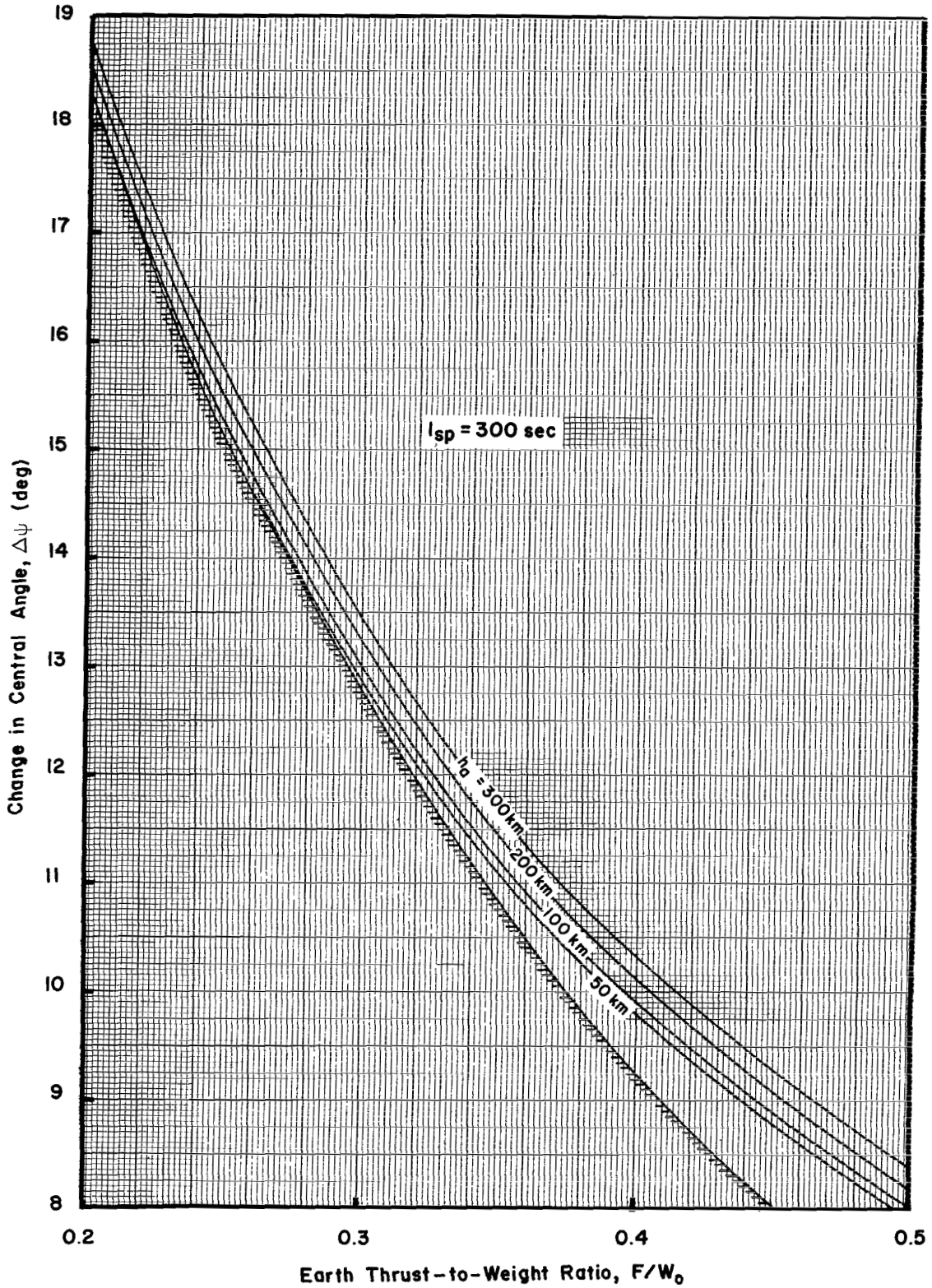

FIGURE 18a. CHANGE IN CENTRAL ANGLE FOR LUNAR DESCENT - I_{sp} = 300 sec

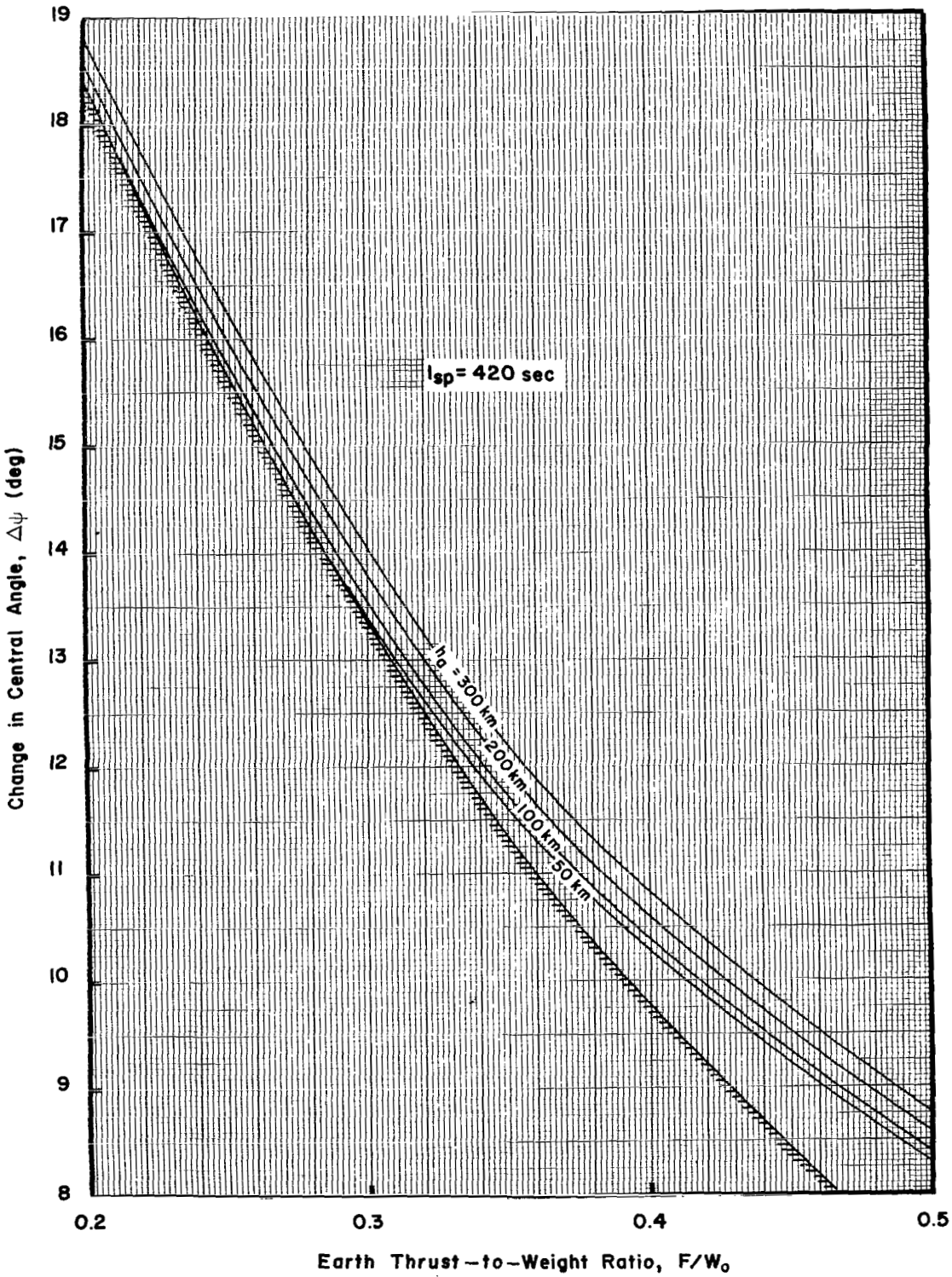

FIGURE 18b. CHANGE IN CENTRAL ANGLE FOR LUNAR DESCENT - I_{sp} = 420 sec

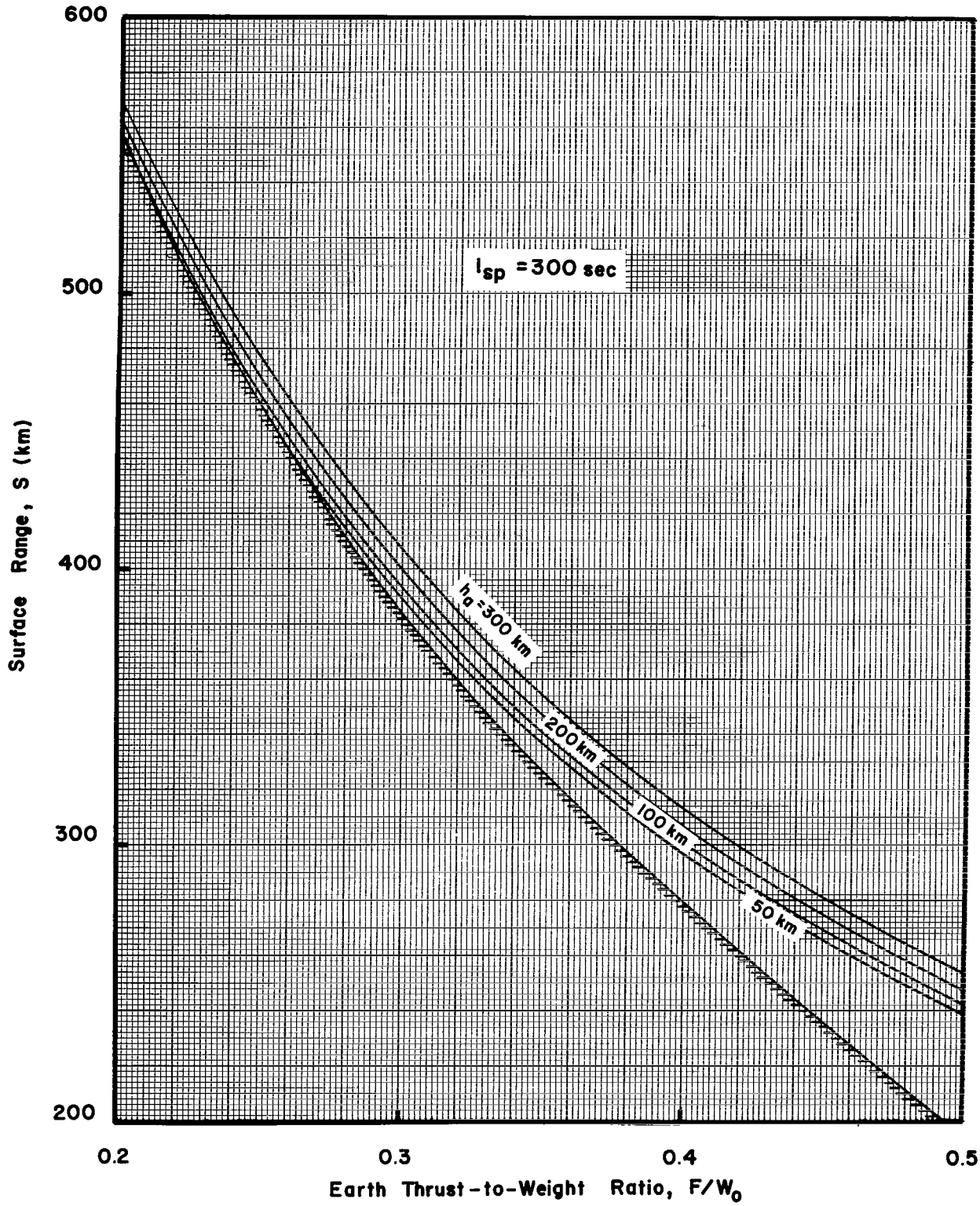

FIGURE 19a. SURFACE RANGE FOR LUNAR DESCENT - I_{sp} = 300 sec

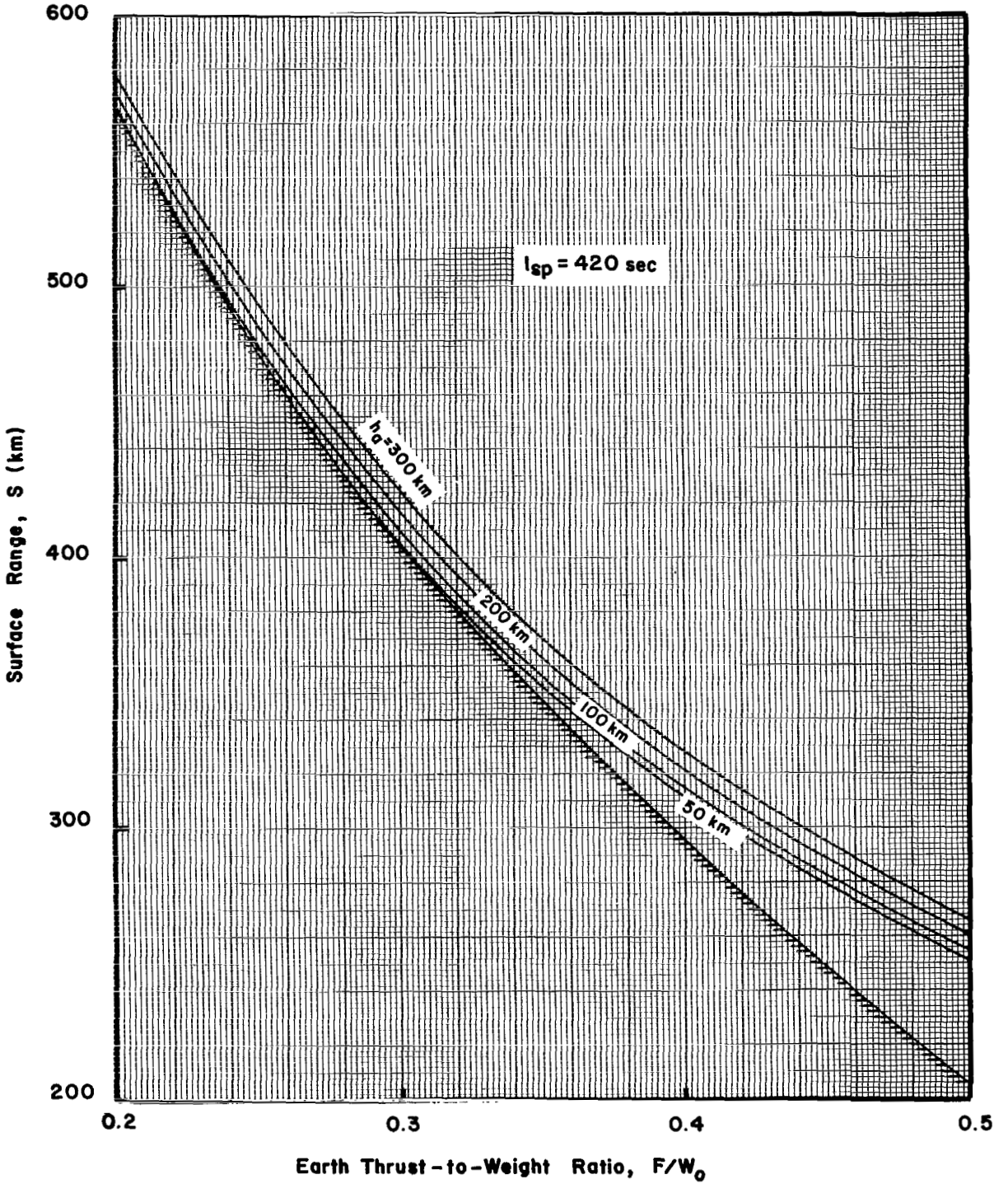

FIGURE 19b. SURFACE RANGE FOR LUNAR DESCENT - I_{sp} = 420 sec

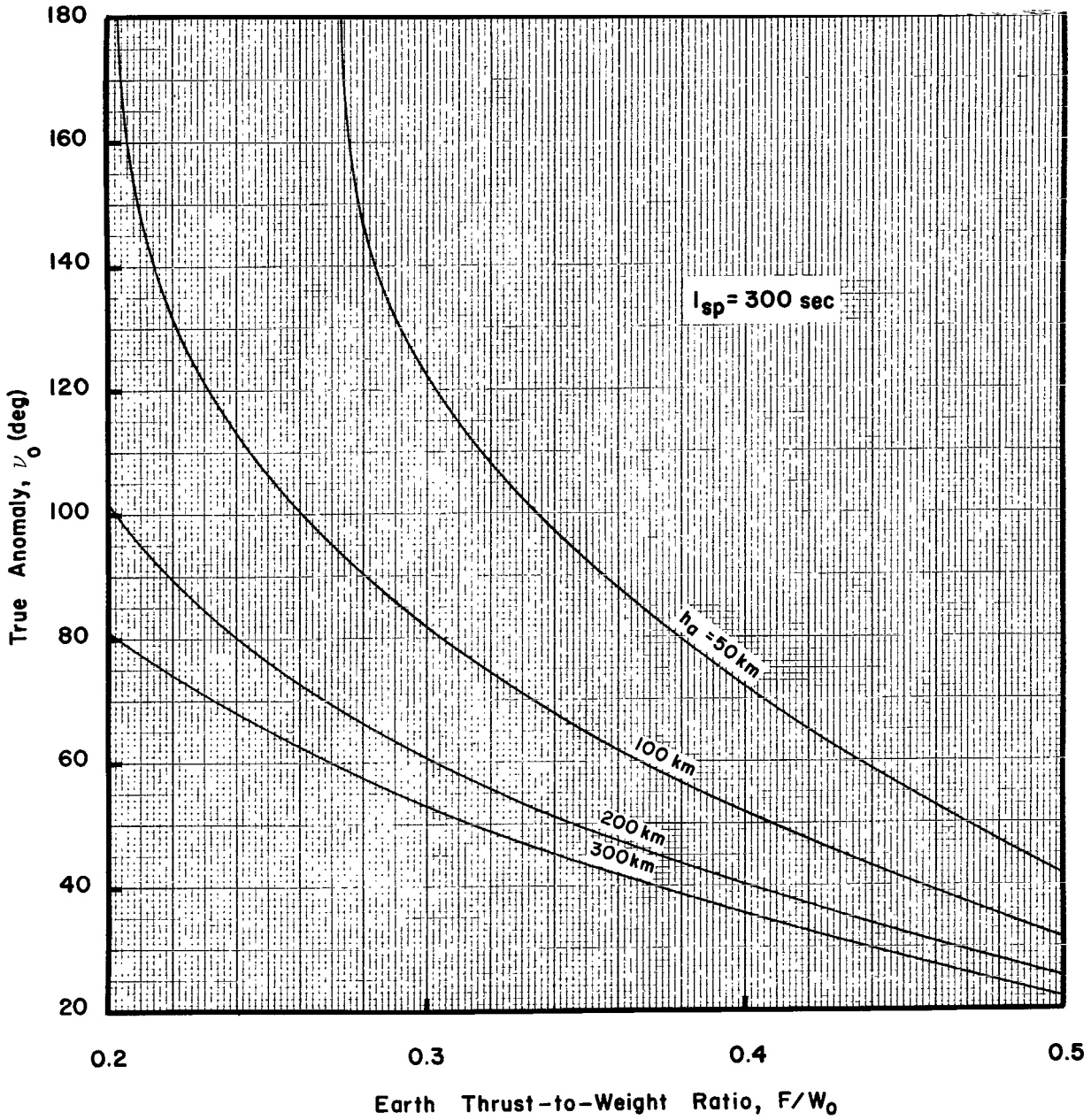

FIGURE 20a. TRUE ANOMALY AT INITIATION OF LUNAR DESCENT - I_{sp} = 300 sec

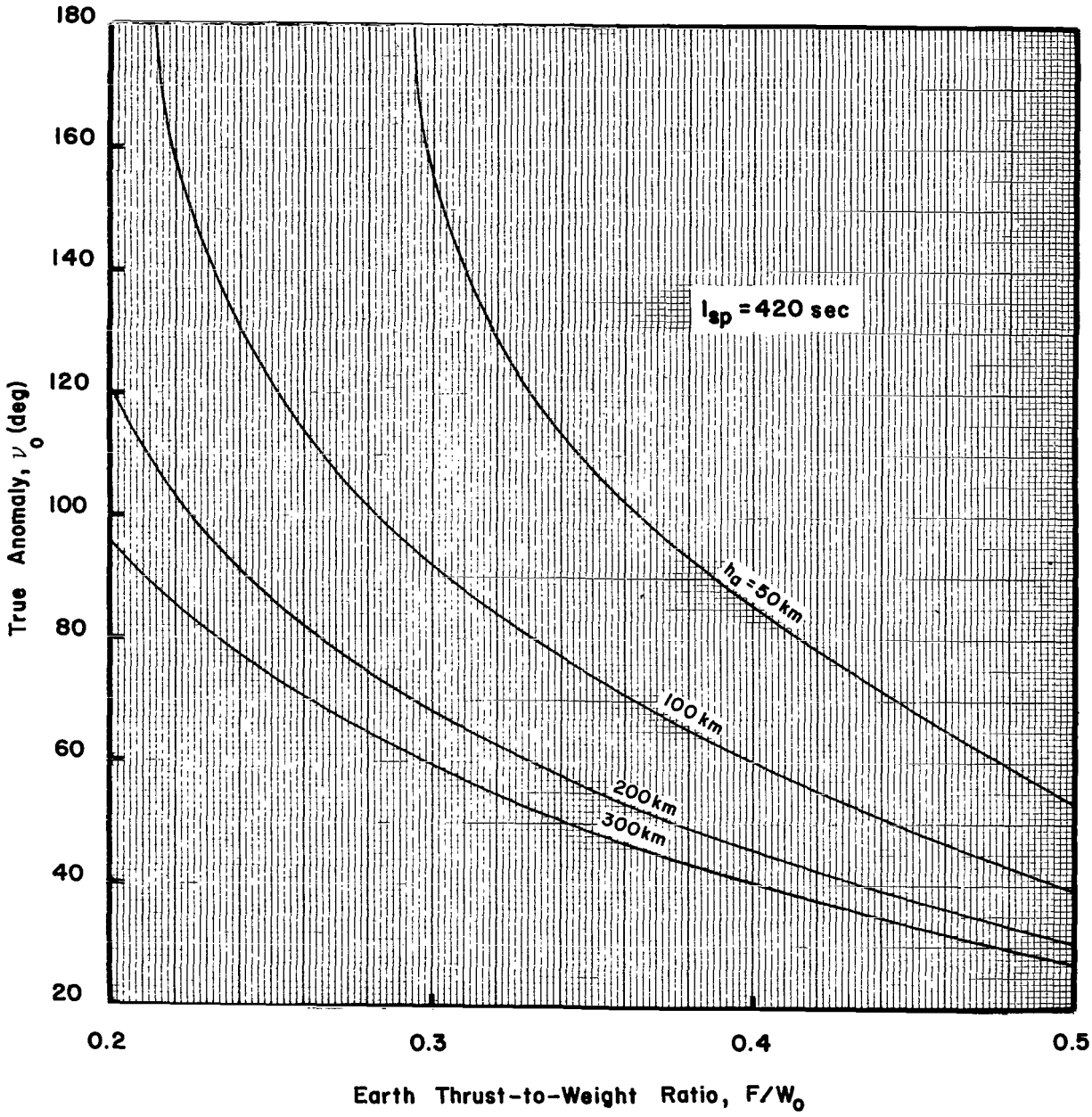

FIGURE 20b. TRUE ANOMALY AT INITIATION OF LUNAR DESCENT - I_{sp} = 420 sec

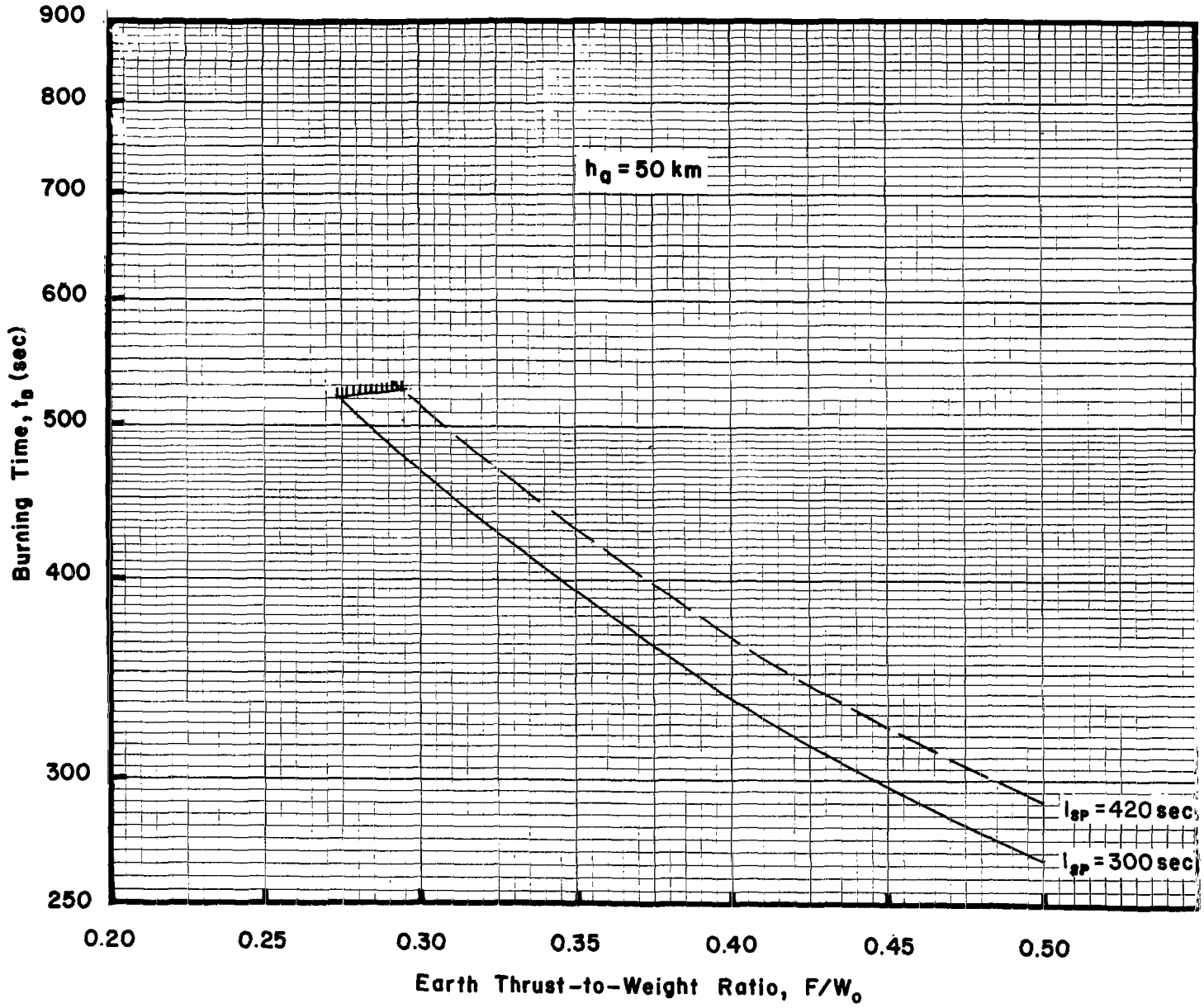

FIGURE 21a. BURNING TIME FOR LUNAR DESCENT - h_a = 50 km

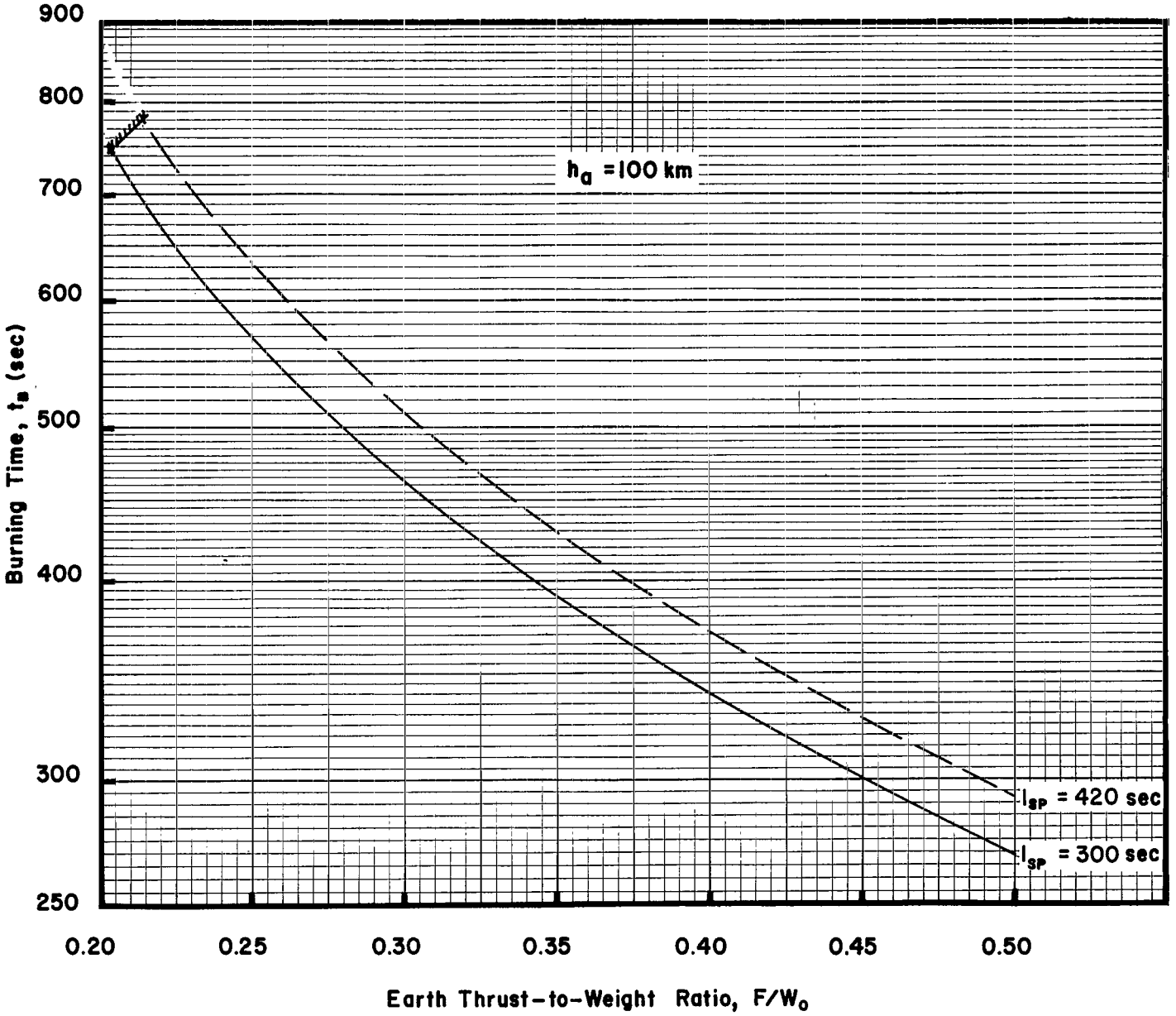

FIGURE 21b. BURNING TIME FOR LUNAR DESCENT - h_a = 100 km

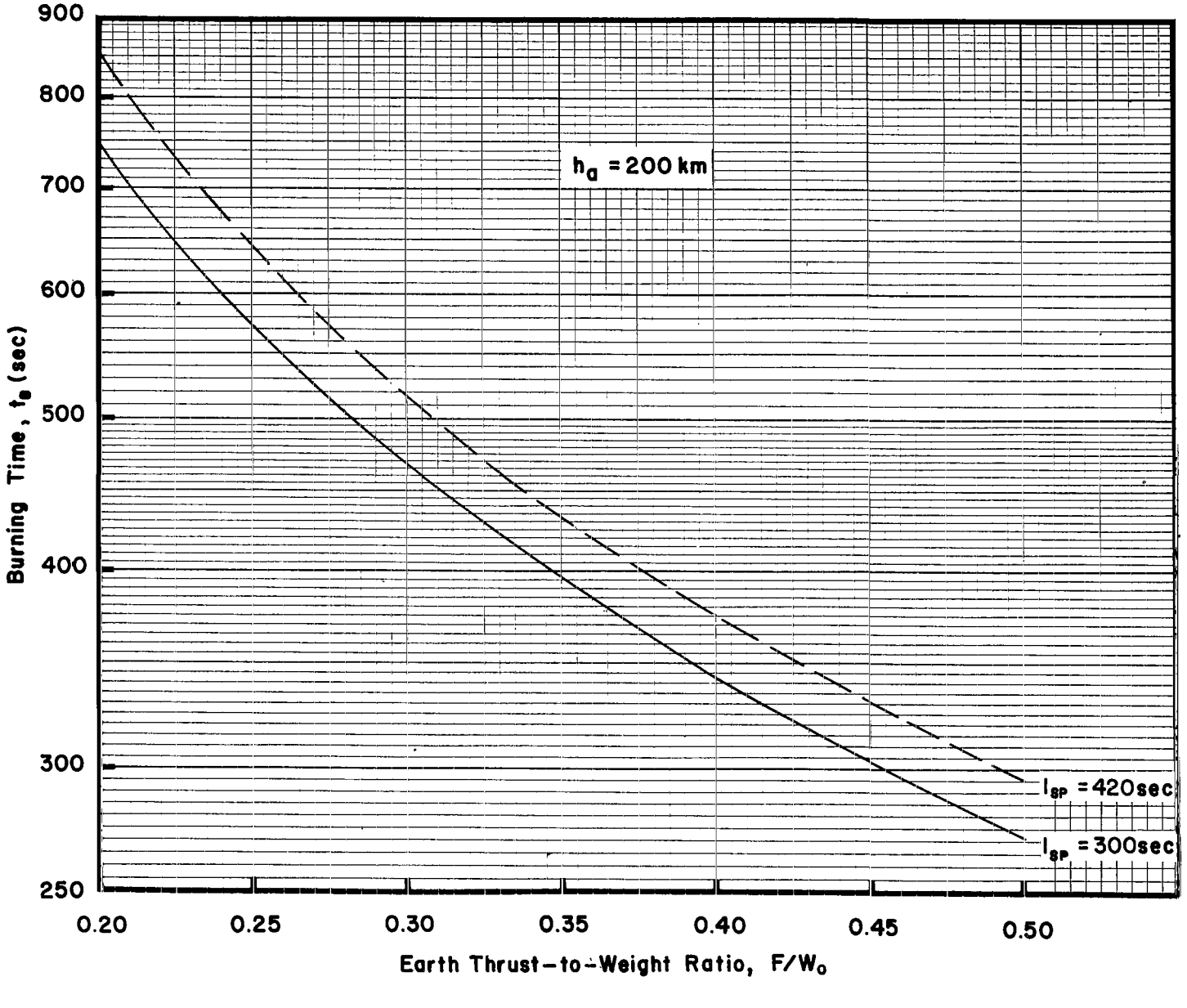

FIGURE 21c. BURNING TIME FOR LUNAR DESCENT - h_a = 200 km

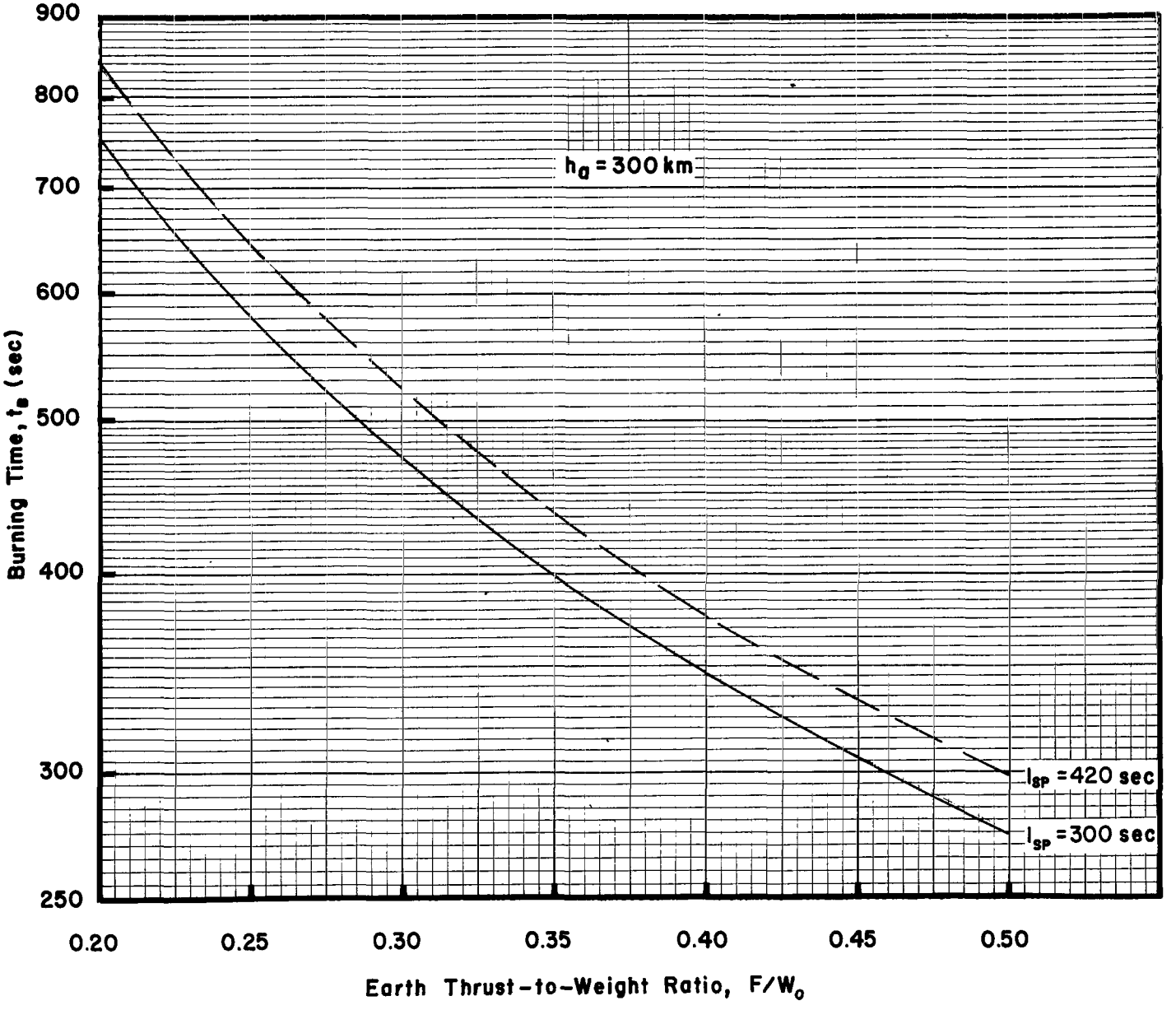

FIGURE 21d. BURNING TIME FOR LUNAR DESCENT - h_a = 300 km

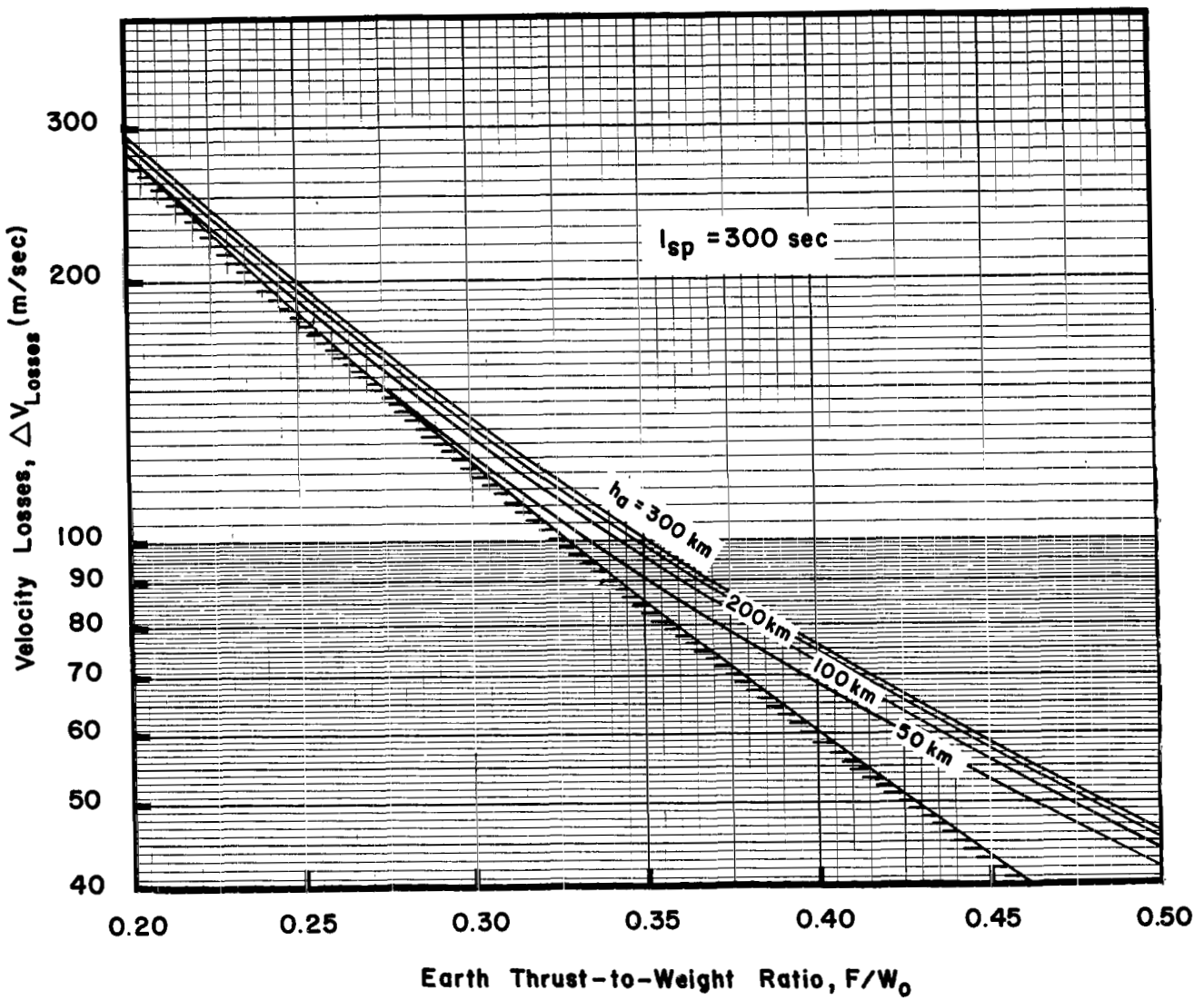

FIGURE 22a. VELOCITY LOSSES FOR LUNAR DESCENT - I_{sp} = 300 sec

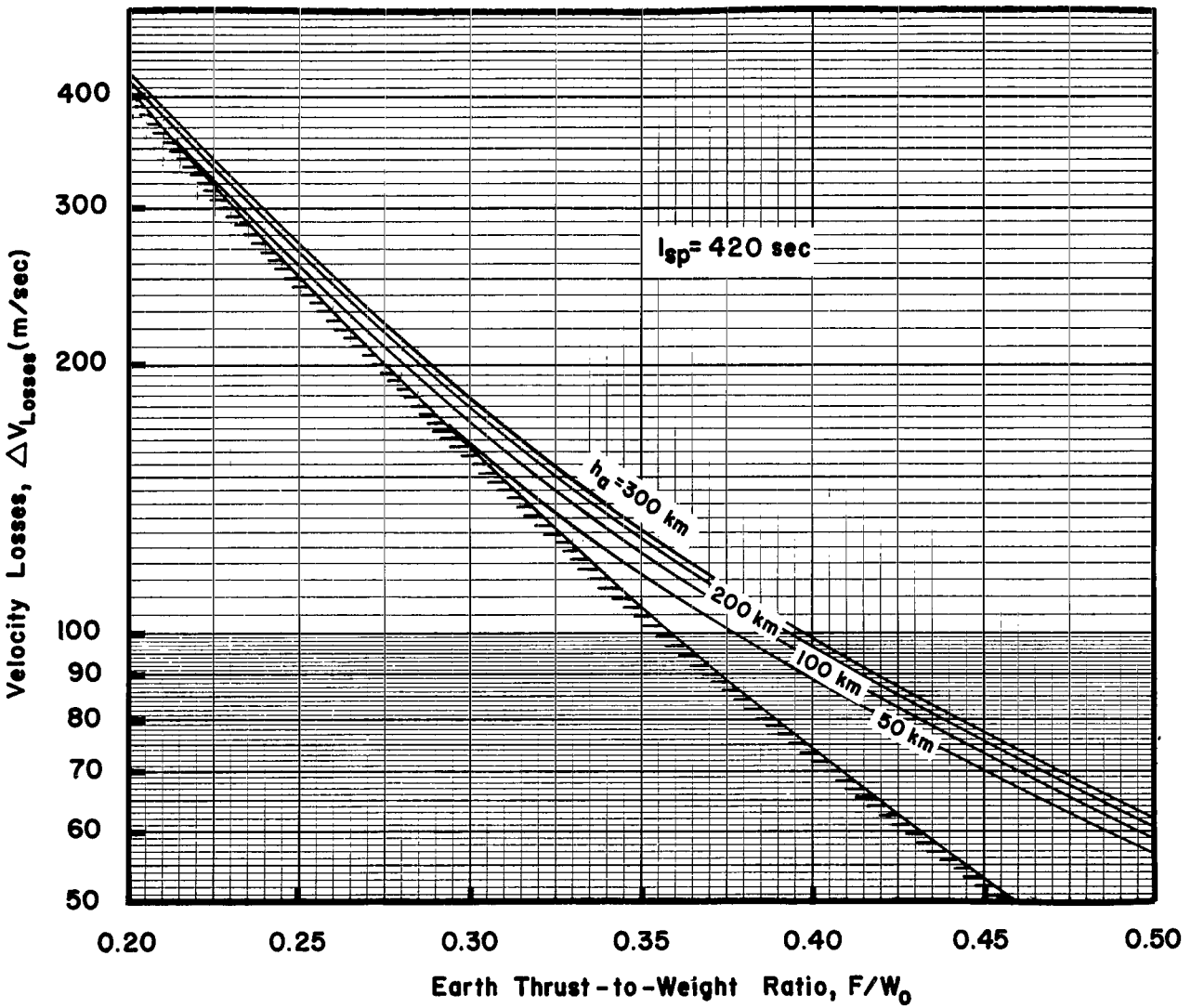

FIGURE 22b. VELOCITY LOSSES FOR LUNAR DESCENT - I_{sp} = 420 sec

BIBLIOGRAPHY

Akridge, C. M. and Sam H. Harlin, Parametric Performance Analysis of Lunar Missions, Brake to Lunar Orbit, MTP-P&VE-F-63-6, March 5, 1963.

Akridge, C. M. and Sam H. Harlin, Parametric Performance Analysis of Lunar Missions, Lunar Descent, MTP-P&VE-F-63-8, May 2, 1963.

Fellenz, Dietrich W. and Ronald J. Harris, Influence of Weight Parameters on the Propulsion Requirements of Orbit-Launched Vehicles, NASA TN D-1525, May 1963.

Jenkins, M. V. and R. E. Munford, Preliminary Survey of Retro-grade Velocities Required for Insertion into Low-Altitude Lunar Orbits, NASA TN D-1081, September 1961.

Mason, Maxwell and S. M. Brainin, Descent Trajectory Optimization for Soft Lunar Landings, IAS 30th Annual Meeting, Paper No. 63-11, January 22-24, 1962.

Queijo, M. J. and G. K. Miller, Jr., Analysis of Two Thrusting Techniques for Soft Lunar Landings Starting from a 50-mile Altitude Circular Orbit, NASA TN D-1230, March 1962.

Stafford, Walter H., Working Graphs for Artificial Lunar Satellites, IN-P&VE-F-62-6, July 3, 1962.

Steiner, P., Lunar Powered Flight, STL Report No. 8976-0004-RU-000, August 10, 1961.

Weber, R. J., W. M. Pauson, and R. R. Burley, Lunar Trajectories, NASA TN D-866, August 1961.

Weber, R. J. and W. M. Pauson, Some Thrust and Trajectory Considerations for Lunar Landings, NASA TN D-134, November 1959.

NASA-Langley, 1965 M323

"The aeronautical and space activities of the United States shall be conducted so as to contribute . . . to the expansion of human knowledge of phenomena in the atmosphere and space. The Administration shall provide for the widest practicable and appropriate dissemination of information concerning its activities and the results thereof."

—NATIONAL AERONAUTICS AND SPACE ACT OF 1958

NASA SCIENTIFIC AND TECHNICAL PUBLICATIONS

TECHNICAL REPORTS: Scientific and technical information considered important, complete, and a lasting contribution to existing knowledge.

TECHNICAL NOTES: Information less broad in scope but nevertheless of importance as a contribution to existing knowledge.

TECHNICAL MEMORANDUMS: Information receiving limited distribution because of preliminary data, security classification, or other reasons.

CONTRACTOR REPORTS: Technical information generated in connection with a NASA contract or grant and released under NASA auspices.

TECHNICAL TRANSLATIONS: Information published in a foreign language considered to merit NASA distribution in English.

TECHNICAL REPRINTS: Information derived from NASA activities and initially published in the form of journal articles.

SPECIAL PUBLICATIONS: Information derived from or of value to NASA activities but not necessarily reporting the results of individual NASA-programmed scientific efforts. Publications include conference proceedings, monographs, data compilations, handbooks, sourcebooks, and special bibliographies.

Details on the availability of these publications may be obtained from:

SCIENTIFIC AND TECHNICAL INFORMATION DIVISION

NATIONAL AERONAUTICS AND SPACE ADMINISTRATION

Washington, D.C. 20546